2

A REVIEW OF LOCALIZED CORROSION OF HIGH-LEVEL NUCLEAR WASTE CONTAINER MATERIALS - I

Prepared for

Nuclear Regulatory Commission
Contract No. NRC-02-88-005

Prepared by

G. Cragnolino and N. Sridhar

Center for Nuclear Waste Regulatory Analyses
San Antonio, Texas

April 1991

TABLE OF CONTENTS

TABLE OF CONTENTS (cont'd)

LIST OF FIGURES

Figure | Page

Figure Page

LIST OF TABLES

ABSTRACT

Literature on localized corrosion, both that which has been published in relation to high-level waste container materials and that in the general literature on similar materials, is reviewed in this report. Particular attention is paid to experimental techniques and the effects of environmental factors on localized corrosion. Since the required period of containment of radioactive wastes (i.e., 300 to 1000 years) is much larger than the test periods and there is no prior experience with these containers, experimental investigations must be combined with suitable models (both mechanistic and probabilistic) in order to predict the performance of container materials. This requires that the experiments be designed such that they yield either bounding parameters or parameters that can be used as inputs in models. The types of experiments that are suitable for this purpose are examined. Published experimental findings of both DOE- and NRC- sponsored programs for the candidate Fe-Cr-Ni alloys (304L and 316L stainless steels (SS) and alloy 825) and the copper-based alloys (CDA 102, CDA 613, and CDA 715) are examined in detail. In terms of short-term electrochemical tests on the effect of environmental variables, the main findings have been the detrimental effects of chloride, the beneficial effects of nitrate and nitrite, and the relative independence of the localized corrosion parameter on temperature at least for one alloy. The main limitations of the current experimental results seem to be: 1) inadequate characterization of the environments, 2) lack of independence of environmental factors assumed to be independent, and 3) the lack of correlation in some materials between electrochemical parameters and visual observation of localized corrosion. The effect of gamma radiation on localized corrosion has been reviewed. While some of the observed effects can be attributed to nascent H_2O_2, the irreversible effects observed point also to possible modification of surface films. Investigations of crevice corrosion in the HLW program have been limited to immersion tests of creviced samples for long periods of time. The need for better control of crevice geometry and especially for electrochemical tests of crevice corrosion which may yield bounding parameters, such as crevice corrosion repassivation potential, is pointed out.

1. INTRODUCTION

The NRC regulation 10 CFR 60.113 requires the waste package to provide substantially complete containment of radionuclides for a minimum period of 300-1000 years. Arising from this is the need for DOE to demonstrate, through proper selection, design, testing, and analyses, the long-term performance of waste packages. In order to evaluate DOE's resolution of these technical issues, NRC must develop an understanding of the important parameters that affect long-term performance of waste package materials and components, the limitations and suitability of various test methods used to demonstrate performance, and factors not addressed by DOE that may affect waste package performance. The Integrated Waste Package Experiments (IWPE) research program at CNWRA supports NRC in attaining this understanding. The current IWPE program plan is divided into six interconnected tasks:

Task 1: Corrosion
Task 2: Stress Corrosion Cracking
Task 3: Materials Stability
Task 4: Microbiologically Influenced Corrosion
Task 5: Other Degradation Modes
Task 6: Reporting

The present report is part of Task 1, being focused on reviewing the literature pertaining to localized corrosion of the classes of candidate container materials. Localized corrosion in this review refers only to pitting and crevice corrosion. Other modes of corrosion that can be considered to be localized, such as intergranular corrosion, dealloying, or microbiologically influenced corrosion, are not addressed in this report.

In an area abounding in literature reviews (Beavers, 1990c; Farmer, 1988a; Farmer 1988b), a question may be reasonably asked as to the need for yet another review. What does the present review offer that has not already been said in previous reviews? First, more experimental results have been published regarding localized corrosion since the previous reviews. Further, in examining the previous reviews, it was observed that scant attention was paid to topics relating to test methods and to the investigations outside the high-level waste area. For example, the topical report by Beavers and Thompson (Beavers, 1990) essentially reviewed only the DOE sponsored experimental research on localized corrosion pertinent to the tuff repository. The degradation mode survey by Farmer et al. (Farmer, 1988c) examined literature outside the high-level waste area, but did not adequately address the literature pertaining to the effects of environmental species other than chloride, pH, and temperature, nor did it survey critically various test techniques available to investigate localized corrosion. The present review addresses both these limitations.

The review is comprised of five sections:

1. General review of localized corrosion test methodology and parameters of importance
2. Localized corrosion of Fe-Cr-Ni-Mo alloys
3. Localized corrosion of Cu-based alloys
4. Recommendations and summary

This is one of two reviews planned under the IWPE Project, the second of which is scheduled for a later date. The current report does not address topics such as the effect of radiation on the

semiconductive surface films formed on a variety of candidate alloys, effect of surface chromium depletion, and localized corrosion of alternate container materials.

The sources of information include the published reports of DOE laboratories, various semi-annual reports and papers of NRC sponsored research at Cortest Columbus Technologies, (formerly Cortest Columbus, Inc.), published reports of research on high-level waste container corrosion from other countries, and open literature. In each of the section pertaining to a specific class of materials, a brief overview of their physical metallurgy is given.

2. A REVIEW OF LOCALIZED CORROSION TEST METHODOLOGIES AND PARAMETERS

2.1 PARAMETERS

A critical question in the design of high-level waste containers is the assessment of material performance over long periods of time. It is generally agreed that this can only be accomplished by a suitable combination of experimentation and modeling. While it is reasonable to assume that the best experiments are those that simulate the actual repository conditions as closely as possible, in reality the actual repository environmental conditions may never be known completely. Hence, the various possible components of the environment have to be examined and their individual and combined effects evaluated by suitable accelerated tests so that the components important to localized corrosion may be delineated. Even if all the components of an environment are known, there may be significant uncertainties in extrapolating short term data and, hence, prediction of actual performance must be bounded using suitable parameters. Only certain experiments have the possibility of yielding parameters that can be used in extrapolation and bounding models. For example, repassivation potential in a crevice corrosion experiment can be used as a bounding parameter, provided this potential is established as a time-independent parameter. In contrast, pitting potential is not a suitable bounding parameter since pit propagation or crevice corrosion can occur at potentials lower than this potential. What follows is a brief review of test techniques available to determine various parameters of interest in pitting and crevice corrosion.

Three electrochemical parameters are commonly used to characterize the material and environmental conditions leading to pitting: a) the open-circuit or corrosion potential (E_c or E_{corr}), b) the pitting potential (E_p or E_{up}), and c) the repassivation or protection potential (E_{rp} or E_{prot}). The corrosion potential is the potential attained by a metal as a result of the balance of anodic reactions, which include metal dissolution, and cathodic reactions, which include simultaneous reduction of several environmental species such as H^+, O_2, H_2O_2, Fe^{3+}, and NO_3^-. Since this is a mixed potential, it is determined by the heterogeneous electrochemical kinetics on the metallic surface of many oxidation and reduction reactions. The pitting and repassivation potentials, on the other hand, are critical potentials for initiation and arrest of pits, respectively, measured by polarizing the metal to anodic (more positive) potentials in environments which can induce pitting in the metal. In these measurements, reducible species, such as O_2 and H_2O_2, should be removed, if possible, so that the mixed potential set up by these species does not reduce the accessible anodic potential range. Thus, for a given alloy, the E_{corr} measured in an environment containing the anticipated redox species is compared to the E_p and E_{rp} measured in the same environment without the redox species.

As a first approximation, we consider that:

a) Nucleation and growth of pits occur if $E > E_p$

b) Arrest of growing pits occurs if $E < E_{rp}$

c) Growth of existing pits occurs if $E_p > E > E_{rp}$

It has been indicated that the difference between E_p and E_{rp} can be used as a measure of the crevice corrosion resistance of alloys (Wilde, 1974), though other experimental results (Manning, 1981) have not always shown this to be valid. E_p is usually determined by measuring the potential above which an appreciable and sustained increase in anodic current is observed. However, since increase in anodic

current can be a result of a variety of anodic processes including the onset of oxygen evolution, the electrochemical measurements must be followed by visual observation of the samples for pits or other forms of localized corrosion. In the absence of visual evidence of localized corrosion, the potential at which a significant increase in anodic current is observed is called a transpassive or break-down potential. Similarly, E_{rp} is measured as the potential below which the anodic current decreases to the passive current. If no visual evidence of localized corrosion is found, E_{rp} refers to the end-point of other transpassive anodic processes.

An alternative approach to characterize the resistance to pitting of an alloy in a given environment has been the use of a critical pitting temperature, CPT or T_p, which is defined as the temperature at which pitting is observed to initiate at any given potential. This approach was pioneered by Brigham (Brigham, 1973). He found that the pitting potential underwent a rapid decrease in a certain temperature range and, hence, the mid-point temperature of this transition region can be used to compare various alloys. The higher the critical pitting temperature, the more superior the alloy is in terms of its resistance to pitting. The same approach can also be used in nonelectrochemical tests where the samples are immersed in a solution containing a redox couple yielding a relatively high open-circuit potential (e.g., Fe^{3+}/Fe^{2+} in $FeCl_3$). In this case pitting is determined only by visual means. This has been a widely used approach by alloy manufacturers. It must be emphasized that T_p is dependent on the applied or redox potential and other environmental factors such as chloride concentration and pH.

Crevice corrosion can be characterized by the same type of parameters as pitting. Indeed, in many electrochemical pitting tests, crevice corrosion at the area of contact of the sample with the electrical connection is difficult to avoid. However, this crevice in the contact area has an ill-defined geometry. In order to perform a controlled crevice corrosion test, there are several additional factors that need to be considered. These are the crevice gap (tightness of the crevice), crevice depth or length, crevice area/open area ratio, crevice forming materials (e.g., metal to metal vs. metal to rock crevice), and crevice surface finish. Tsujikawa et al. (Tsujikawa, 1982, 1987, 1990; Okayama, 1987) have investigated the concepts of crevice corrosion initiation and repassivation potentials extensively. The crevice corrosion initiation potential, termed E_{crev}, is the potential at which a rapid and sustained anodic current is observed on a creviced sample. In analogy to pitting, the repassivation potential for crevice corrosion, termed E_{rcrev} is the potential at which the anodic current density decreases to 2 $\mu A/cm^2$ and remains at this level for a sustained period of time (ranging from 1 to 3 hours).

An alternative approach is the determination of the highest pH of a solution where no passivity is observed, termed depassivation pH or pH_d (Okayama, 1987). The significance of this parameter is related to the chemical changes occurring within the crevice leading up to the initiation of corrosion. Because of the limited transport of ionic species and hydrolysis of metallic ions within the restricted volume of the crevice, the pH in the crevice tends to decrease with time. Simultaneously, the chloride content inside the crevice increases with time due to transport of these ions from the outside environment in order to maintain charge balance. At a critical pH and chloride concentration that depend on the alloy, the passive film is no longer stable inside the crevice and crevice corrosion initiates. Hence, pH_d, can be used to characterize an alloy's resistance to initiation of crevice corrosion. The lower the pH_d, the superior the resistance to crevice corrosion. The measured value of pH_d has been shown to be relatively independent of chloride concentration from 0.05N to 2N and temperature from 25°C to 80°C (Okayama, 1987; Crolet, 1977). The dependence of pH_d on other environmental species within the crevice has not been established.

In similarity to pitting corrosion, temperature can also be used as a characteristic parameter for crevice corrosion (Brigham, 1974; Hibner, 1986). The critical crevice corrosion temperature, termed

CCT or T_c, is the temperature at which crevice corrosion is observed to initiate. The higher T_c is in an environment, the more superior the alloy is to crevice corrosion in that environment.

Other types of parameters that have been used for both pitting and crevice corrosion include initiation time (t_i), propagation rate (either in terms of current density or units of penetration rate, such as mm/year), depth of pitting or crevice corrosion (d), density of pitting or number of pits per unit area (N), and fraction of area affected by crevice corrosion. It must be emphasized that rates of corrosion calculated from overall weight-loss measurements can be highly misleading in localized corrosion except in cases where the degree of localized corrosion is quite high.

The electrochemical parameters discussed above are arrived at by using d.c (direct current) techniques. Some a.c. (alternating current) techniques have been attempted and can yield useful parameters to characterize initiation and propagation of pits. These parameters include the total impedance (Z_{tot}), total resistance (R_{tot}), capacitance (C), and charge transfer resistance (R_t). The advantages and limitations of a.c techniques will be discussed in Section 2.4.

2.2 PITTING CORROSION TEST METHODS

Various test techniques used to determine the pitting parameters have been described in several excellent reviews (Smialowska, 1986; Oldfield, 1987). It is not the intent here to review all these techniques exhaustively. The more common of these techniques will be discussed along with experimental factors that can influence the measured parameters.

In general, the techniques can be classified as electrochemical and nonelectrochemical techniques. The electrochemical techniques can be potentiostatic (controlled potential held constant over a given period of time), potentiodynamic (controlled potential that is scanned continuously), combinations of the two, galvanostatic (controlled current), galvanodynamic (controlled current that is scanned continuously or in a stepwise manner), and combinations of the two. The advantages and disadvantages of the controlled potential and current tests have been reviewed by Smialowska (Smialowska, 1986). The controlled potential tests have been used more widely than controlled current tests. Potentiodynamic tests have been used in many screening investigations of pitting corrosion and are part of the ASTM standard electrochemical tests (ASTM G-5 and G-61). The advantages of the potentiodynamic test is, of course, the ease of operation especially with the advent of computer controlled data acquisition systems. However, aside from experimental factors such as sample and solution preparation, many important factors relating to the electrochemical technique can affect the measured variables. These include: the starting potential, scan rate, maximum current density at which the scan is reversed, ohmic drops in the system, and sample crevice. Generally, for pitting studies, the potentiodynamic scan is started from the corrosion potential. This is also prescribed in the ASTM G-61 standard. A sample polarization curve resulting from this procedure is shown in Figure 1. In some experimental studies (Beavers, 1988a), the scan is started from cathodic potentials, typically 100 mV negative to the corrosion potential. The effect of this relatively small cathodic polarization on the resulting anodic behavior has not been established and is probably dependent on the material. Cathodic polarization can reduce the passive film on materials such as Fe, Cu, or Ni which are not strong passive-film formers, whereas, it may not have a significant effect on Cr-containing alloys which form passive films not easily reduced. As evidence of the effect of passive film growth, it has been shown that longer residence time in the passive region can result in an increase in pitting potentials (Lizlovs, 1968) and crevice corrosion temperature (Hibner, 1986) due to the growth of the passive film. The effect of potential scan rate on pitting potential has been studied in greater detail by many investigators (Smialowska, 1986), although the agreement is poor. Many argue that a rapid scan rate tends to increase the pitting potential because not enough time is provided for pits to nucleate at the lower potentials. However, some have argued that the high scan rate results in a lower residence time

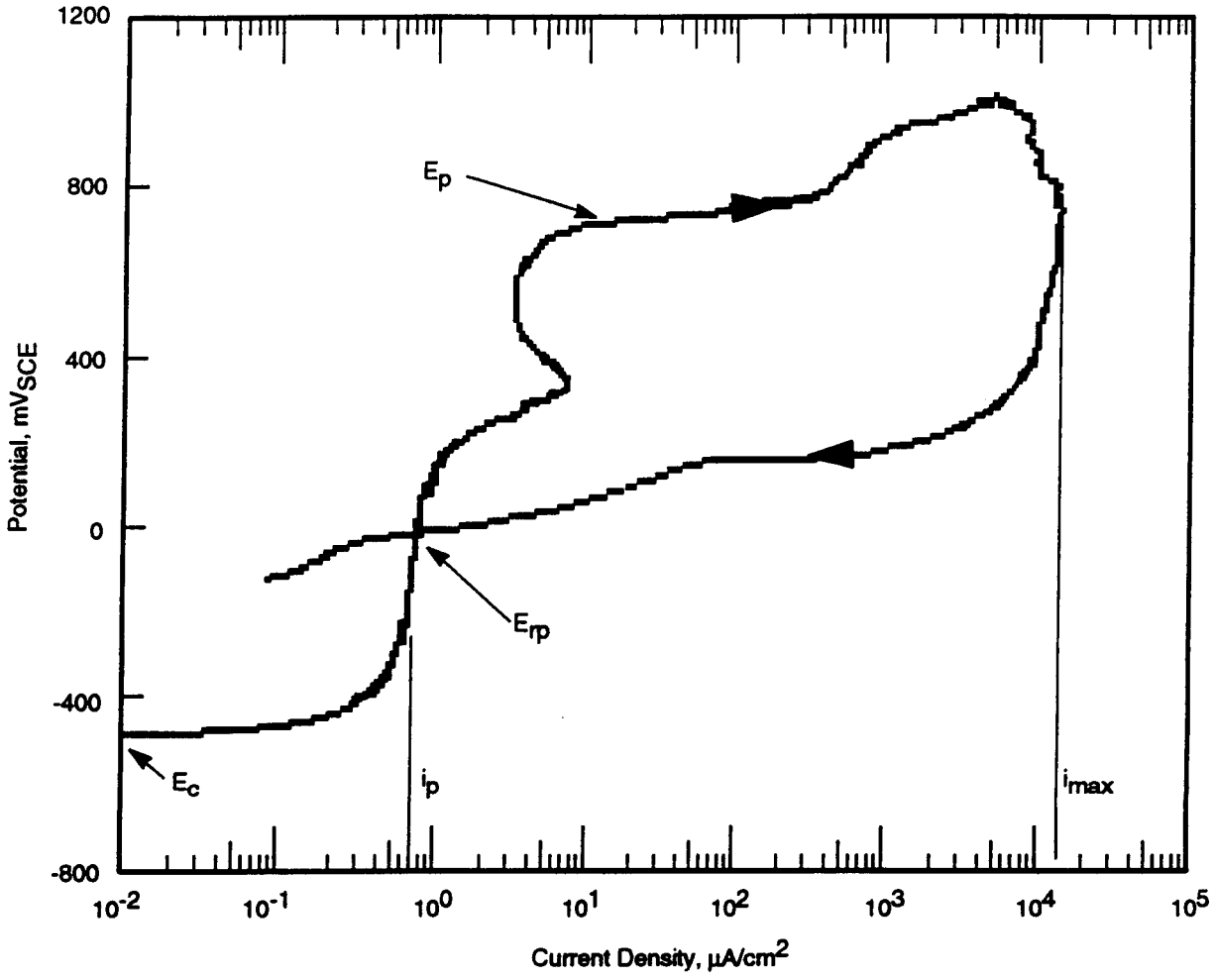

Figure 1. A typical cyclic polarization curve for alloy 825 in a Cl^- containing solution indicating various electrochemical parameters.

in the passive region thus resulting in thinner or imperfect films which are more susceptible to pitting at a lower potentials. Since, potentiostatic conditions (or very slowly changing potentiodynamic condition) represent the closest simulation of most real exposure conditions, a scan rate that is as slow as possible (approximating potentiostatic conditions) without increasing the test time unduly is usually preferred. The scan rate recommended by ASTM G-61 is 0.167 mV/sec and is close to the scan rate that is widely used. The maximum current density at which the scan is reversed controls the extent of pit growth and nucleation of new pits. It has been shown by Wilde (Wilde, 1974) in a low-Cr containing alloy that the higher the current density at which the scan is reversed, the lower the repassivation potential, E_{rp}. This is because the solution inside the pit becomes increasingly acidic and, hence, more difficult to repassivate. However, one may expect that a steady-state pH may be established after a certain pit depth and the repassivation potential may then become independent of pit growth. This has been shown by Newman and Franz (Newman, 1984) with carefully established pit growth conditions. Further studies are necessary to verify this.

Ohmic drops (also termed IR drops, where I is the total current and R the solution resistivity between the reference electrode and the sample) due to high solution resistivity and high currents can be a problem especially in dealing with relatively dilute environments such as J-13 water. The effects of ohmic drop on pitting potential measurements have been addressed by Mansfeld (Mansfeld, 1988). Generally, the pitting potential may appear to be higher because of the contribution of IR potential to the overall potential. In extreme cases, the transition to high current densities may become gradual and make pitting potential difficult to discern. Another problem with the use of high-resistivity solutions is the propensity for noise pick-up which can obscure the critical potential measurements. Ohmic drop can be mitigated by suitable design such as minimizing the current path and sample size (Hack, 1990). Compensation for ohmic drops can be performed on the resulting polarization curves by a variety of methods (Ehrhardt, 1990). The noise pick-up due to high-resistivity solution is also dependent on the electronic circuitry of the potentiostat, but can be minimized by using a high-concentration solution in the salt bridge of the reference electrode or by providing a high-conductivity path such as a platinum auxiliary wire to the reference electrode circuitry.

Potentiostatic tests are used commonly to measure incubation times, growth rates (by measurement of current density), and critical pitting temperature. Pit incubation (nucleation) time has been considered by many to be stochastic in nature. Shibata et al. (Shibata, 1977) used a multiple sample approach to measure the pitting potential distribution using a potentiodynamic technique as well as incubation times using a potentiostatic technique. They found a distribution of induction time which they modeled using a Markov-type process. Others have used potentiostatic techniques to measure current noise as pre-pitting events (Bertocci, 1986; Williams, 1985). Pit growth has also been modeled (Cottis, 1990) in a stochastic format using results from an immersion test in which the potential was maintained by Fe^{3+} redox reaction (10% $FeCl_3$, 50°C). Critical pitting temperature tests (Bernhardsson, 1983) have been performed by maintaining a constant potential and changing the temperature in a stepwise manner while monitoring the current. The temperature at which the current increased in a sustained manner beyond a preset value (usually 10uA/cm^2) is called the critical pitting temperature.

The nonelectrochemical pitting tests rely on either a known redox couple to provide a controlled potential (e.g., ferric chloride tests) or on simulating as closely as possible the actual exposure conditions (e.g., seawater tests). In the former case, pit initiation is usually measured by progressively increasing the solution temperature or by testing separate samples in solutions at different temperatures. The temperature at which pitting is observed in 50% of the samples is usually referred to as pitting temperature. In the latter case, both the pit initiation time and pit growth rate (density and depth) are measured.

2.3 CREVICE CORROSION TEST METHODS

Crevice corrosion tests are affected by the factors of crevice geometry in addition to the factors already mentioned for pitting tests. The tests are again electrochemical and nonelectrochemical in nature.

The electrochemical tests for crevice corrosion have been reviewed extensively (IJessling, 1980; Oldfield, 1987). Two types of electrochemical tests may be distinguished: 1) Mechanism or model oriented tests, and 2) Design parameter oriented tests. The purposes of the first type of tests are to determine the chemical changes that occur inside a crevice and to determine the critical chemical and electrochemical parameters that lead to crevice corrosion. An example of this type of tests is shown in Figure 2 (Efird, 1977). These tests may not use crevices or artificial cells to simulate an occluded region that has poor communication with the bulk solution, and do not completely reproduce the crevice geometry. The results of these tests may then be used as inputs in a mechanistic model which predicts failure time or some other measure of crevice corrosion resistance. On the other hand, the second type of tests is focused in measuring macroscopic parameters that can be used to measure and control crevice corrosion. These tests generally use crevices created by placing suitable mating surfaces against each other with reproducible geometry (crevice gap, length, etc.). Some examples of types of crevice assembly are shown in Figure 3.

The type of parameters measured in the second type of crevice corrosion tests are similar to those in pitting tests. For example, similar to the pitting and repassivation potentials, crevice initiation and repassivation potentials have been measured (Drugli, 1978; Tsujikawa, 1982). The advantage in crevice repassivation potential seems to be the relative independence of the potential to the extent of crevice corrosion (Tsujikawa, 1987a). This is illustrated in Figure 4. This then can form an important bounding condition for crevice corrosion. The crevice corrosion initiation and growth rate has also been measured (IJessling, 1980; Diegle, 1981) by coupling a completely creviced sample to an open sample through a zero resistance ammeter (ZRA). When the creviced sample starts corroding, its potential will be more active than that of the open sample and the resulting galvanic current can then be a measure of the crevice corrosion growth rate. Care must be taken, however, that the ZRA measurement indeed corresponds to crevice corrosion growth rate by periodic visual measurements of crevice corrosion depth.

Another type of measurement involves temperature as the critical parameter in similarity to critical pitting temperature (Nagaswami, 1983). A sample fitted with a suitable crevice device is held at a pre-determined potential for a short duration (typically 15 minutes) and the resulting current monitored. If the current does not increase to a preset limit, the temperature is increased by 5°C and the measurement repeated. The temperature at which the current increases beyond $1 A/m^2$ is regarded as the critical crevice corrosion temperature. The biggest difficulty of the critical temperature approach is how to relate it to prediction of actual performance. Other disadvantages of this technique include the short duration and the arbitrariness of the preset current limit of $1 A/m^2$. Crevice corrosion could have occurred at a much lower current and, hence, the experiment yields a nonconservative critical temperature.

The nonelectrochemical techniques are similar in nature to the nonelectrochemical pitting tests. Typically a standard crevice geometry is created by means of a nonmetallic crevice washer as described in ASTM G-46 and G-78. Some typical examples of crevices created by this method are shown in Figure 3. It must be noted that crevice corrosion is dependent on the type of crevice device. The tests can be used to arrive at a critical crevice temperature as described before for pitting tests or measure the initiation time and extent of crevice corrosion. The measurement of a critical crevice temperature by these immersion tests has the same limitations as mentioned before for crevice temperature measurement by electrochemical means. However, these measurements have been used widely to compare and rank

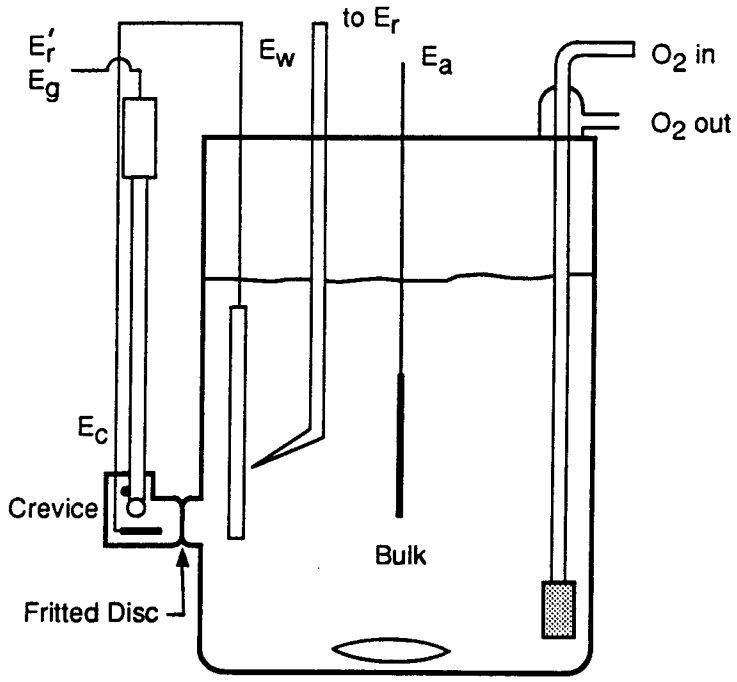

Figure 2. Crevice corrosion test cell used to generate mechanistic information on crevice corrosion. E_c = crevice sample, E_g = glass pH electrode, E_w = Boldly exposed sample, E_r = open reference electrode, E'_r = crevice reference electrode, and E_a = Pt counter electrode. (Efird, 1977).

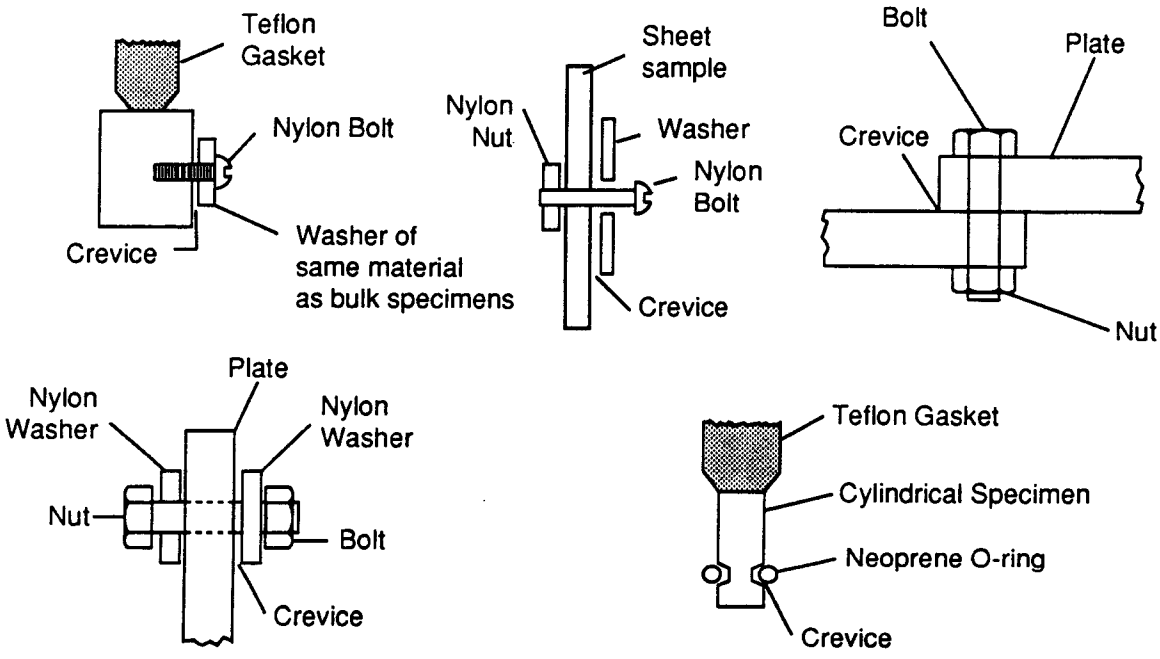

Figure 3. Schematic diagrams of various types of crevice assembly. (IJessling, 1980).

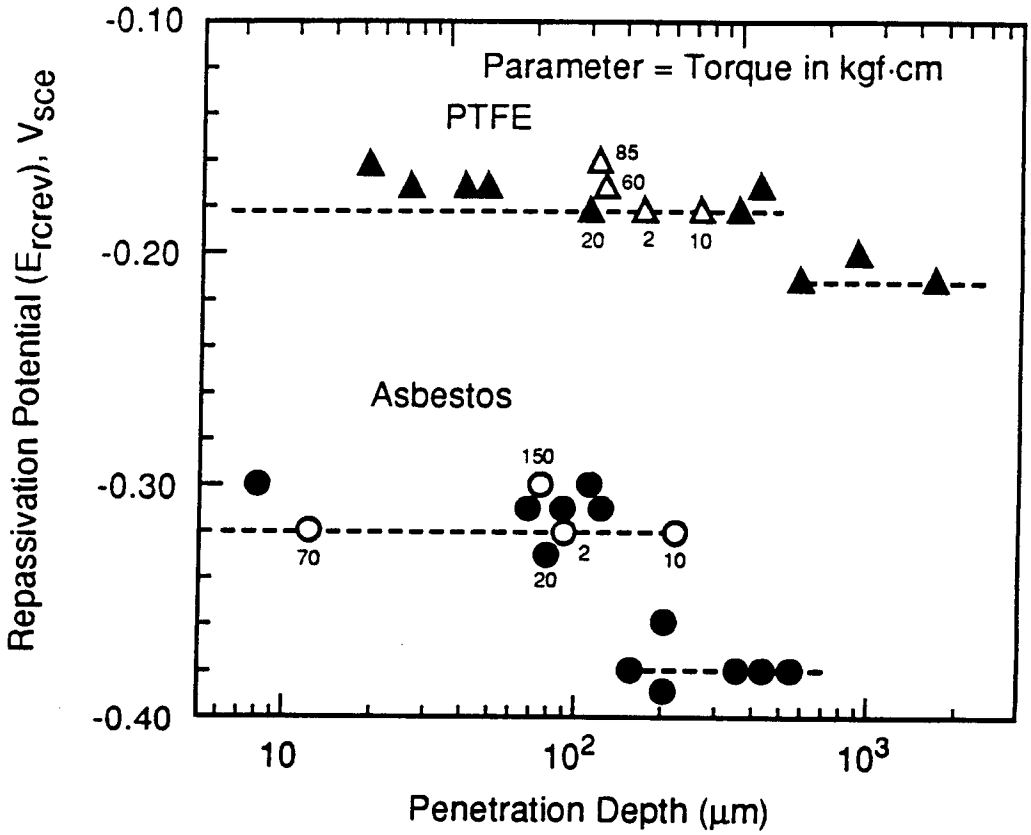

Figure 4. Repassivation potential vs. extent of previous crevice corrosion for two crevice devices. The numbers next to some points show crevice tightening torque in Kgf· cm. Test sample: Type 316 stainless steel. Solution: 3% NaCl. (Tsujikawa, 1982).

alloys in terms of their resistance to localized corrosion. Measurement of crevice initiation time, crevice corrosion depth and area have been made in many environments, most notably ambient sea water. Accurate measurement of initiation time is difficult in a nonelectrochemical test because of the time intervals involved between sample observations and because of the lack of sensitivity of visual observation compared to electrochemical measurements. However, measurements of depth of crevice corrosion and also the proportion of crevices corroded in a multiple crevice assembly have been made to characterize the performance of many alloys in sea water (Nagaswami, 1983), and in pollution control equipment (Silence, 1983).

2.4 A.C. IMPEDANCE TECHNIQUES

The advantage of the a.c technique over the d.c. technique is the ability to distinguish processes with various time constants by measuring the response of a system to cyclic applied potentials of various frequencies (Macdonald, 1987). The main disadvantage of the technique is the need for an appropriate mechanistic model or a electrical circuit analog that can be used to deconvolute the impedance data and account for the various processes. The difficulty in the latter approach is that the electrical analog selected may not be unique (many different circuits can result in the same impedance response) and assignment of circuit elements to various electrochemical processes may be difficult. Localized corrosion of aluminum alloys has been studied using a.c. impedance techniques (Shih, 1989; Scully, 1990). The equivalent circuit model they used is shown in Figure 5. It consists of parallel combination of RC circuits corresponding to reactions in pits and open surface. The R_{ox} and C_{ox} correspond to the charge transfer resistance through the passive film and capacitance associated with the passive film. The R_{pit} and C_{pit} are similarly associated with the pit, while the R_s corresponds to the solution resistivity. They showed that a decrease in the total charge transfer resistance occurs with exposure time which corresponded to an increase in pitting. Wang et al. (Wang, 1988) examined the pitting of AISI 304 stainless steels in various NaCl solutions using a.c. impedance. While they did not postulate any model for the pitting, they showed that the charge transfer resistance, R_t, decreased considerably when pitting occurred and the capacitance (which presumably was a combination of double layer capacitance and oxide capacitance) increased. In both cases, the transition between nonpitting and pitting conditions seemed to be continuous.

2.5 SELECTION OF SUITABLE TEST TECHNIQUES

A brief description was given of the types of test techniques available to characterize the localized corrosion behavior. It is well to remember that many of these accelerated laboratory tests predict the relative performance of a range of alloys or performance of a single alloy in a range of environments which is then compared to the field performance of the same alloys either in the same application or a closely similar application. In the case of the HLW container application, no such field experience exists and the time frames for performance requirement are much longer than normally encountered in engineering applications. Hence, given below are some criteria that need to be formulated to select the most appropriate accelerated test methods.

1) Bounding Parameters

The first question is whether the test technique can yield bounding parameters. For example, if E_{rcrev} can be shown to be independent of the extent of prior localized corrosion (Tsujikawa, 1990), then it can be used as a reasonably good bounding parameter. In this approach, if the redox (or mixed) potential (which is time dependent) of an environment is higher than the E_{rcrev}, it can cause crevice corrosion of a given alloy. Hence, this approach must be explored more fully. Critical pitting/crevice

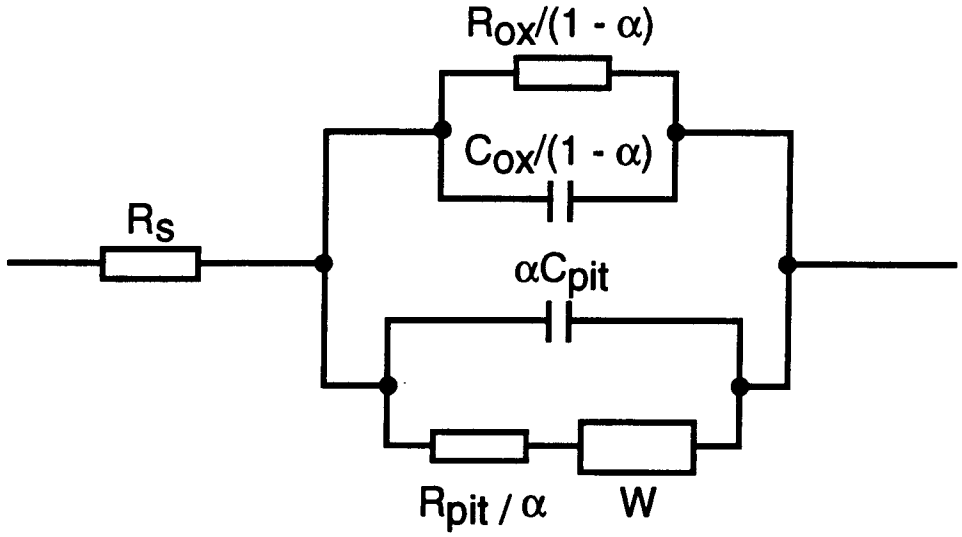

Figure 5. Equivalent circuit model for pitting corrosion of aluminum. (Scully, 1990).

corrosion temperature can also be used as a bounding parameter provided it can be shown that the environmental conditions (redox potential, chloride concentration, etc.) of the test environment are estimated conservatively.

2) *Time Extrapolation*

The second question is whether the test yields data that can be extrapolated to longer times. For example, measurements of initiation time, E_p, and critical temperatures cannot be extrapolated to longer times unless the test performed can be linked to a mechanistic model. Simply measuring the extent of corrosion on a sample immersed in an aggressive environment cannot yield information on its performance beyond the test period unless the test is designed such that the test parameters are similar to the parameters used in the model (model verification over a relatively short period of time) or the test can yield parameters that can be used as inputs to a model. Tests that measure pH_d, for example, fit into the latter category and may be worthy of further evaluation.

3) *Size Extrapolation*

Since the number of containers and the size of each container are expected to far exceed those of the test samples, the test results must be capable of being extrapolated in size scale. This has been done on the basis of extreme value statistical techniques in terms of areal density of pits/crevice corrosion and depth of attack (e.g., Laycock, 1990). However, many of the current experimental results using this type of technique have resorted to extremely aggressive environments where pitting initiation is guaranteed and only growth events are studied. Use of extreme value statistics on pit/crevice initiation is possible but has not been attempted. In the case of crevice corrosion growth, a more deterministic approach is possible by examining various crevice area/open area ratios. In both pitting and crevice corrosion, probabilistic extrapolation of initiation times to larger size scale needs to be explored.

3. LOCALIZED CORROSION OF Fe-Cr-Ni ALLOYS

3.1 HIGH-LEVEL WASTE RELATED LITERATURE

3.1.1 Electrochemical Experiments

3.1.1.1 DOE and LLNL Experimental Results

The nominal compositions of the various Fe-Cr-Ni alloys that are being considered either as candidate or as alternate alloys are shown in Table 1.

Two consecutive studies on localized corrosion of the candidate Fe-Cr-Ni alloys were conducted at the Lawrence Livermore National Laboratory (LLNL) using electrochemical techniques (McCright, 1984; Glass, 1984). The latter results have been summarized and included in a recent publication (McCright, 1987). In these studies, cyclic potentiodynamic polarization curves were obtained to determine the anodic behavior of AISI 304L and 316L SS and alloy 825 in tuff conditioned J-13 well water at temperatures ranging from 50 to 90°C.

It is known that water extracted from the J-13 well, located in the proximity of the proposed repository site at Yucca Mountain, has been used as the reference groundwater for experimental studies (Glassley, 1986), assuming that its composition is close to that of the vadose water in the unsaturated zone in the Topopah Spring tuff. However, it should be noted that the composition of J-13 well water reported by various authors varies. Only recently the range of concentrations found by different authors for all the species of interest has been reported (Glassley, 1990). As shown in Table 2, J-13 water is a neutral pH water in which the prevailing ionic species are HCO_3^- and Na^+. Other anions, such as Cl^-, F^-, SO_4^{2-} and NO_3^- are present at lower concentrations. It should be noted that the silicon content of the water, in the form of silicic acid, is relatively high. Waters from other wells in the vicinity of Yucca Mountain have similar chemical composition, but differences in pH and ion concentration ratios are considered to be significant (Murphy, 1989).

Although no complete experimental details are provided in the aforementioned publications, it is reported that water extracted from the J-13 well was conditioned by contact with crushed Topopah Spring tuff (2 mm average particle size). Whether the concentrations of anionic and cationic species in the water increased as a consequence of the interaction with the crushed tuff or remained constant, is not reported. It can be presumed, however, that the concentration should be extremely dependent on the mineralogical composition of the rock and the temperature and also, unless equilibrium conditions were rapidly established, on the duration of the conditioning process and the volume ratio of the rock to the water. At boiling temperatures (100°C), it has been shown (Abraham, 1986) that the concentration of several anions and cations, such as SO_4^{2-}, NO_3^-, Cl^-, Na^+, K^+ and Ca^{2+}, increases significantly with time when synthetic J-13 water was heated in the presence of crushed tuff, as shown in Figure 6.

The previous results may be not necessarily applicable to the conditions or the procedure adopted in the LLNL study, but it is apparent that the composition of the testing environment is by no means well defined. It should be noted, however, that Glassley has indicated (Glassley, 1986), after reviewing rock-water interaction experiments performed at LLNL, that no significant changes from the initial J-13 values were found for chloride, fluoride, nitrate and sulfate and only a slight decrease in the dissolved carbonate content was observed. The most significant compositional change was due to the dissolution of silicon from the tuff, accompanied by a decrease in

Table 1. NOMINAL CHEMICAL COMPOSITION IN WEIGHT PERCENT OF VARIOUS Fe-Cr-Ni ALLOYS OF INTEREST IN HIGH-LEVEL NUCLEAR WASTE DISPOSAL PROGRAMS

Alloy	UNS No.	C max	Cr	Cu	Fe	Mo	Ni	Ti	Others
304L SS	S30403	0.03	19	-	Bal.	-	10	-	Mn = 2 max. S = 0.03 max.
316L SS	S31603	0.03	17	-	Bal.	2.5	12	-	Mn = 2 max. S = 0.03 max.
825	NO8825	0.05	21.5	2	29	3	42	1	-
600	N06600	.08	16	-	8	-	75	-	-
800	N08800	0.1	21	-	44	-	32.5	0.38	-
G-3	N06985	0.015	22	2	19.5	7	44	-	0.8 max. nB
G-30	N06030	0.03	29.5	2	15	5.5	43	-	W = 2.5 Nb = 0.8
625	N06625	0.1	21.5	-	5 max	9	62	-	Nb = 4
C-276	N10276	0.01	15.5	-	5.5	16	57	-	W = 4
C-4	NO6455	0.01	16	-	3 max	15.5	65	-	Ti = 0.7 max
C-22	NO6022	0.015	22	-	3 max	13	56	-	W = 3
904L	N08904	0.02	21	1.5	Bal.	4.5	25	-	Mn = 2 max. S = 0.035 max.
Alloy 28	N08028	0.03	27	1	Bal.	3.5	31	-	-
254SMO	S31254	0.02	20	0.75	Bal.	6	18	-	N = 0.2

Table 2. CHEMICAL COMPOSITION RANGES OF J-13 WELL WATER (GLASSLEY, 1990)

Species	mMoles/liter	mg/liter
Li^+	0.006 - 0.024	0.04 - 0.17
Na^+	1.83 - 2.17	42 - 50
K^+	0.10 - 0.17	3.7 - 6.6
Mg^{2+}	0.07 - 0.10	1.7 - 2.5
Ca^{2+}	0.29 - 0.37	11.5 - 15
Sr^{2+}	0.0002 - 0.001	0.02 - 0.1
Fe^{3+}	<0.0002 - 0.003	<0.01 - 0.16
Al^{3+}	0.0003 - 0.004	0.008 - 0.11
$Si(SiO_2)$	0.95 - 1.14	26.6 - 31.9
NO_3^-	0.113 - 0.168	6.8 - 10.1
F^-	0.029 - 0.135	1.7 - 2.7
Cl^-	0.178 - 0.237	6.3 - 8.4
HCO_3^-	1.93 - 2.34	118 - 143
SO_4^{2-}	0.18 - 0.22	17 - 21
pH	6.8 - 8.3	

the concentration of magnesium and calcium in the water as a result of the precipitation of insoluble salts. Confronted with this discrepancy, we have assumed for the purpose of the following discussion that at least the initial composition of the solution in the electrochemical experiments corresponds approximately to that given in Table 2 for J-13 water. The solutions were saturated with air at the testing temperature, but no provisions were made to bubble air or other gases, such as CO_2, through the solution. It can be expected that the concentration of HCO_3^- and the pH during the electrochemical experiments are not the same as those reported in Table 2, as a result of the release of CO_2 from the solution at temperatures above room temperature.

All three alloys, namely AISI 304L SS, AISI 316L SS, and alloy 825, were tested in the mill-annealed condition. Specimens of each alloy were mechanically polished with 400 grit SiC paper. A potential sweep rate of 1 mV/s was used in the polarization scans. A typical polarization curve for AISI 304L SS in J-13 water at 90°C is shown in Figure 7 (Glass, 1984). Although pitting (E_p) and repassivation (E_{rp}) potentials are indicated on the anodic curve, in the absence of any reported visual observation of localized corrosion it is most probable that the potential at which an abrupt increase of current occurred in the forward potential scan is associated with oxygen evolution and not with passivity breakdown. The minor hysteresis noted in the reverse scan may be due to surface modifications which enhance the rate of oxygen evolution rather than the result of pit growth as expected when pit initiation takes place in the forward scan.

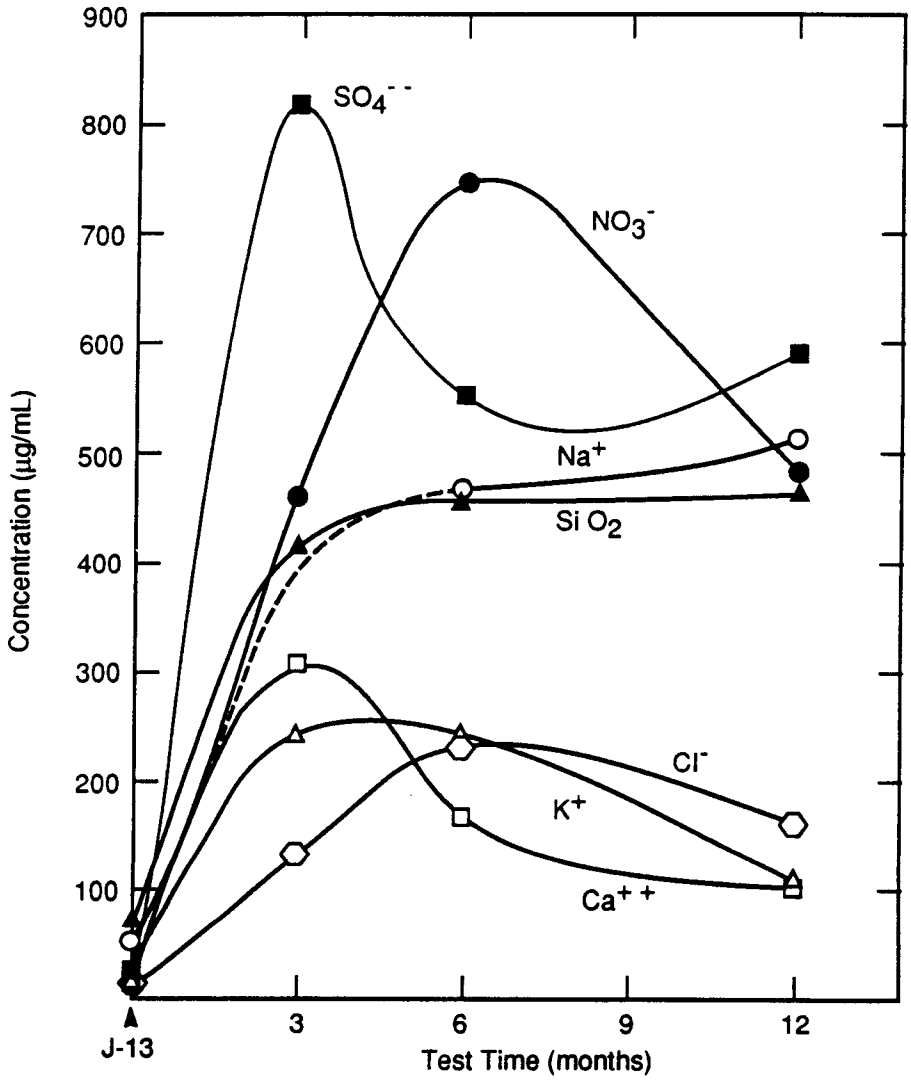

Figure 6. Concentration changes in J-13 water during reaction with crushed tuff and stainless steel corrosion samples at 100°C. (Abraham, 1986).

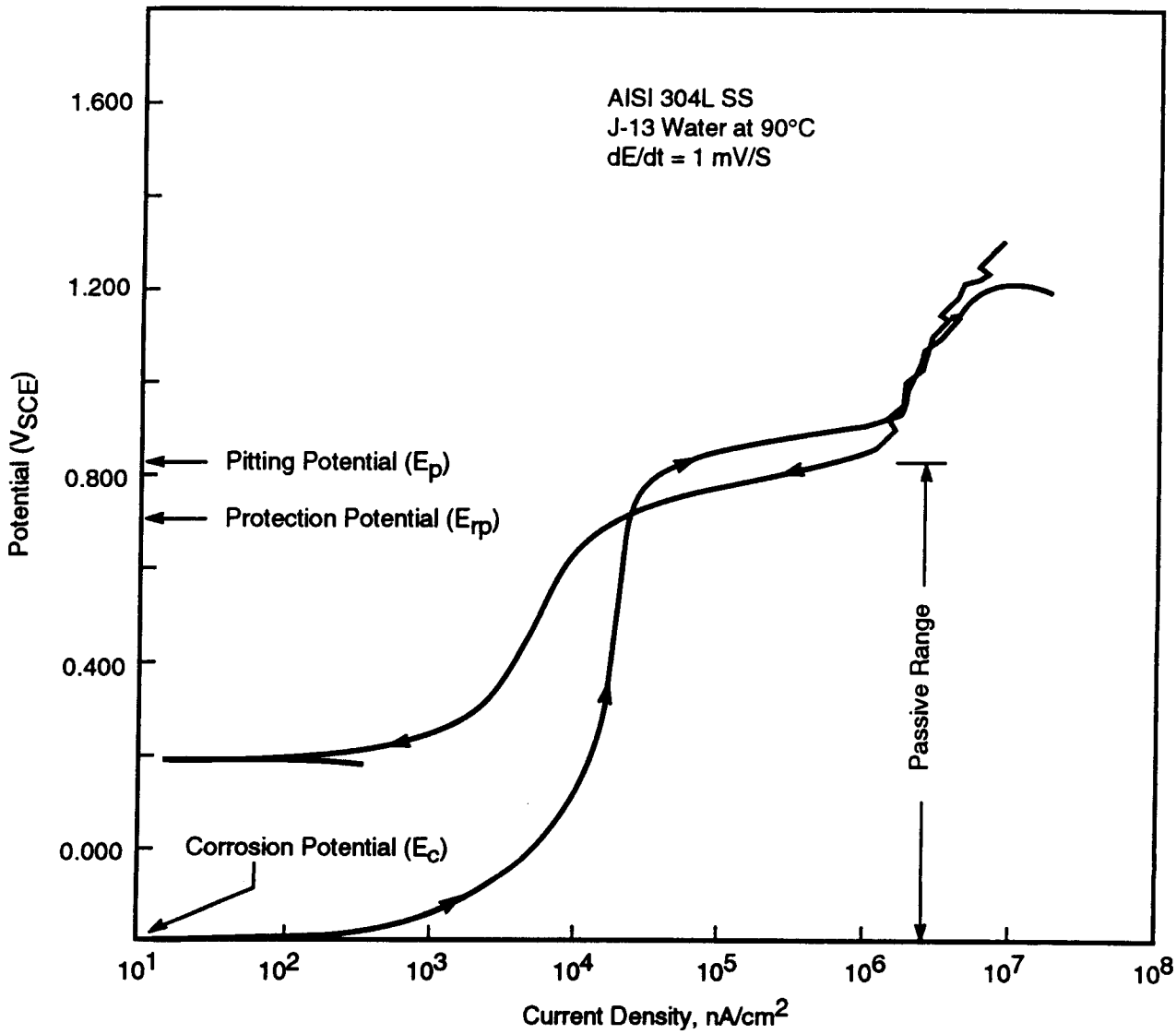

Figure 7. Cyclic polarization curve for type 304L stainless steel in J-13 water at 90°C. Scan rate = 1mV/sec. Note that without observation of localized corrosion E_p and E_{rp} relate to oxygen evolution, not pitting. (Glass, 1984).

Plots of corrosion (E_c), pitting (E_p), and repassivation (E_{rp}) potentials as a function of temperature are shown in Figures 8, 9 and 10 for AISI 304L SS, AISI 316L SS, and alloy 825, respectively, according to the data provided in the original publications (McCright, 1984; Glass, 1984). It is clearly seen that the three alloys exhibited relatively high pitting potentials (above 800 mV_{SCE}) which are almost independent of temperature, suggesting, as noted above, that the so called pitting potentials are those potentials at which the oxygen evolution reaction occurred. Clearly, different repassivation potentials were measured in both studies. In the first work (McCright, 1984) the repassivation potentials were significantly lower than those measured in the latter study, as clearly noticeable in Figures 8, 9 and 10. For 304L and 316L SS, the differences are greater than 400 mV at all the temperatures studied. Since pitting potentials were not reported in the initial study, it is not possible to offer an explanation for such discrepancy. In the second study (Glass, 1984; McCright, 1987), the repassivation potentials were found to be almost identical to the pitting potentials in the case of AISI 304L SS, but approximately 100 mV lower for the other alloys. No explanation can be offered for this observation either. Precisely the opposite behavior should be expected if pit initiation was involved, because 304L SS usually exhibits the lowest pitting potential of the three alloys in chloride-containing solutions and, as a consequence, a lower repassivation potential would be predicted for the least resistant alloy. In addition, a very slight dependence of the repassivation potentials with temperature was noted for the three alloys within the 50 to 90°C range. All these observations confirm that the breakdown observed in the potential-current density curves at high anodic potentials was the result of oxygen evolution as a consequence of water oxidation and it cannot be attributed to pit initiation. It should be noted that no visual observation of the metal surfaces after the polarization tests are reported in these publications.

As shown in Figures 8, 9 and 10, corrosion potentials ranging from -200 to -100 mV_{SCE} were measured on the three alloys in air saturated J-13 well water. A remarkable coincidence in the values reported in the two studies can be observed in these figures. Also, the slight influence of temperature and alloy composition on the corrosion potential should be noted.

Of the three candidate Fe-Cr-Ni alloys, AISI 304L SS was the single material in which the effect of higher chloride concentrations was studied (Glass, 1984). A significant decrease in the pitting potential (E_p) was observed when NaCl at concentrations higher than 25 ppm was added to tuff-conditioned J-13 well water (which already had about 6 ppm chloride) at 90°C. For example, by increasing the added NaCl concentration from 25 to 50 ppm the pitting potential decreased from 730 to 220 mV_{SCE}. At even higher concentrations (10000 and 30000 ppm) E_p decreased to values which were very close to the corrosion potential (-100 to -200 mV_{SCE}), confirming the occurrence of pitting corrosion at high chloride concentrations. Their results are replotted in Figure 11, where the pitting and corrosion potentials are given as a function of the total chloride concentration instead of in terms of the added NaCl concentration as reported in the original publication. Following an abrupt decrease from potentials at which the oxygen evolution reaction occurs, the variation of E_p with the decimal logarithm of the Cl^- concentration appears to become linear at concentrations above 600 ppm exhibiting a slope of approximately 80 mV per decade, similar to that observed by other authors for AISI 304 SS (Smialowska, 1986). As shown also in Figure 11, no clear dependence of the corrosion potential with Cl^- concentration was observed, except at high concentrations. At low concentrations the values of the corrosion potential exhibited a rather erratic variation.

As noted above and illustrated in Figure 12, no significant effect of temperature on E_p of AISI 304L SS was observed (Glass, 1984) within the 50 to 90°C range at the low chloride concentrations ($\simeq$ 7 ppm) corresponding to J-13 water. This is due to the fact that no pitting occurred at these low chloride concentrations in the cyclic polarization tests. However, it is rather

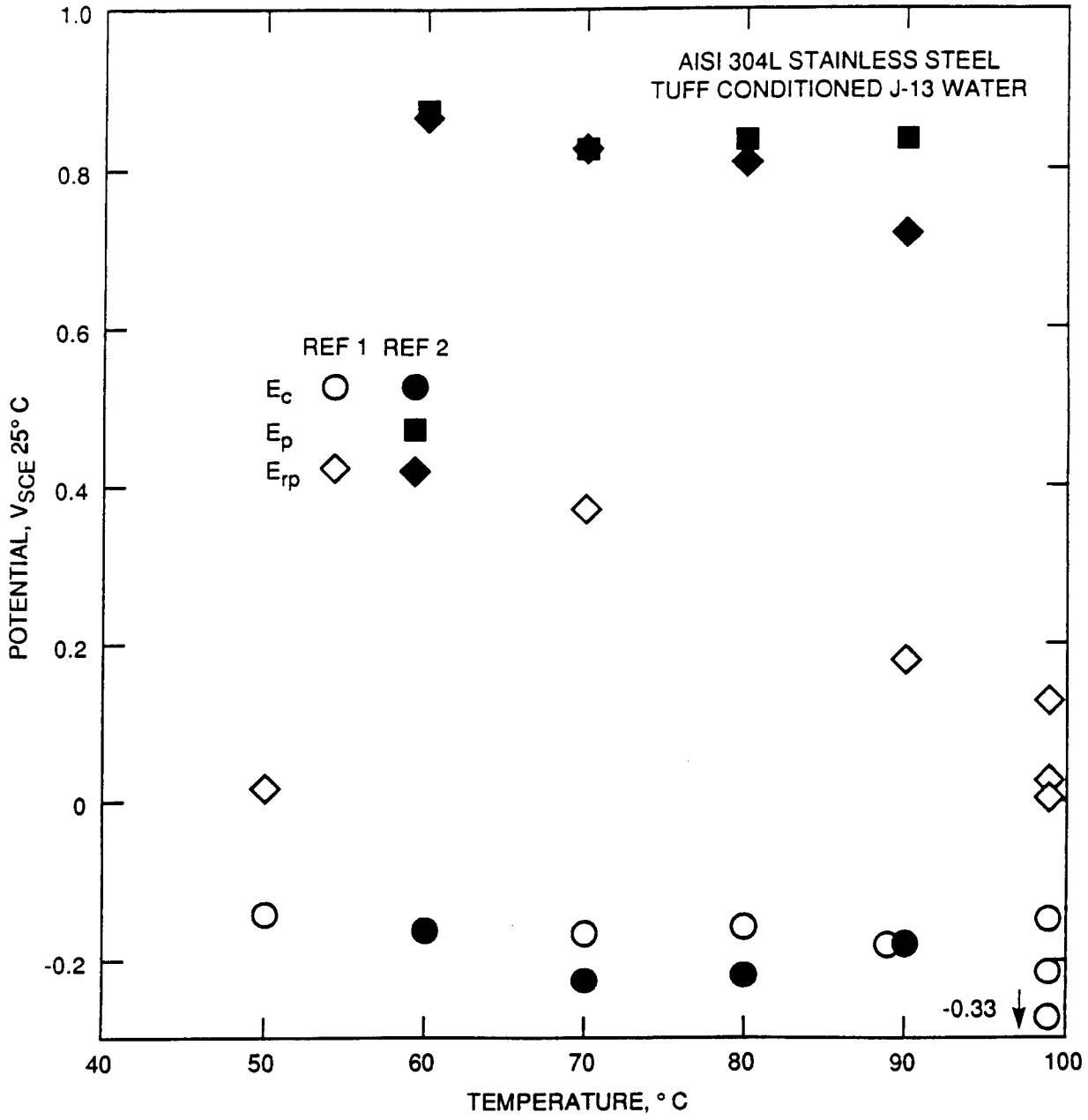

Figure 8. Compendium of data from cyclic polarization curves on type 304L stainless steel in tuff conditioned J-13 water conducted by LLNL. Reference 1: McCright, 1984; Reference 2: Glass, 1984.

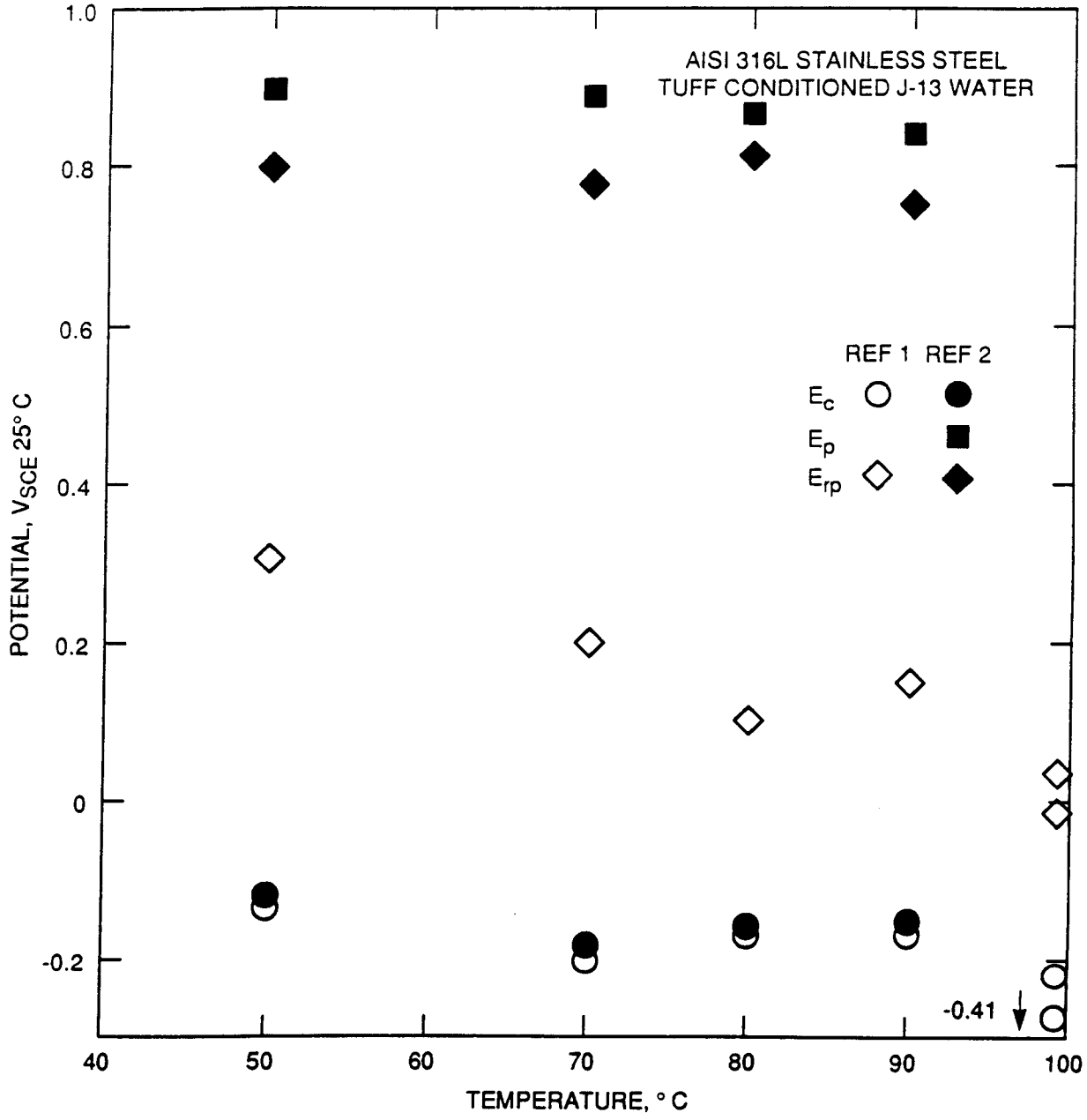

Figure 9. Compendium of data from cyclic polarization curves on type 316L stainless steel in tuff conditioned J-13 water conducted by LLNL. Reference 1: McCright, 1984; Reference 2: Glass, 1984.

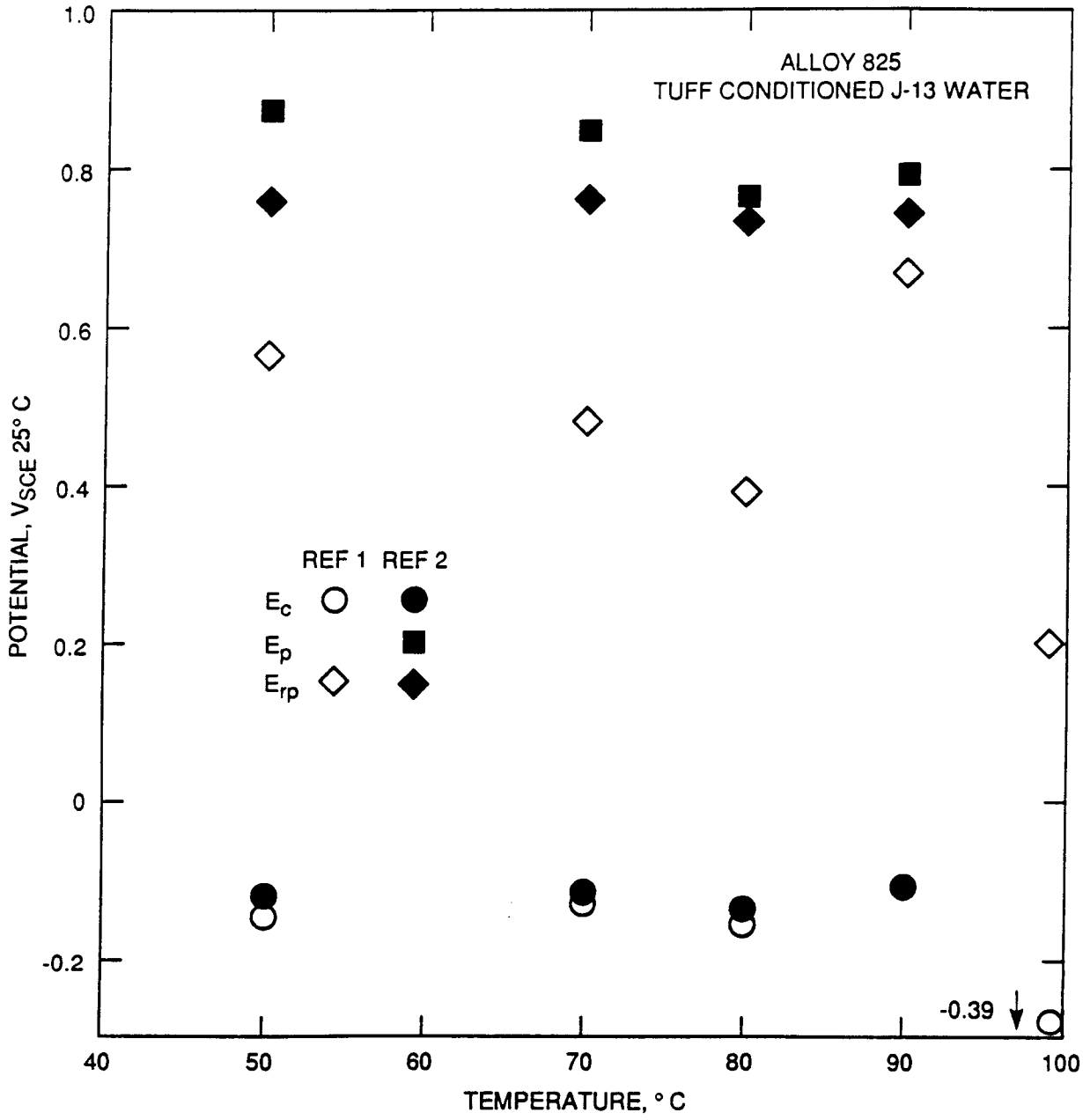

Figure 10. Compendium of data from cyclic polarization curves on alloy 825 in tuff conditioned J-13 water conducted by LLNL. Reference 1: McCright, 1984; Reference 2: Glass, 1984.

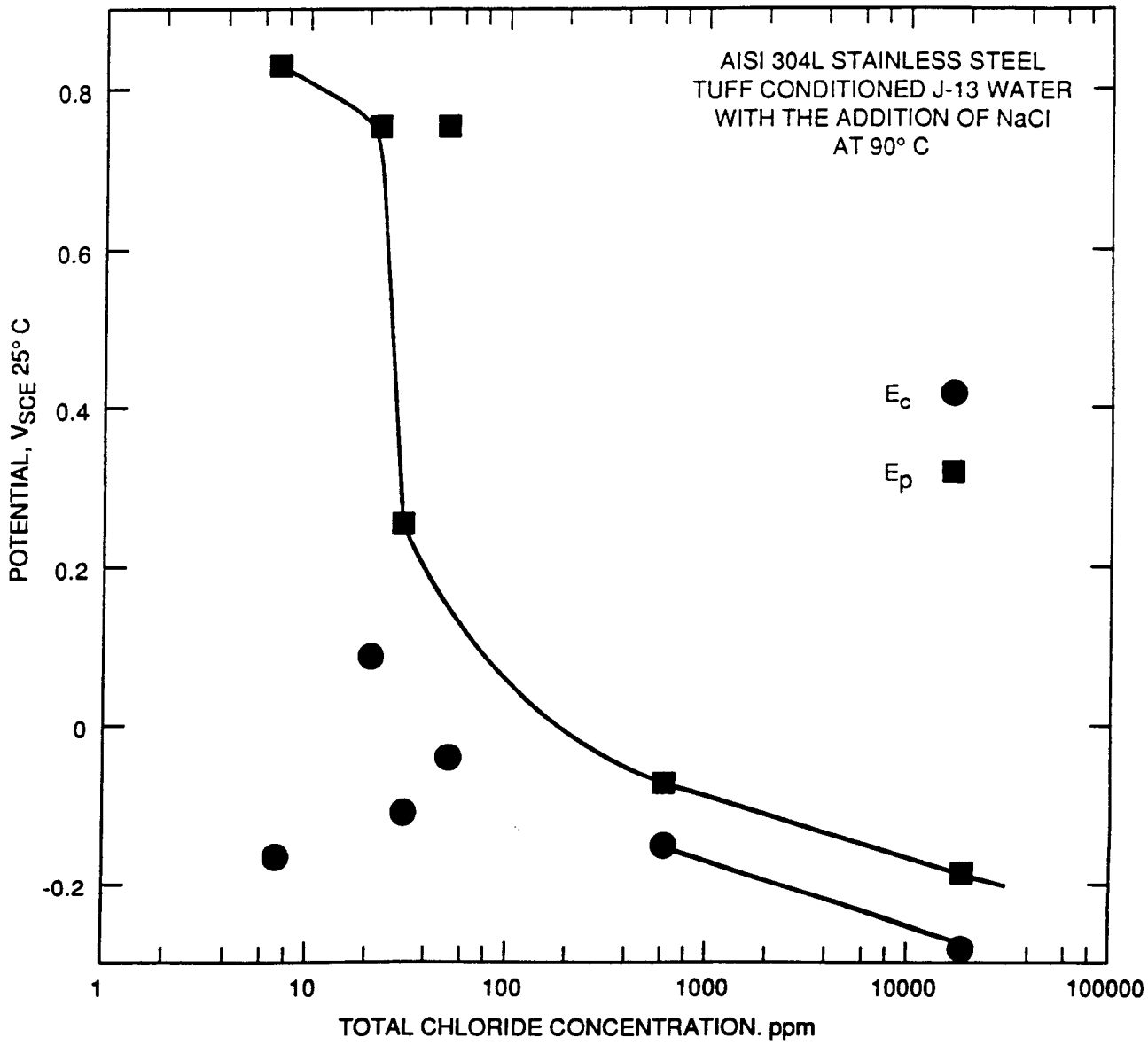

Figure 11. Pitting and corrosion potentials vs. total chloride content in tuff conditioned J-13 water for type 304L stainless steel. Scan rate = 1 mV/sec. (data taken from Glass, 1984)

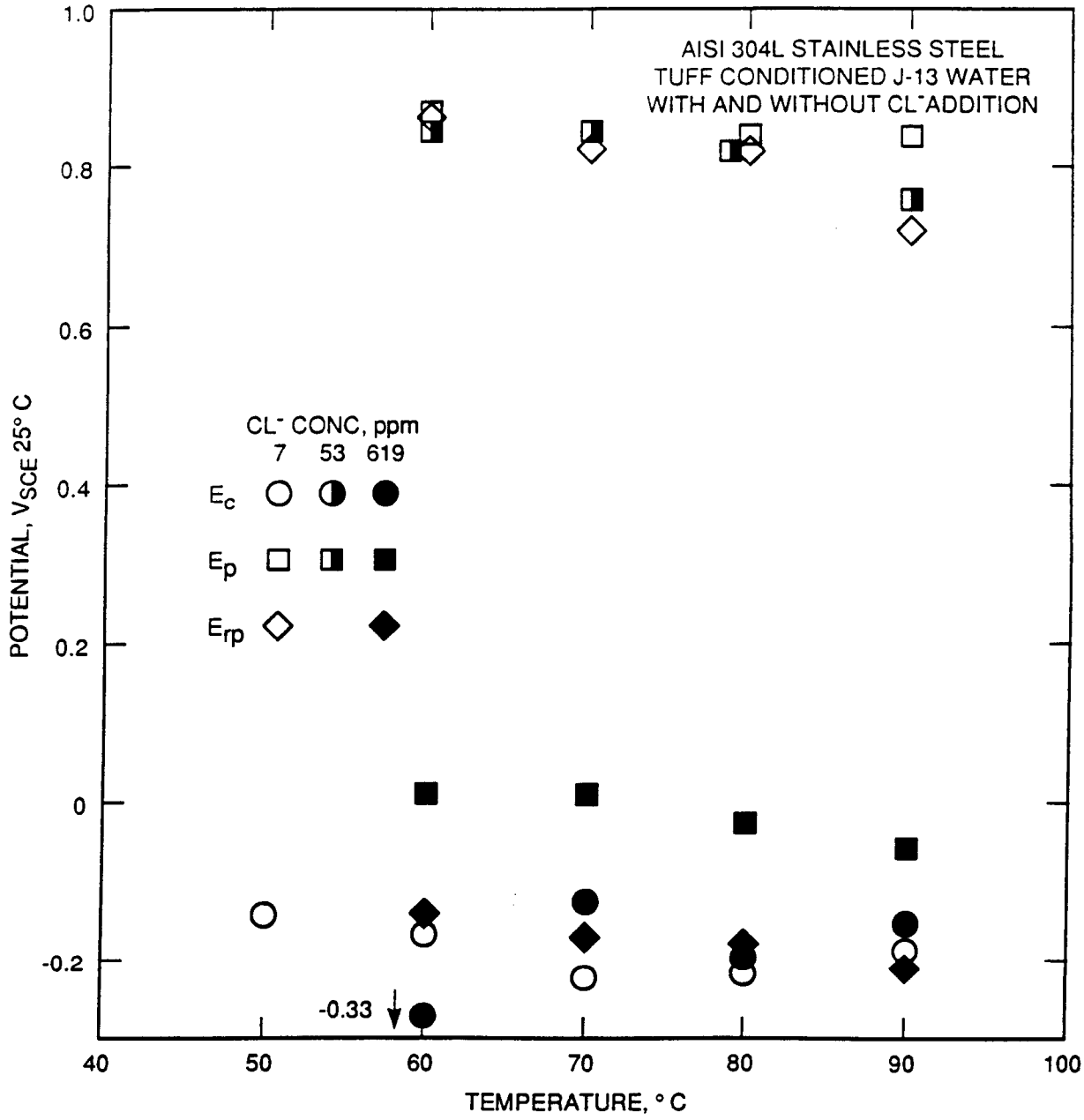

Figure 12. Temperature vs. localized corrosion parameters measured from cyclic polarization curves. (data taken from Glass, 1984)

surprising that even in the presence of 619 ppm Cl^- (1000 ppm NaCl) a relatively small effect of temperature is observed. This is in contrast with the relatively strong dependence of the pitting potential on temperature (at least 5 mV/°C) observed for many metals and alloys in the 25 to 150°C range (Smialowska, 1986; Brigham, 1973). These diverse observations may be understood by considering the pitting potential vs. temperature curve described by Brigham and Tozer (Brigham, 1973). At low chloride concentrations, the alloy/solution system is in the upper plateau region of the E_p vs. temperature curve, conditions under which the electrochemical behavior is dominated by the evolution of oxygen from the solution or eventually the oxidation of chromium to CrO_4^{2-}. Within the temperature range of 50 to 90°C, the repassivation potential (E_{rp}) decreased from -140 to -220 mV_{SCE} with increasing temperature in the solution containing 619 ppm Cl^- (Glass, 1984). The corrosion potentials were found to be very close to the E_{rp} values at temperatures equal to and greater than 70°C, indicating the possible occurrence of localized corrosion at these temperatures in a naturally aerated solution. No visual observation of pitting corrosion was reported, but it is apparent that in J-13 well water containing NaCl at concentrations greater than 50 ppm pitting corrosion occurred in the electrochemical tests as indicated by the measurement of relatively low pitting potentials. As noted above, no data were reported for the other candidate alloys at chloride concentrations higher than that present in J-13 well water.

A limited number of relevant experiments have been conducted for the candidate Fe-Cr-Ni-Mo alloys. As described, most of the work has been confined to a specific solution which by no means covers the variations in groundwater chemistry that may exist in the repository environment. Only in the case of AISI 304L SS was the effect of higher chloride concentrations studied. As expected, localized corrosion occurred at Cl^- concentrations above 25 ppm at relatively low anodic potentials, suggesting that any alteration of the water chemistry brought about by the presence of increasing chloride concentrations may be extremely detrimental for this alloy. This is in agreement with the available information in the open literature (Smialowska, 1986). However, the specific conditions of the tuff repository environment in terms of other ionic species have not been studied sufficiently. It should be emphasized that an adequate and complete characterization of the tuff repository environment, and in particular its evolution with time taking into consideration the combined effects of radiation and heat, does not exist. An appropriate description, in terms of water chemistry, pH, E_h, trapped and dissolved gases among other variables, is not yet available (Murphy, 1989).

In later works, the influence of a gamma-radiation field on the localized corrosion of AISI 316L SS was evaluated (Glass, 1985; Glass, 1986). A cylindrical array of Co-60 sources was used and a dose rate of 3.3 $\pm$ 0.7 Mrad/h was obtained in the electrochemical cell. The experiments were performed at 30°C using as electrolyte J-13 well water and in some cases more concentrated forms (10X and 100X) of the same water.

One of the important observations in this work is shown in Figure 13. It is seen that the corrosion potential of AISI 316L SS in aerated 10X concentrated J-13 water increased by almost 200 mV in the presence of gamma-radiation. When the electrochemical cell was removed from the radiation field, the potential decreased approximately 50 mV. Two additional cycles of exposure to and removal of the radiation field (on-off) indicated that steady-state conditions were attained. It should be noted that in the "off" condition the potential did not recover the low value measured before irradiation. The increase in the potential upon irradiation was attributed to the generation of oxidizing species in the solution. In particular, a concentration of H_2O_2 of approximately 0.14 mM was measured after 3.5 hours of exposure at the dose rate mentioned above.

The authors concluded that the potential increase was the result of the generation of H_2O_2 as a consequence of radiolysis of water in the presence of air (or oxygen) dissolved in water. This was essentially confirmed in a separate experiment conducted in the absence of irradiation

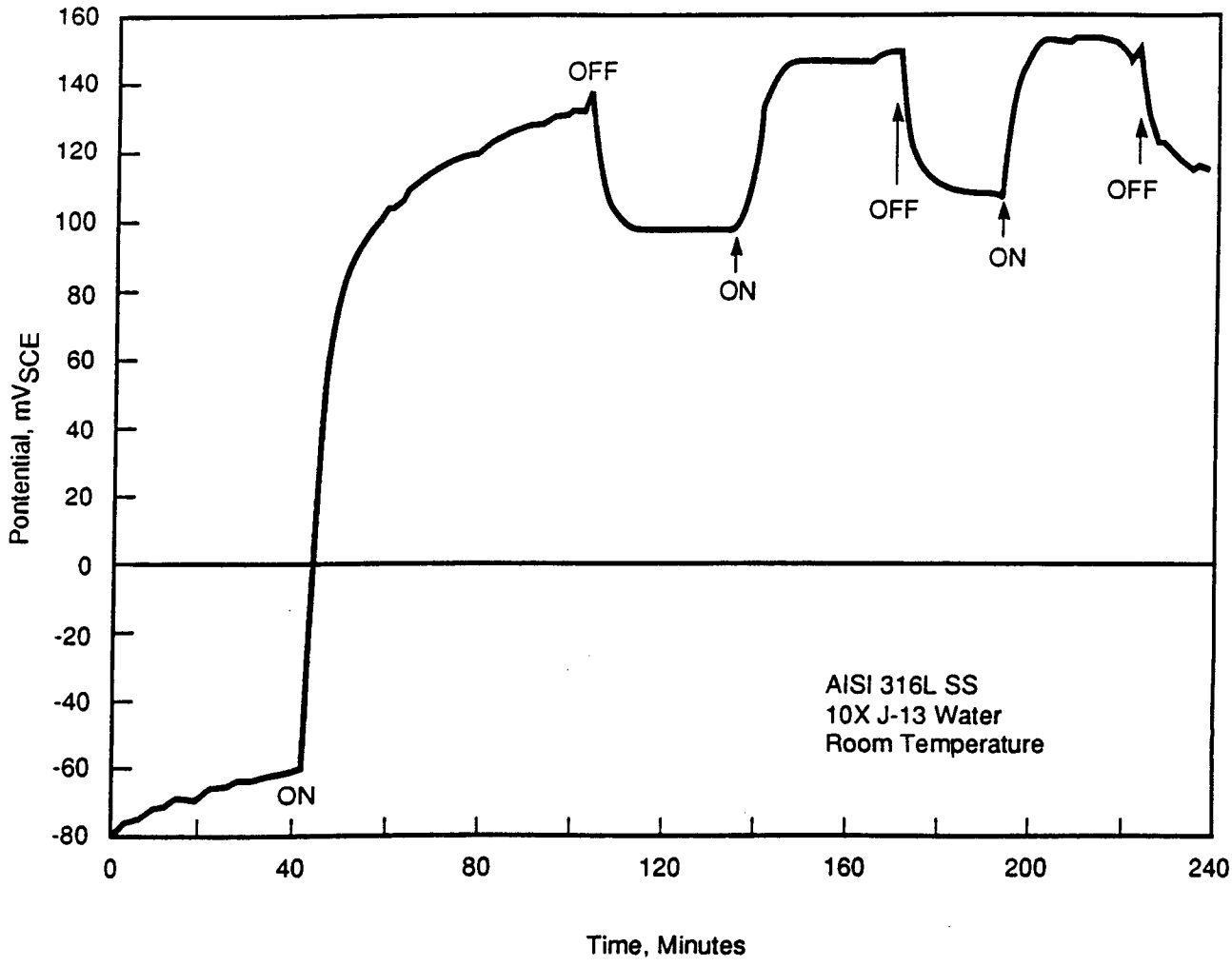

Figure 13. Corrosion potential changes with exposure to gamma radiation for type 316L stainless steel in 10X concentrated J-13 water. No prior exposure to radiation. (Glass, 1985).

in which the addition of H_2O_2 to the solution produced a potential increase almost equivalent to that found in the presence of gamma radiation. They also suggested that other species, i.e., unstable radicals such as OH, may have also contributed to the potential increase but their effect, due to the short half-life of these free-radicals, is difficult to demonstrate.

It should be noted, however, that in a separate experiment in which irradiated J-13 was replaced by fresh water (without irradiation) the corrosion potential did not drop to the low values measured before irradiation, as shown in Figure 14. The result of this experiment seems to indicate that an irreversible change occurred in the metal surface, presumably in the passive film. It is possible that bound water in the passive film, known to be present in this range of potentials in Fe-Cr-Ni alloys, underwent radiolysis and this process had an impact in the corrosion potential. Other changes in the semiconductive properties of passive films have been associated to the effect of radiation, but instead of gamma radiation, as a result of the action of alpha or beta particles (Elfenthal, 1989). Localized states can be created close to the conduction band in n-type semiconductor oxides or even in insulators. Nevertheless, the variation of the corrosion potential cannot be attributed to the metal anodic process because in the passive range the current density usually exhibits a very slight dependence on potential. Most of the significant changes in potential should, therefore, be related to the cathodic reaction (essentially, the partial anodic and cathodic electron transfer reactions of the oxidizing species). It is possible that the alteration of the passive film electronic conductivity by the action of gamma radiation may have affected the kinetics of the cathodic reactions.

Results from anodic polarization curves for AISI 316L SS in chloride-containing solutions (0.018 M NaCl corresponding to 650 ppm Cl^-) indicate that the pitting potential remained essentially unchanged by gamma radiation (Glass, 1986). On the other hand, the corrosion potential was found to be displaced by approximately 200 mV in the anodic direction. The authors claimed that even though this is a significant reduction in the difference between pitting and corrosion potential as a result of irradiation, the potential shift is not enough to induce pitting in the material. It should be emphasized, however, that this criterion is not adequate because localized corrosion may occur at potentials lower than the pitting potential as determined in the potentiodynamic tests. As a mater of fact, in experiments in which the repassivation potential was also measured, it was found that under irradiation this potential is lower than the corrosion potential measured in the same conditions, as shown in Figure 15 (Glass, 1985; McCright, 1987). These results suggest that at least for AISI 316L, and also for AISI 304L which exhibits lower pitting and repassivation potentials in chloride-containing groundwater, gamma radiation may induce localized corrosion by increasing the corrosion potentials to values at which crevice corrosion may be easily initiated or existing pits may grow without being repassivated.

3.1.1.2 Cortest Columbus Experimental Results

The experimental work conducted by Cortest Columbus Technologies under NRC sponsorship has been published in six reports (Beavers, 1988a, 1988b, 1989a, 1989b, 1990a, 1990b). In addition to these reports, Cortest prepared a review of the literature relevant to the tuff repository (Beavers, 1990c). The initial experimental results from this project have also been published in the Proceedings of a Conference (Beavers, 1990d).

The literature review by Beavers and Thompson covers the influence of environmental variables on the corrosion behavior of the candidate container materials for the Yucca Mountain Project. The review is a good summary of the literature available for the specific case of the tuff repository and contains updated information on the more common forms of localized corrosion and stress corrosion cracking (SCC) for the austenitic Fe-Cr-Ni alloys and Cu-base alloys. The effects of heat

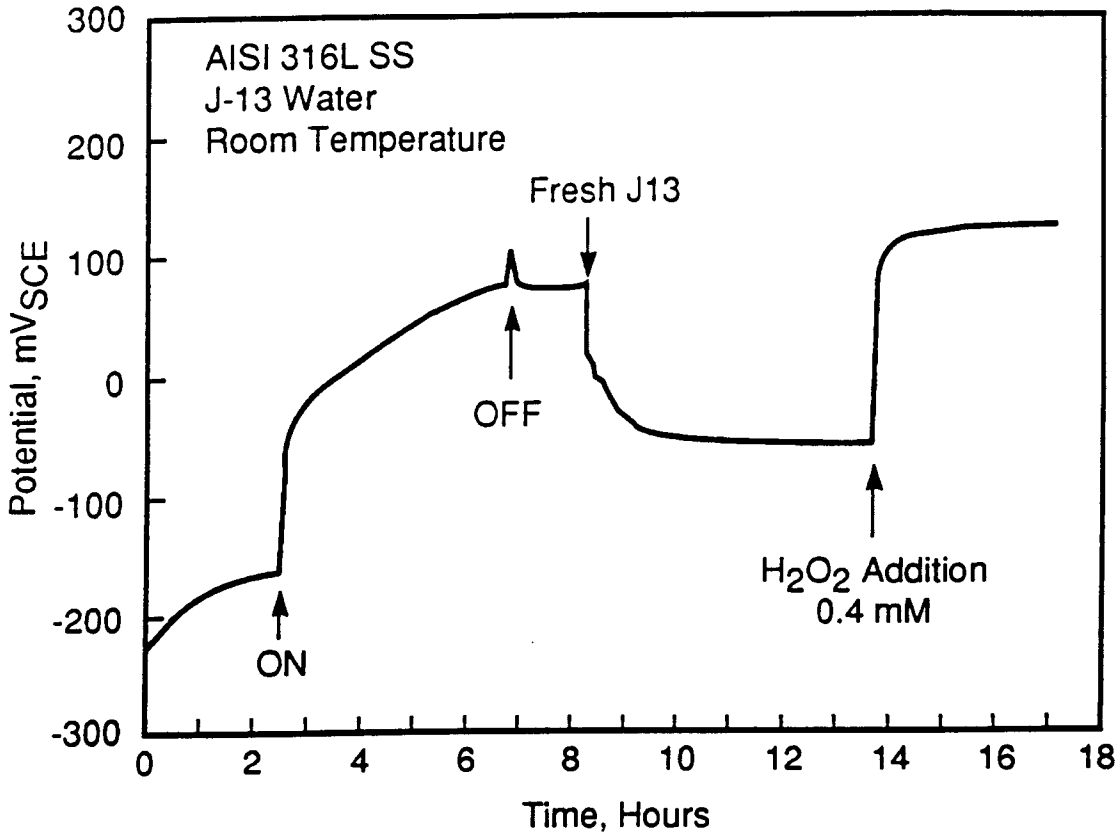

Figure 14. Corrosion potential changes with gamma radiation for type 316L stainless steel. Solution was changed after the first "off" cycle and H_2O_2 was added to the new solution. (Glass, 1986).

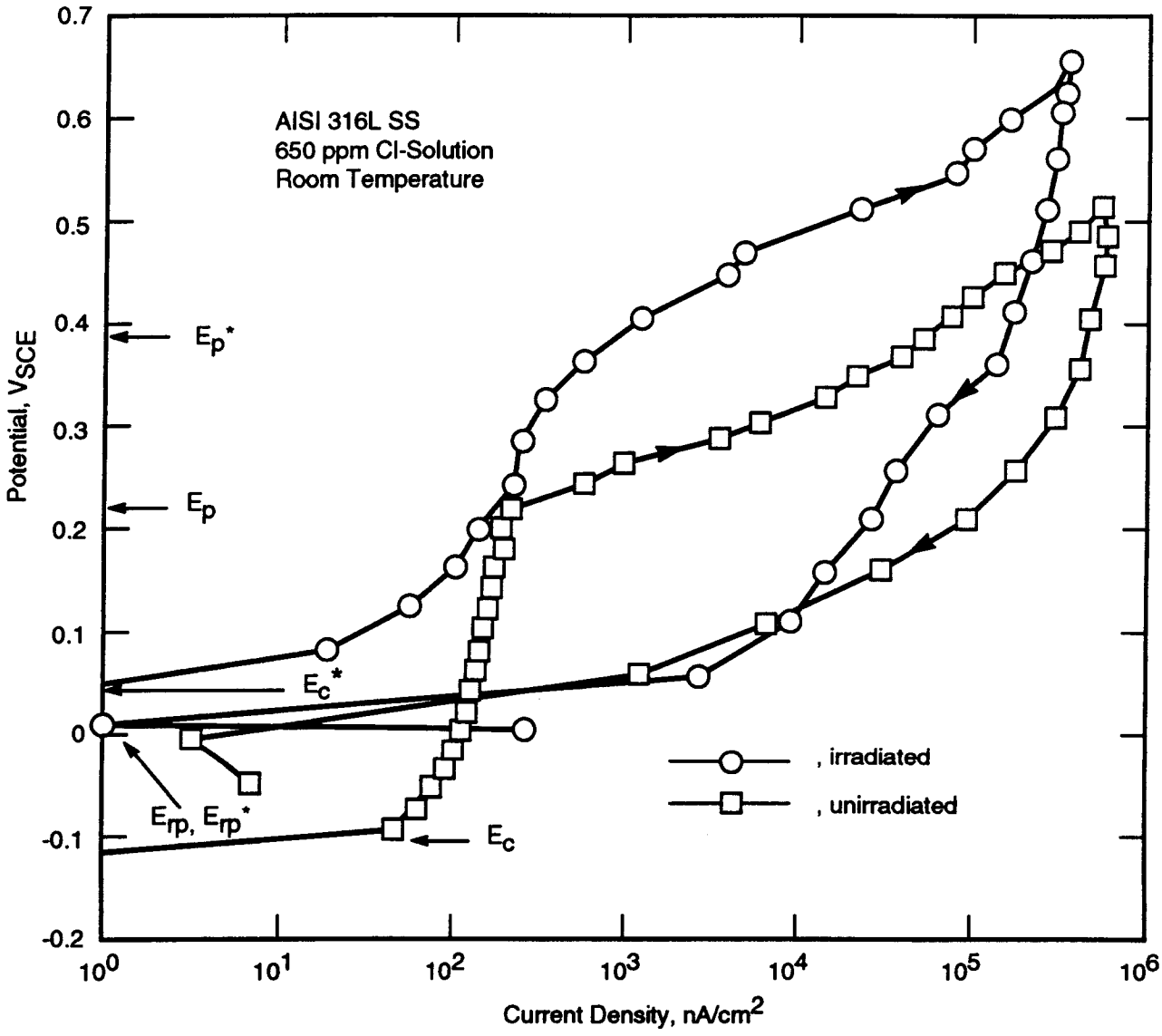

Figure 15. Effect of gamma radiation on cyclic polarization behavior of type 316L stainless steel in J-13 water with 650 ppm Cl$^-$. E^*_p, E^*_{rp}, E^*_c = irradiated condition. (Glass, 1985).

decay and radiation on corrosion are included, as well as a brief discussion of the possible impact of microbiologically influenced corrosion on the performance of the container alloys. However, it would be highly desirable to have a critical assessment of other possible metal/environment failure modes, even though some of them may not be anticipated with current experience. The review contains an initial section on the tuff repository environment, in which a good discussion of the available information is presented, as well as the possible impact of thermal, radiational and microbiological effects. However, as noted above, an adequate and complete characterization of the environment and its eventual evolution with time does not exist.

The purpose of the Cortest experimental work on cyclic potentiodynamic polarization was to examine the effects of environmental and metallurgical variables on the electrochemical behavior of candidate container materials. Two of the three Fe-Cr-Ni alloys initially selected by LLNL were used by Cortest. They are: AISI 304L SS and alloy 825. In Appendix C of the first report in the Cortest's series (Beavers, 1988a), the laboratory procedure adopted for conducting cyclic potentiodynamic polarization curves was described, as well as the procedure used for the preparation of a simulated tuff groundwater with a chemical composition similar to that of J-13 well water. Polarization curves were obtained by using a forward potential scanning at a scan rate of 0.167 mV/s from a cathodic potential towards anodic potentials, followed by a reverse scanning when the current density reached $1x10^{-3}$ A/cm2. Using this method the pitting potential and the repassivation potential as well the corrosion, passivation (maximum current), and passive currents were determined. Apparently, the corrosion potential was measured initially, before the potential scan was started and after the specimen was exposed to the solution overnight.

In an initial set of cyclic polarization curves, the anodic behavior of AISI 304L and alloy 825 were determined at 90°C under naturally aerated conditions in simulated J-13 water and in the same water with the addition of 1000 ppm Cl^- (Beavers, 1989a). The behavior of both alloys was almost identical in J-13 water, in which the Cl^- content is approximately 6 ppm. No hysteresis loop was observed in the cyclic polarization curves, which exhibited a "break-off" potential of about 700 to 800 mV_{SCE}, and examination of the specimens after testing indicated no pitting or other forms of localized corrosion. On the other hand, both alloys exhibited a pronounced hysteresis loop in J-13 water containing 1000 ppm Cl^- and extensive pitting corrosion was observed on the specimen surfaces after testing. A pitting potential of approximately 160 mV_{SCE} and a repassivation potential of -160 mV_{SCE} were measured on AISI 304L SS, whereas, the values for alloy 825 were 700 and 160 mV_{SCE}, respectively. Since the corrosion potential measured on AISI 304L was approximately -250 mV_{SCE}, it was concluded that this value is sufficiently close to the repassivation potential to consider the behavior of the alloy marginal in an environment similar to J-13 water, but with a high chloride content. Pitting corrosion was considered to be unlikely in the case of alloy 825, since the range for pit growth (160 to 700 mV_{SCE}) was found to be 600 to 700 mV more positive than the free corrosion potential. However, it should be noted that the value reported (-480 mV_{SCE}) seems to be abnormally low for an air-saturated solution. Nevertheless, from the results reported in this work it is apparent that alloy 825 is significantly more resistant to localized corrosion than AISI 304L SS. These results are also in agreement with the conclusions of other recent work on alloy 825 in which the effect of chloride concentrations in J-13 water has been examined systematically (Sridhar, 1990; Cragnolino, 1991).

A second aspect of the approach adopted by Cortest is the use of a fractional factorial experimental matrix for the evaluation of the effect of many environmental variables including pH and temperature. This methodology was previously used for corrosion studies of various alloy/environment systems encountered in different industrial applications in which several dissolved species were known to affect the resistance to localized corrosion (Koch, 1988). It was also used to study the corrosion behavior of carbon steels in high temperature groundwater for high-level waste packaging

within the scope of the Basalt Waste Isolation Project (Thompson, 1990). The valuable aspect of this approach is the attempt to identify the role of the different anionic and cationic species that may accelerate or inhibit localized corrosion. However, the success of the approach depends heavily on the criteria used in the selection of the independent and dependent variables. Fifteen variables were chosen by selecting the concentration of thirteen different species in addition to pH and temperature. Nine of these species ($HSiO_3^-$, HCO_3^-, F^-, Cl^-, NO_3^-, Ca^{2+}, Mg^{2+}, Al^{3+} and PO_4^{3-}) are present in J-13 well water; three species (NO_2^-, H_2O_2 and oxalic acid) are considered to be formed by radiolysis, and the remaining one (O_2) is present in the unsaturated zone from air and also can be formed by radiolysis of water.

Several problems arise from this particular selection of species and concentration values studied. They are as follows:

1) The concentration of HCO_3^- is dependent on pH. This means, for example, that for an initial concentration of HCO_3^- equal to 2000 mg/l or 32 mmoles/l the actual concentration will be significantly lower at pH 5 than at pH 10. At the lowest pH, HCO_3^- has been mostly transformed to CO_2 which has evolved from the solution. Therefore, the effect of HCO_3^- concentration on the dependent parameters cannot be assessed independently of the effect of pH, unless the partial pressure of CO_2 is controlled.

2) The concentrations of Si and Al in solution are dependent on the concentration of F^-, which acts as a complexing agent. In the case of Al, which is added to the solution as a cation [in the form of $Al_2(SO_4^{2-})_3 \cdot 16H_2O$], the stable complex is AlF_6^-. The formation of this complex reduces the concentration of Al^{3+} well below the initial concentration, mainly when the F^- concentration is 200 mg/l, equivalent to 10.5 mmoles/l, and represents a concentration that is more than 10 times higher than the highest Al^{+3} concentration used in the test matrix [20 mg/l or 0.74 mmoles/l]. Si is added in the form of $SiO_2 \cdot xH_2O$, but it can be easily converted to SiF_6^-. This is particularly true at the lowest concentration included in the test matrix, which is 0.035 mmoles/l. Even at the highest initial concentration, 3.5 mmoles/l, the concentration of noncomplexed Si is significantly reduced, making invalid the adoption of the initial concentration as representative of the particular environment. An additional aspect to consider is the low solubility of $SiO_2 \cdot xH_2O$, coupled with its slow rate of dissolution, which implies that in the high concentration condition (100 mg/l) a significant proportion did not dissolve.

3) Several species were included in the test matrix because they may be generated in the repository environment as a result of radiolysis. These species are NO_2^-, H_2O_2, $H_2C_2O_4$ (oxalic acid) and also O_2, although O_2 was also included as a consequence of the aerobic nature of the repository. The reasons for the inclusion of oxalic acid in favor of other organic species is not clear. Although it can be argued that in the repository the presence of organic compounds can be expected, by no means can it be assumed that oxalic acid is the prevailing species. Acetic acid is stable up to 300°C, while oxalic

decomposes above 150 to 170°C. The additional fact that oxalic acid is a good complexing agent for iron may complicate even further the interpretation of the results.

4) Regarding the reducible/oxidizable species, such as NO_2^-, NO_3^-, H_2O_2 and O_2, it should be noted that these species interfere with the measurement of the true anodic behavior of the material because the current associated with their reduction or oxidation cannot be distinguished from that corresponding to metal dissolution or passivation. The ideal situation is to remove all the electrochemically active species that may participate in charge transfer reactions at the metal surface (i.e., species such as oxygen and H_2O_2) and study the anodic behavior of such a surface by applying controlled potentials. The role of the radiolytically generated species should be studied under open-circuit conditions to interpret their effect on the redox potential of the environment and the corrosion potential of the metal. The role of anionic species which are able to act as reducible species as well as inhibitors, such as nitrate and nitrite, can be studied using potentiodynamic/potentiostatic methods. At neutral or slightly alkaline pH, the kinetics of their reduction is sufficiently slow and, as a consequence, they do not interfere with the anodic response of the metallic electrode. Under such conditions, their behavior as inhibitors tend to predominate.

From the statistical analysis of the data, conducted with the Statistical Analysis System program (SAS Institute, Cary, NC), the magnitude of the beneficial and detrimental effect of the environmental variables on the different electrochemical parameters was assessed in quantitative terms, according to the following general expression for the regression equations:

$$Y = A_o + \sum_{j=1} A_j X_j$$

where Y is the electrochemical parameter, A_o is the intercept, A_j is the coefficient for the jth environmental variable and X_j is the value of the variable j.

The regression coefficients for the fifteen environmental variables were calculated for each dependent variable (E_c, E_p, E_{rp} and i_c), based on a 80% confidence level. This means that it is accepted a 20% probability that a given variable does not have an effect. The data has been presented in a bar-chart format, as shown in Figures 16 and 17 for AISI 304L SS. The value of E or i for each environmental variable is the product of its coefficient and the range of the variable, in terms of concentration, °C or pH units. It was found, as shown in Figure 16, that for AISI 304L SS, chloride promotes a significant decrease of pitting and repassivation potentials, whereas, nitrate increases the value of both parameters. No other variable was found to have an effect on the repassivation potential. The pitting potential increases with pH and HCO_3^- and decreases with temperature. However, as noted above, pH and HCO_3^- are not independent variables. Nevertheless, all these observations are in qualitative agreement with the expected behavior of AISI 304 stainless steel on the basis of experimental results in less complex environments (Smialowska, 1986; Sedriks, 1979). From a quantitative point of view the

correlations are relatively poor, since the adjusted R^2 values for E_p and E_{rp} were found to be 0.32 and 0.55, respectively.

For alloy 825, the results are not easily explainable, since no anion including chloride was found to have a detrimental effect on pitting potential (Figure 18). In contrast, F^- exhibited a beneficial effect by increasing that potential. Both Mg^{2+} and H_2O_2 decrease E_p and E_{rp}. E_{rp} also decreases with pH and chloride concentration, and increases with NO_3^- and oxalic acid. From a quantitative point of view the correlations are also relatively poor for alloy 825, since the adjusted R^2 values for E_p and E_{rp} were found to be 0.19 and 0.47, respectively. As recognized by the authors (Beavers, 1990d), the very low R^2 value for E_p seems to reflect the fact that the potentials measured in this case are not true pitting potentials but potentials corresponding to the oxidation of water to oxygen in agreement with the relatively high E_p values.

The corrosion potential is the third parameter of interest to evaluate the tendency to localized corrosion of a given alloy in a particular environment. If the corrosion potential (E_c) is higher than the pitting potential, the alloy is susceptible to pitting corrosion and if it is lower than the pitting potential but higher than the repassivation potential propagation of localized corrosion (crevice and/or pitting corrosion) may occur. For AISI 304L, as shown in Figure 17, it was found (Beavers, 1990a) that H_2O_2, Ca^{2+}, and pH increase the corrosion potential, whereas, Si, HCO_3^-, F^-, Cl^-, Al^{3+}, O_2 and temperature decreased it. Although the effect of H_2O_2 is understandable as an oxidizing species, the observation that O_2 has the opposite effect is puzzling. In the case of alloy 825, the results seem to be more consistent with previous observations since pH, H_2O_2 and O_2 increase the corrosion potential and HCO_3^-, F^- and temperature decrease it. Also, the adjusted R^2 values exhibited a better correlation for the corrosion potential than for the other electrochemical parameters. Values of 0.57 and 0.66 were calculated for AISI 304 SS and alloy 825, respectively.

Some of the problems and limitations associated with the lack of independence of some variables were recognized by the authors in a previous publication (Thompson, 1990). Despite the above mentioned limitations, it should be noted that the approach used by Beavers and Thompson is an important attempt at defining the quantitative effects of relevant environmental variables on localized corrosion. By conducting studies in solutions containing anionic and cationic species found in J-13 well water, but covering a wide range of concentrations, they were able to identify regions of the environmental space where additional research is needed.

3.1.2 Crevice Corrosion Studies

Crevice corrosion is a form of localized attack that occurs within crevices and other shielded areas where a stagnant solution is present. The occurrence of crevice corrosion, as a plausible degradation mode for the current design of containers and their emplacement in the boreholes of the proposed Yucca Mountain repository, needs particular consideration. Contact of the container outer surface with rocks, packing fillers, dirt, or other materials inadvertently placed in the borehole gap may lead to the formation of creviced or shielded areas where the initiation of crevice corrosion is possible in the presence of an appropriate aqueous environment. In addition, weldment voids and flaws or deep surface scratches and marks may act as microcrevice sites. It should be noted, however, that independent of any particular design all engineered structures and components are more prone to be affected by crevice corrosion than by pitting corrosion. Obviously, an adequate design can reduce the risk of crevice corrosion, but in many industrial applications fabrication defects or the deposition of particulate matter, sometimes under abnormal operating conditions, lead to the premature initiation of this form of localized attack.

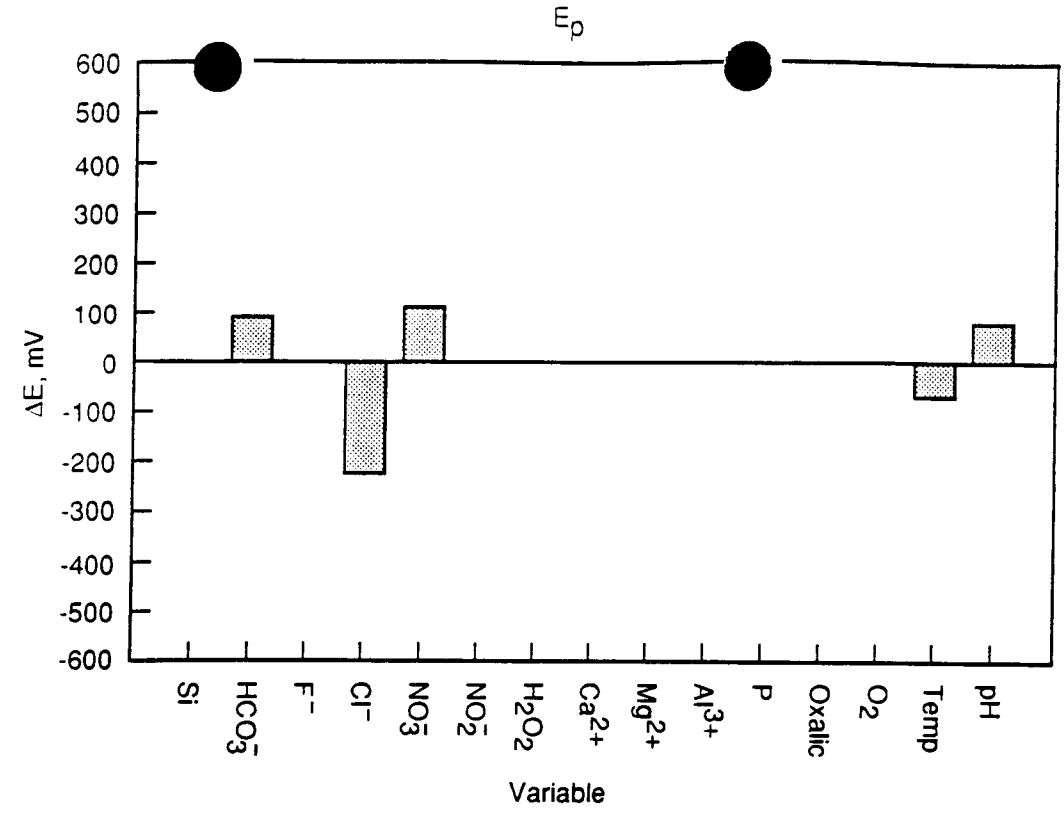

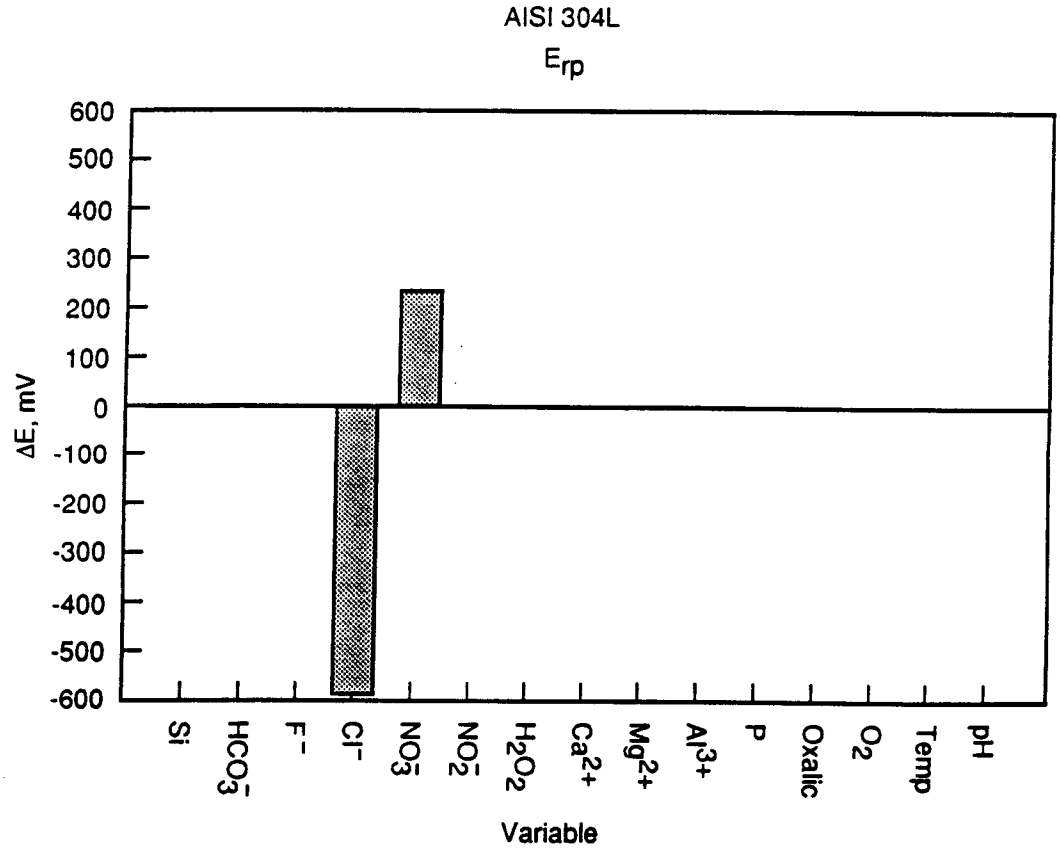

Figure 16. Amplitude of changes in E_p and E_{rp} due to changes in environmental factors (from min. to max.) as calculated by multiple regression analysis. Type 304L stainless steel. (Beavers, 1990a).

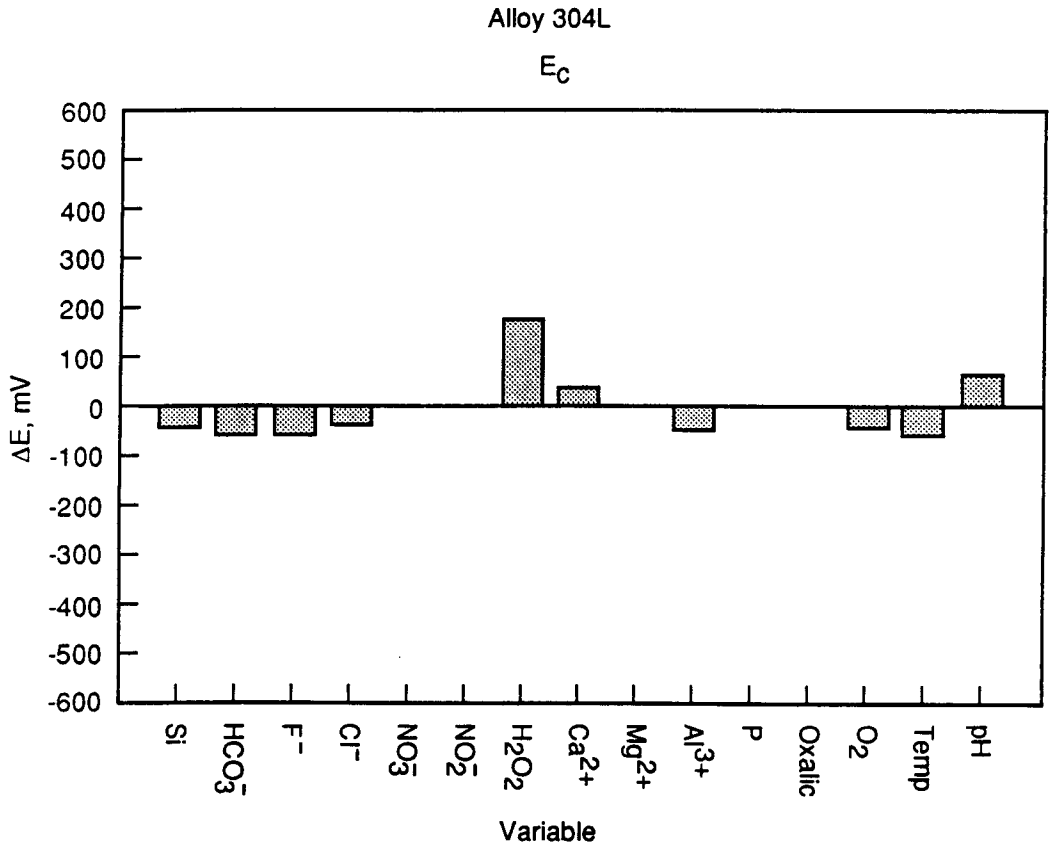

Figure 17. Amplitude of changes in E_c due to changes in environmental factors (from min. to max.) as calculated by multiple regression analysis. Type 304L stainless steel. (Beavers, 1990a).

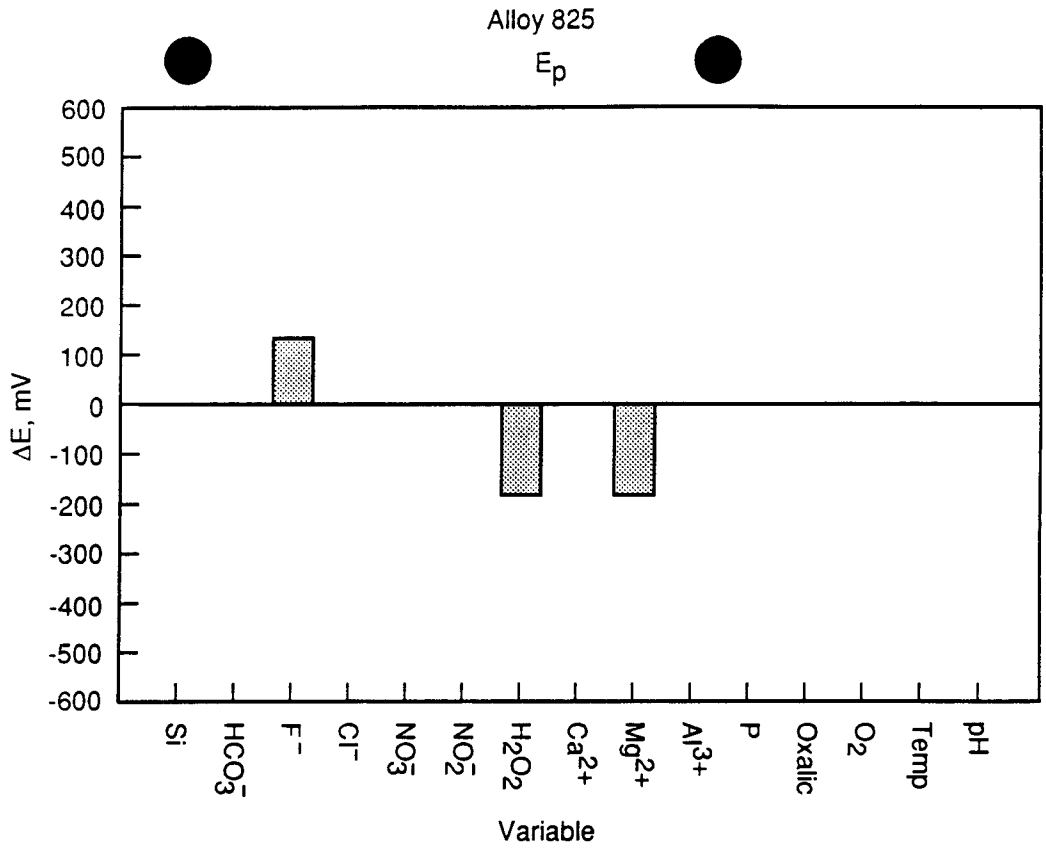

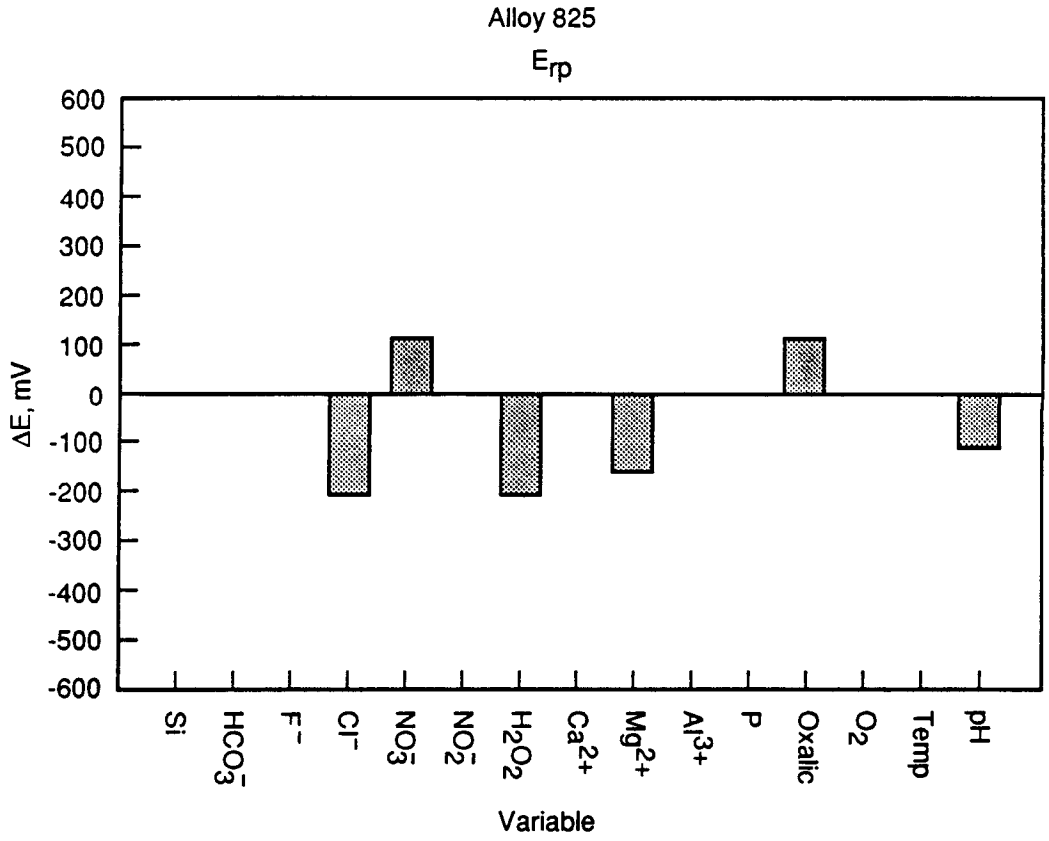

Figure 18. Amplitude of changes in E_p and E_{rp} due to changes in environmental factors (from min. to max.) as calculated by multiple regression analysis. Alloy 825. (Beavers, 1990a).

3.1.2.1 *DOE and LLNL Experimental Results*

Despite the above noted reasons, crevice corrosion of the candidate materials for high-level nuclear waste containers has not been studied systematically in the experimental program conducted at LLNL as a part of the Yucca Mountain Project Waste Package Plan.

Initial tests were carried out using rectangular coupons, fitted with (PTFE) washers which contain 12 separate slots in order to promote crevice corrosion conditions (McCright, 1984). Specimens of AISI 304L, 316L and 317L stainless steels were tested, among other steels, in J-13 well water conditioned with crushed tuff rock at 100°C and in the gaseous phase in equilibrium with that solution, i.e., air saturated with water vapor. Triplicate specimens of each alloy were used in the tests. No attempt was made to control the crevice gap. After 1000 hours exposure to both environments, specimens were weighed, weight losses were determined and the surfaces were examined to detect the occurrence of localized corrosion in the freely exposed surface and in the creviced surface. No signs of localized corrosion were detected in any of the specimens tested. Weight-loss data are given in Table 3.

Table 3. CORROSION TEST RESULTS FOR STAINLESS STEEL SPECIMENS (McCRIGHT, 1984).

	CORROSION RATE (μm/y)					
	J-13 Well Water (100°C)			Air Saturated with Water Vapor (100°C)		
ALLOY	#1	#2	#3	#1	#2	#3
304L SS	nil	0.25	nil	nil	0.25	nil
316L SS	nil	nil	nil	0.51	0.51	0.51
317L SS	0.25	nil	0.13	0.25	0.51	0.76

Nil is less than 0.13 μm/year which is the weight loss detection limit.

The results of more extended crevice corrosion tests were also reported (Glass, 1984). After approximately one year exposure to J-13 well water at temperatures ranging from 50 to 100°C, it was found that all the alloys tested, including AISI 304L, 316L, 321 and 347 SS, as well as alloy 825, exhibited preferential attack in the creviced area. Although the attack was considered to be minor and described as "staining", it is possible that breakdown of the passive film occurred within the crevice, even in a relatively mild environment such as J-13 well water. Prolonged exposure time and more aggressive environmental conditions may have led to a more severe attack. It was concluded from weight loss measurements that all the stainless steels tested exhibited very low corrosion rates, as shown in Table 4. The corrosion rates were found to be comparable to that of alloy 825. The authors (Glass, 1984) suggested on the basis of these results that any one of these candidate alloys could meet the minimum 300-1000 year containment objective. However, they also indicated that the different materials may exhibit varying degrees of susceptibility to crevice corrosion even in J-13 well water. A more sensitive technique for evaluating the tendency to crevice corrosion is required.

Table 4. CORROSION RATE OF CANDIDATE CONTAINER MATERIALS IN J-13 WATER AS DETERMINED FROM WEIGHT-LOSS DATA (GLASS, 1984)

	TEST DURATION	CORROSION RATE (μm/y)				
		Temperature (°C)				
ALLOY	(hrs)	50	70	80	90	100
304L	3548	0.03	0.20	0.20	0.15	0.10
	5000	0.23	0.20	0.23	0.15	0.13
316L	3548	0.23	0.25	0.28	0.15	0.18
	5000	0.10	0.23	0.25	0.25	0.20
317L	3548	0.35	0.28	0.28	0.18	0.08
	5000	0.03	0.25	0.20	0.28	0.10
321	3548	0.18	0.30	0.20	0.20	0.20
	5000	0.13	0.28	0.20	0.33	0.03
347	3548	0.23	0.38	0.25	0.20	0.25
	5000	0.28	0.33	0.25	0.28	1.05
825	3548	0.30	0.28	0.18	0.20	0.15
	5000	0.38	0.38	0.20	0.28	0.28

3.1.2.2 Cortest Columbus Experimental Results

Beavers and Durr (Beavers, 1990b) have recently reported the results of crevice corrosion tests. For both AISI 304L SS and alloy 825, no attack was observed after 8065 hours exposure to aerated, simulated J-13 water at 90°C. As in the case of the tests conducted at LLNL, ribbed PTFE washers were used to define the crevice geometry and triplicate specimens of each alloy were tested. The testing solution was allowed to evaporate in approximately one week by controlling the rate of air flow through the solution and the cooling water flow rate in the condensers located in the cover of the testing flasks. Then, fresh J-13 water was replaced into the flask and the operation was repeated on a weekly basis for the duration of the test. The corrosion rate was determined by weight loss and was found to be lower than 0.009 μm/y for both alloys. In a previous report (Beavers, 1990a), a corrosion rate lower than 0.02 μm/y was reported after 4056 hours. This variation represents an improvement in the level of weight-loss detection. However, another possibility is that no additional weight loss was detected after the initial 4000 hours. No signs of localized corrosion were detected in these long-term boil down tests. Slight scaling of the specimens was reported.

As a result of the evaporation process, it can be expected that in these tests the solutions will become concentrated with time, giving rise to high concentrations of soluble salts over the prolonged testing period, finally reaching saturation conditions for most of the salts. For these reasons, it is difficult to understand why crevice corrosion was not observed in AISI 304L SS, which is an alloy extremely susceptible to this type of localized attack. For example, Sedriks (Sedriks, 1979) has reviewed data showing that the probability of crevice corrosion initiation for AISI 304L SS after 30 days exposure to sea water (19.4 g Cl^-/kg H_2O) rise from 70 to 90% of the specimens tested by increasing the

temperature from 25 to 50°C. This is a clear indication of poor resistance to crevice corrosion in relatively concentrated chloride solutions. Since no data on the concentration of the different species has been reported, no conclusion can be drawn regarding possible inhibiting effects of the passivating anions, such as sulfate, nitrate, or even bicarbonate.

In these tests, corrosion rates were also measured monthly by using polarization resistance techniques. In addition, corrosion potential measurements were conducted. The use of electrochemical impedance measurements was indicated in the initial program. However, no experimental details regarding these measurements have been provided, and it is not known if electrochemical impedance spectroscopy was used to confirm the polarization resistance values. Table 5 summarizes the results of the electrochemical measurements performed on AISI 304L SS and alloy 825, and Figure 19 illustrates the trends in the corrosion potential. It is apparent from the data that the polarization resistance decreased with time for both alloys. Therefore, the corrosion rate should increase. The corrosion potential exhibited significant variations with time, but for both alloys remained within a band ranging from -250 to -100 mV_{SCE} which indicates a passive behavior in a rather mild oxidizing environment. Although minor, the increase of corrosion rate with time is not clearly understandable because a small drop or an almost constant value should be expected as a result of the passive behavior of the alloys.

The corrosion rate, related to i_{corr}, is calculated according to:

$$i_{corr} = B / R_p \qquad (1)$$

where R_p is the polarization resistance.

The expression of B is as follows:

$$B = B_a B_c / 2.303 (B_a + B_c) \qquad (2)$$

The values of B_a and B_c, given in Table 5, were measured from polarization curves. This gives values of B equal to 44.9 and 48.9 mV/decade for AISI 304L SS and alloy 825, respectively.

Beavers and Durr concluded that the data reveals that polarization resistance measurements overestimated the corrosion rates for both alloys. However, it should be noted in Table 5, that the authors adopted a value independent of time for each of the Tafel slopes (B_a and B_c) required to obtain corrosion rates from the polarization resistance measurements using the Stern-Geary relationship. It is doubtful that the Tafel slopes remained constant over such an extended period during which film growth was taking place on the surface. Nevertheless, since the discrepancy between the weight-loss and the electrochemical measurements of the corrosion rate is far greater than one order of magnitude, the cause of the difference cannot be only the value of the coefficient B used to calculate i_{corr}.

It cannot be expected that under any circumstance a decrease greater than an order of magnitude in the measured value of B could occur to explain the above noted discrepancy. Therefore, the discrepancy should be ascribed, at least partially, to the polarization resistance measurements and to the considerable uncertainties in the measured values of B_a and B_c. It is also possible that an additional electrochemical reaction occurring simultaneously is the reason for the low R_p values measured.

Table 5. SUMMARY OF RESULTS OF ELECTROCHEMICAL MEASUREMENTS FOR FE-CR-NI ALLOYS IN AERATED SIMULATED J-13 WELL WATER AT 90°C

ALLOY	HOURS	POLARIZATION RESISTANCE kohm-cm^2	TAFEL SLOPES mV/decade Ba	Bc	CORROSION RATE μm/yr	E_c mV (SCE)
I825	356	1230	211	221	0.39	-149
I825	1341	1740	211	221	0.27	-284
I825	2713	9450	211	221	0.05	-101
I825	4055	264	211	221	1.81	-208
I825	6382	242	211	221	1.97	-227
I825	8061	117	211	221	4.08	-168
I825	9410	214	211	221	2.24	-205
304L	339	4960	493	131	0.10	-67
304L	1515	1800	493	131	0.26	-91
304L	2688	438	493	131	1.08	-103
304L	5374	601	493	131	0.78	-168
304L	6719	105	493	131	4.49	-176
304L	8065	142	493	131	3.34	-190
304L	9407	222	493	131	2.13	-115

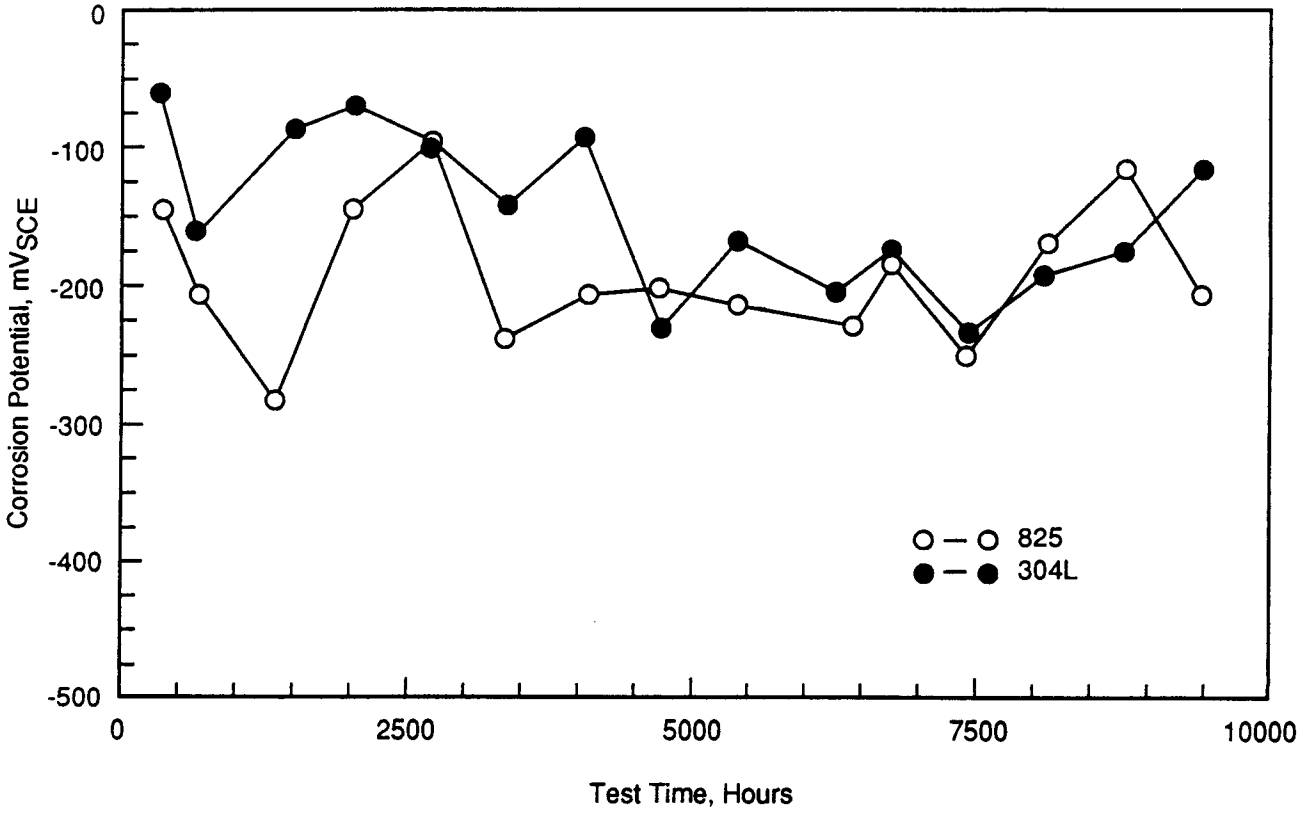

Figure 19. Corrosion potential vs. test time in aerated, simulated J-13 water at 90°C under weekly wet/dry cycles. (Beavers, 1990b).

Additional data on the behavior of AISI 304L SS and alloy 825 have been provided by Beavers and Durr (Beavers, 1990a). After approximately 3000 hours exposure to an aerated solution of pH 10 containing 1000 ppm Cl^- as the main aggressive species and to the vapor phase above the solution at 90°C, crevice corrosion of AISI 304L SS was observed in both the vapor and the liquid phases, being more severe in the latter case. In both cases, the development of pits was observed in the crevice region. Average corrosion rates, based in weight loss measurements for three specimens exposed to each condition, were estimated to be 0.29 and 0.03 μm/y in the liquid and vapor phases, respectively. The maximum pit depth was found to be 62 μm in the liquid phase and 15 μm in the vapor. Specimens exposed to alternate immersion conditions also exhibited pitting, with a maximum pit depth of 41 μm and an average corrosion rate of 0.43 μm/y. These results suggested that under alternate immersion conditions, the corrosion rates and the severity of the localized attack may be comparable or even higher than under fully immersed conditions. It is apparent that additional experiments are necessary to obtain a definitive conclusion regarding the detrimental effect of alternate immersion vs. full immersion. On the other hand, no evidence of localized corrosion was observed on alloy 825, with the exception of a relatively shallow pit of 10 μm in one of the three specimens exposed to the liquid phase. No attack was detected on specimens exposed to the vapor phase or to alternate immersion conditions. The average corrosion rate for the three exposure conditions was estimated to be less than 0.002 μm/y, which is the detection limit. These results confirm that for the isothermal testing conditions used in this work alloy 825 is far more resistant to localized corrosion in the presence of a crevice than AISI 304L SS.

A valuable aspect of this set of experiments is the fact that the corrosion potentials were measured at various time intervals during the exposure of AISI 304L SS and alloy 825 to the aqueous solution at 90°C. The results are shown in Figure 19, where it is seen that AISI 304L SS exhibited higher potentials than alloy 825 during the whole testing period. Beavers and Durr emphasize that the corrosion potential for alloy 825 was always lower than the repassivation potential measured in the same solution, whereas, in the case of AISI 304L SS, in which the repassivation potential was -150 mV_{SCE}, the corrosion potential was consistently higher. These observations provide an explanation for the difference in resistance to localized attack between both alloys. During the course of the experiments, successive additions of H_2O_2 were made to the solution in an attempt to promote localized corrosion on alloy 825. Although the potential increased to about 250 mV_{SCE} upon H_2O_2 addition (200 ppm), no localized corrosion was initiated. The authors indicate that the possible cause is the relatively rapid decline of potential as soon as the highest value is reached as a result of the accelerated decomposition of H_2O_2.

It is apparent that limited experimental work has been done to assess the resistance of the austenitic alloys to crevice corrosion under simulated tuff repository conditions. In addition, the scarce data is essentially confined to the behavior in very few environments (i.e., in J-13 well water in the case of LLNL and in a solution selected by Cortest because it promotes pitting in cyclic polarization tests) without considering variations in pH, temperature and concentration of anionic and cationic species. It should be noted also that the initiation of crevice corrosion is critically related to the geometry and dimensions of the crevice, i.e., crevice gap and depth. The creviced/uncreviced area ratio is also an important factor. The effect of these parameters has not been evaluated in the studies discussed above. Finally, an additional factor to consider is the nonmetallic material used to configure the crevice. PTFE is the single material used in the tests reviewed above. This material, as do many polymers, creeps under mechanical loading at relatively low temperatures and hence, crevice dimensions may be altered. No attempt has been made to test other materials. Ceramic or tuff as nonmetallic components of the crevice may have a different effect that requires experimental evaluation. The effect of different crevice forming materials on corrosion was shown in Figure 4.

3.2 GENERAL LITERATURE

3.2.1 Effect of Microstructure

The nominal compositions of the various Fe-Cr-Ni alloys that are being considered either as candidate or as alternate alloys are shown in Table 1. Some of these alloys have also been examined in other HLW repository programs (Accary, 1986). The compositions range from those of the austenitic stainless steels to Ni-base alloys. These alloys all consist essentially of a single phase, the face-centered cubic crystalline phase, which for the Fe-base alloys is referred to as the austenitic phase. However, depending on the specific compositions, other relatively minor microstructural constituents can be present in some of these alloys. For example, in many stainless steels, inclusion stringers consisting mainly of MnS may be present. In addition, oxide inclusions may also be present either separately or surrounding the sulfide inclusions. In the case of some Ni-base alloys such as alloy 625, carbides of composition MC (M being mainly niobium) and M_6C (M being Mo,Cr) will be present. For alloy 825, nitrides of titanium are present in the microstructure. These microstructural constituents are present essentially inside the grains. Most of them are primary precipitates i.e., they form during the solidification of ingots before further processing. The effects of sulfide and oxide inclusions on localized corrosion behavior of the 300-series stainless steels have been reviewed quite extensively (Sedriks, 1990; Smialowska, 1986). Initiation of pits at MnS inclusion occurs by the adsorption of chloride on these inclusions, dissolution of MnS, and creation of an acidic environment inside the pit originally occupied by the inclusion.

Recent surface analysis studies (Castel, 1990) have affirmed many of the previous findings, but also have shown that the mixed Fe, Cr oxide inclusions are immune to local dissolution. This is in contrast to the results of Cihal et al. (Smialowska, 1986) who found TiO to be effective pit nucleation site. The effect of primary carbides (such as NbC) or nitrides (such as TiN) on localized corrosion has not been investigated to any great degree. In the case of alloy 825, inclusion containing Ti and V (presumably in the form of nitrides) have been shown to be susceptible to pit initiation (Smialowska, 1986). Generally, these primary oxides, carbides, and nitrides are quite stable and, since they are formed during the primary solidification stage, are not associated with depletion zones. Hence, it is unlikely that they will be the main sites of pit initiation. An indirect confirmation of the stability of the oxides is the resistance to localized corrosion of Ni-base alloy welds performed by the Shielded Metal Arc process. In this process, numerous oxide inclusions are present in the weld from the coating on the welding electrode. Yet, this weld shows the same resistance to pitting as a weld made by the Gas Metal Arc process which has no measurable inclusion content (Sridhar, 1990). Similarly, powder metallurgically processed materials, which contain numerous chromium oxide inclusions, show similar localized corrosion resistance as conventionally processed materials of the same chemical composition.

Secondary precipitates are those that form after ingot solidification, during subsequent processing or fabrication. These usually initiate at grain boundaries and are associated with depletion zones. The secondary precipitates can be either carbides, nitrides, or intermetallic compounds. The compositions of these precipitates depend on the alloy composition. For example, in high Cr, low Mo alloys, the carbides are typically high in Cr and are of the type $M_{23}C_6$ or $M_{12}C$, whereas, in high Mo,Cr alloys they are rich in Mo and of the type M_6C. It is not the intent of this review to examine the precipitation reactions in these alloys in detail. The effects of these secondary precipitates on pitting/crevice corrosion of austenitic alloys has not been studied as extensively, the focus of most investigations being intergranular corrosion and stress corrosion cracking. The results of the few studies in austenitic materials seem to be conflicting. Stefec et al. (Smialowska, 1986) found a good correlation between pitting in a NaCl solution and intergranular corrosion in ASTM A-262E test (Sulfuric acid plus copper sulfate solution) for a type 316 stainless steel. However, Manning (Manning, 1985) did not find

any significant effect of intergranular precipitation on pitting in a Ni-Cr-Mo alloy (alloy C-276). In contrast, in duplex and ferritic stainless steels, precipitation of sigma phase (Cr-rich intermetallic compound) and Cr_2N has been shown to clearly increase the susceptibility to pitting (Sridhar, 1987). This area needs more systematic examination in the future.

The effect of microchemical changes due to welding on pitting/crevice corrosion of austenitic alloys has been examined in detail by many investigators (Garner, 1982; Marshall, 1986; Redmerski, 1983). There is a general agreement, at least qualitatively, that fusion welding processes decrease the resistance of an alloy to localized corrosion. This decrease in localized corrosion resistance is caused by the segregation of alloying elements such as Cr, Mo, and W to the interdendritic areas during solidification of the weld and solid state reactions after solidification. The decrease in pitting resistance by autogenous (no filler metal) GTA welding process is exemplified by the data shown in Figure 20 (Garner, 1982). Here the pitting resistance is characterized by the critical pitting temperature and a variety of commercial alloys are represented by their Mo content. The extent of the decrease in resistance is dependent on factors such as the severity of the environment, composition of the weld filler metal, and to a lesser extent on welding parameters. It is important to note that most of the emphasis on localized corrosion studies of welds has been on weld metal and not on the Heat-Affected-Zone (HAZ). To compensate for the segregation induced depletion of alloying elements in the weld metal, filler metals with higher concentrations of some alloying elements (over-alloyed fillers) have been tried successfully.

The welding method that has been chosen as the most preferable for closure of container is not fusion welding, but friction welding where very little melting occurs (Robitz, 1990). This is followed by four fusion welding processes--Electron Beam Welding (EBW), Plasma Arc Welding (PAW), Laser Beam Welding (LBW), and Gas Tungsten Arc Welding (GTAW)--all autogenous. With the exception of GTAW, for which a significant data base on localized corrosion exists, much work needs to be done to characterize the localized corrosion of other welding processes systematically.

3.2.2 Effect of Composition

The effect of alloy composition on base-metal localized corrosion resistance has been studied extensively (e.g., Sedriks, 1990; Sridhar, 1990; Smialowska, 1986). No attempt is made to review this vast literature. However, the effect of various alloying elements on localized corrosion has been summarized in Figure 21 which has been adapted from Sedriks (Sedriks, 1990). It must be noted that the beneficial/detrimental effects of many elements in this figure depend not only on their concentration but also on the concentrations of other elements in an alloy. For example, nitrogen (up to about 0.4%) has been shown to improve the resistance of alloys containing both Cr and Mo, but not only Cr (Bandy, 1983). Copper has no significant effect up to about 1% beyond which it is detrimental (Sridhar, 1990). Chromium equivalence has been used as a measure of pitting resistance to quantify the effects of various alloying elements. Two such Cr equivalence numbers are shown below (all percentages in weight percent):

$$Cr_{Equivalent} = \%\ Cr + 3\ (\%Mo) \quad (3)$$

$$Cr_{Equivalent} = \%\ Cr + 2.6\ (\%Mo) + 4.4\ (\%Nb) + 6(\%W) \quad (4)$$

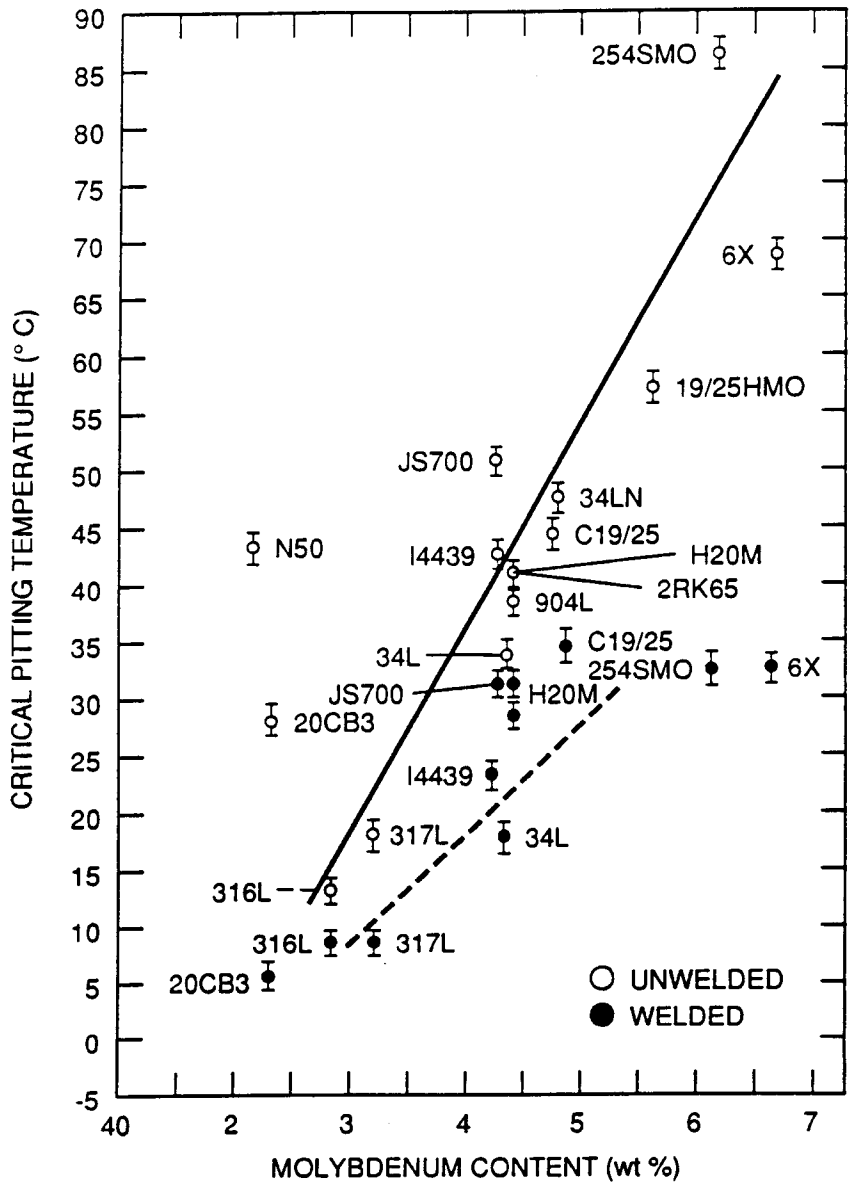

Figure 20. Critical pitting temperature vs. molybdenum content of austenitic alloys in 10% $FeCl_3$ solution. Welding was done by GTAW autogenously at a power input of 0.5KJ/mm. (Garner, 1982).

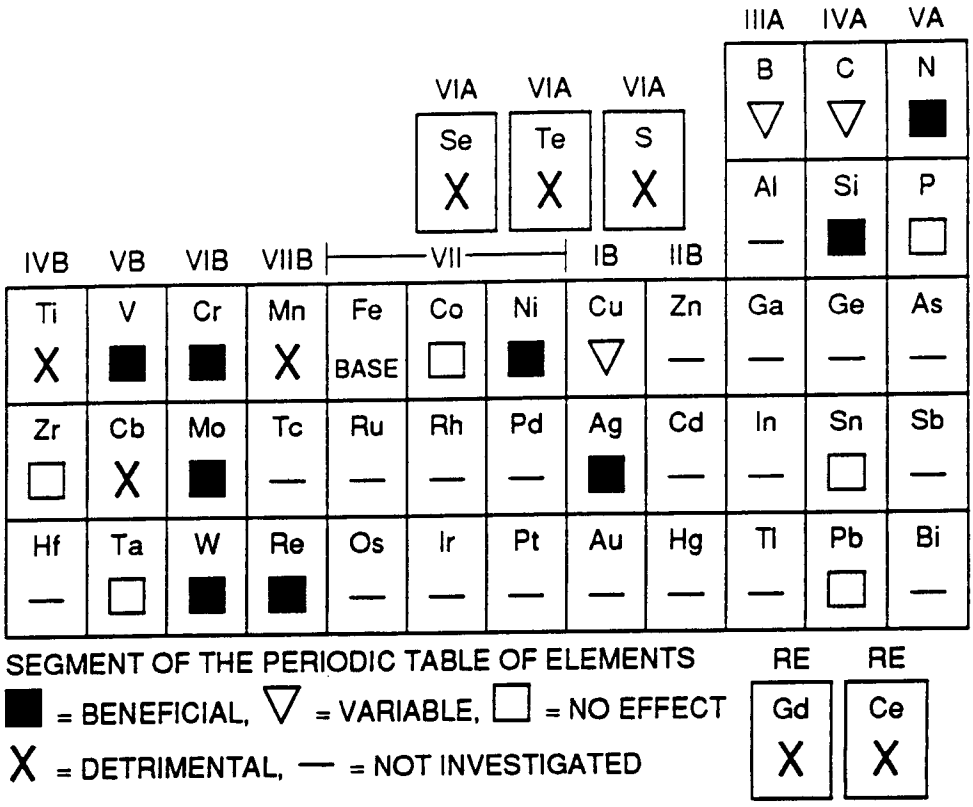

Figure 21. Effect of alloying elements in austenitic alloys on localized corrosion resistance in chloride solutions. (Sedriks, 1982).

It must be noted that these equations are empirical and based on multiple regression analyses of localized corrosion data on various commercial alloys with a wide range in composition in a single environment (e.g., 10% $FeCl_3$). While these equations have been successful in ranking alloys with a wide range of compositions, they do not accurately predict the ranking of alloys with relatively small but significant variations in composition (Sridhar, 1990). Nor are they valid for environments that differ in severity from the one used to develop the equations. Nevertheless, the concept offers ease of plotting localized corrosion data for a variety of alloys in terms of a single parameter.

3.2.3 Effect of Environmental Factors

The effects of a wide variety of anionic species on localized corrosion of austenitic materials have been examined in the literature.

3.2.3.1 Effect of Chloride

Smialowska has reviewed much of the literature pertaining to the quantitative effects of chloride concentration on various localized corrosion parameters such as E_p and E_{rp}. Generally, a logarithmic relationship is found as shown below:

$$E_p = A \, Log \, (Cl^-) + B \qquad (5)$$

with the constants A and B depending on the alloy and environment. Most of the investigations revealing this type of relationship appear to be confined to relatively high chloride concentrations (0.1M or higher) or low alloys. However, Matamala (Matamala, 1987) investigated type 316 stainless steel in pulp and paper mill spent bleach plant solutions (pH = 3.7), containing relatively low chloride concentrations (3 x 10^{-4} M to 0.03 M Cl^-) and found a logarithmic dependance as shown below:

$$E_p = 719 - 147 \, Log \, (Cl^-, ppm), \, mV_{SCE} \qquad (6)$$

The author also measured the effects of temperature ranging from 35° to 65°C in a 3 x 10^{-4} M Cl^- solution at a pH of 3.7 and the effects of pH (2.3 - 6.5) at the same chloride concentration at 54°C. Based on the above set of data, a multiple regression analysis was conducted which indicated the following relationship:

$$E_p = 2570 - 5.81 \, T + 0.18 \, T \cdot pH - 0.60 \, T \cdot log \, (Cl^-) - 0.11 \, T \cdot pH \cdot log \, (Cl^-) \qquad (7)$$

While the above equation purports to indicate interactions between the three variables, T, pH, and Cl^-, the experimental design is not a full factorial design (it has only half the requisite number of combinations of the factors for a full factorial design) and, hence, does not permit establishment of such interactions independent of the effect of other factors. There are other aspects of this investigation that plague interpretation of the results: 1) Repassivation potentials were not measured by the author, 2) No visual observations were reported and, hence, it is difficult to attribute all the

measured E_p values to pitting, 3) The bleach plant solution contained 3 x 10^{-4}M Cl^- but 1 x 10^{-2}M total chlorine so that in the low chloride environments significant amount of residual chlorine was probably present, and 4) It is difficult from only the reported E_p values to determine the threshold Cl^- value at which pitting occurred.

Kain et al. (Kain, 1990) reported crevice corrosion of AISI 304 SS in simulated Colorado River water and potable waters containing 10 ppm chloride. They also examined crevice corrosion of a variety of austenitic alloys ranging from AISI 304 SS (0% Mo) to alloy 254 SMO (6% Mo and 0.2% N) in naturally aerated, flowing (5 cm/sec), sea water diluted by distilled water to a chloride concentration of 1000 ppm. The crevices were formed between flat samples and acrylic blocks with a flexible PTFE tape between them. The sample and acrylic block were placed in a holder and tightened against each other with controlled torque so that the crevice gaps were reproducible. The current flowing between the creviced sample and an open sample while short-circuited was also measured and used as an indicator for crevice corrosion initiation and propagation. At 30°C, crevice corrosion initiated rather quickly on AISI 304 and 316 stainless steels while the higher Mo containing alloys did not exhibit any crevice corrosion in 30 days. Some of the crevice corrosion initiation data are excerpted in Table 6.

Table 6. INITIATION TIME FOR CREVICE CORROSION OF SOME AUSTENITIC ALLOYS IN DILUTED SEAWATER AND SIMULATED SEAWATER (KAIN, 1990)

Environment	Initiation Time, Days			
	304 SS	316 SS	904L	254SMO
Dilute Natural Sea Water, 1g/l Cl + 0.1g/l SO_4	1,0.5	1,1	None*	None
Simulated Sea Water, 1g/l Cl + 1g/l SO_4	3,1	10-13,10-13	None	None
Simulated Sea Water, 1g/l Cl + 10g/l SO_4	13, 10	None	None	None

It can be seen from Table 6 that crevice corrosion can initiate under these conditions in relatively short periods of time in the 0 - 2.5% Mo stainless steels. Postlethwaite et al. (Postlethwaite, 1988) examined the effects of chloride and temperature on localized corrosion of two Ni-base alloys using the cyclic polarization technique. They noted crevice corrosion at the PTFE/sample contact area before pitting occurred, and in some cases, the correlation between electrochemical curves and visual observation of localized corrosion was poor. Their data for alloy C-276 (16% Cr-16%Mo) and alloy 625 (22%Cr-9%Mo) are shown in Figures 22 and 23. It can be seen that in the lowest chloride environment (600 ppm Cl^-), crevice corrosion does not occur in alloy C-276 below 100°C, whereas, alloy 625 exhibits crevice corrosion even at a temperature of 50°C.

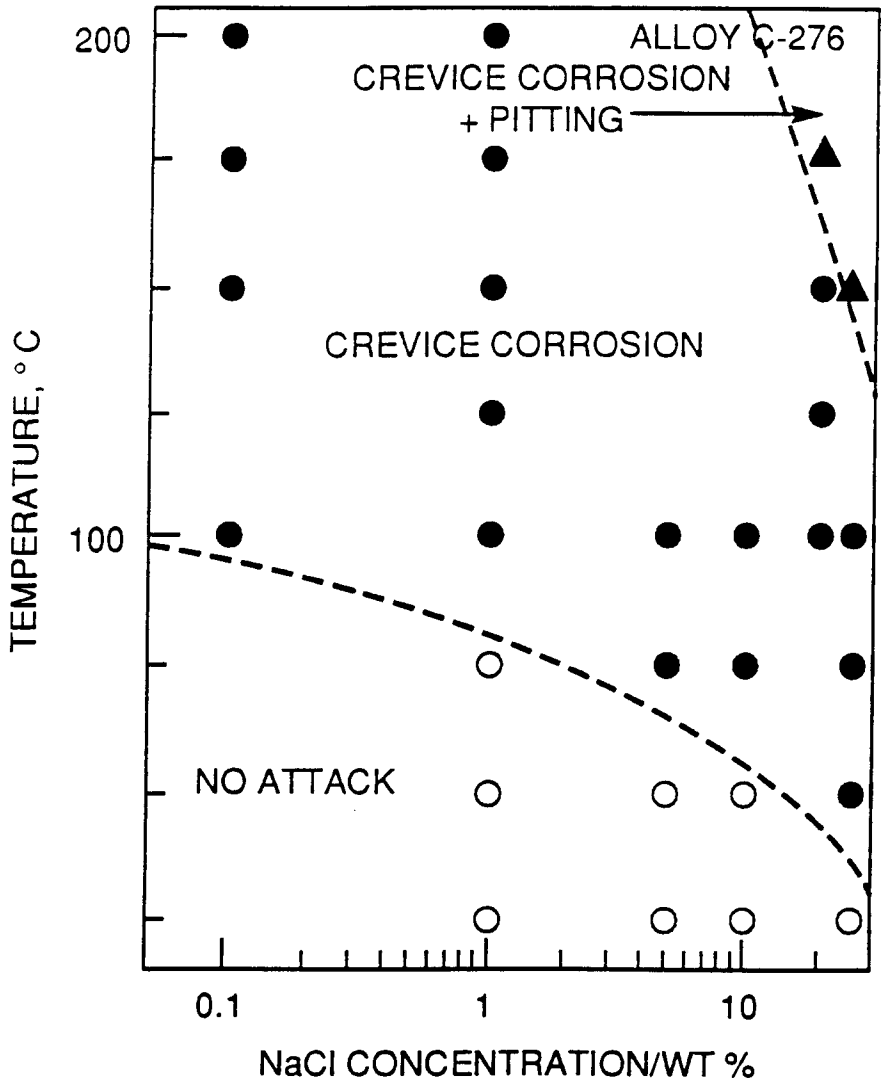

Figure 22. Effects of temperature and chloride concentration on localized corrosion of alloy C-276 in cyclic polarization tests. (Postlethwaite, 1988).

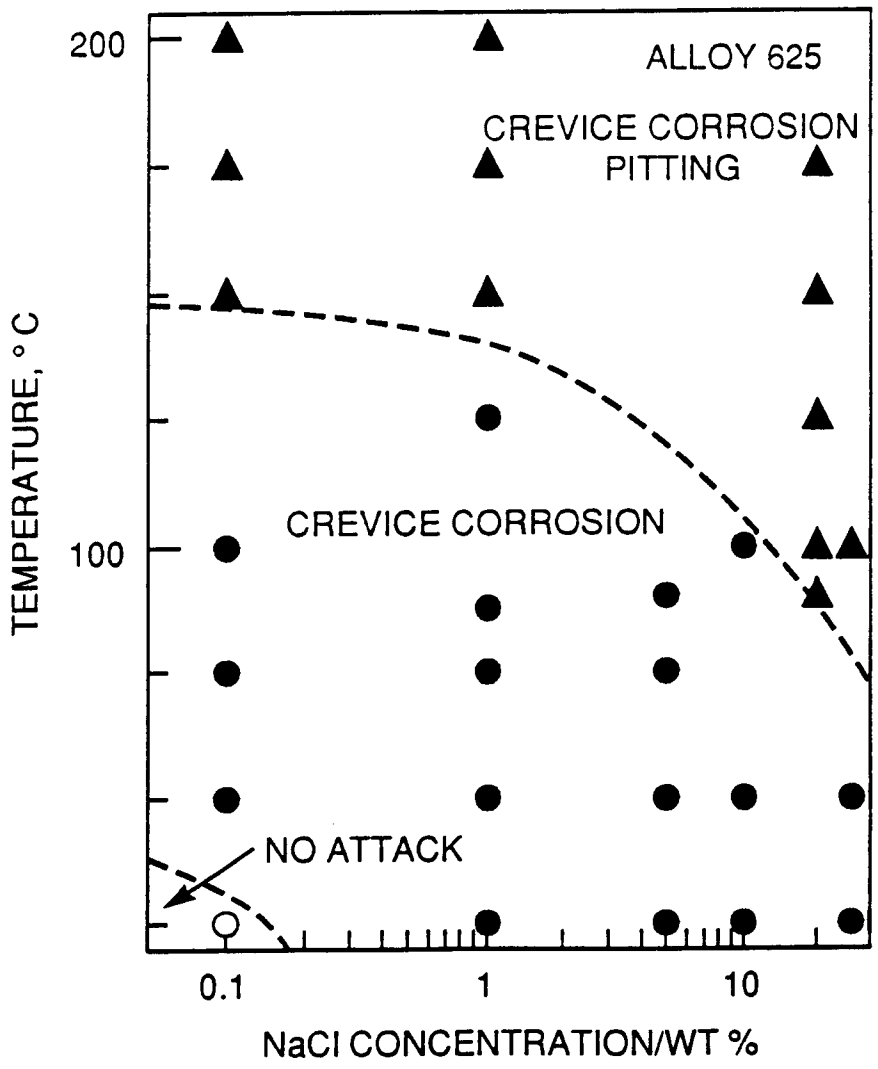

Figure 23. Effects of temperature and chloride concentration on localized corrosion of alloy 625 in cyclic polarization tests. (Postlethwaite, 1988).

3.2.3.2 *Effect of Bicarbonate*

Many natural waters contain bicarbonate as a major ingredient. Yet, the effect of bicarbonate on localized corrosion, free of its interactions with pH, has not been studied. Bogaerts and Van Haute (Bogaerts, 1985) examined the effect of the addition of 0.1M HCO_3^- to 0.1M Cl^- on localized corrosion of AISI 304 and 316 stainless steels and alloy 600 at 150° and 175°C. The authors did not report the pH and, hence, it is not clear whether addition of bicarbonate altered the pH. A slight increase in E_p was noted with the addition of bicarbonate. However, the E_{rp} was lower with bicarbonate. Since these are single sample data, the statistical significance of these observed differences is not clear. Hence, their results on the effect of bicarbonate/pH is inconclusive.

Jallerat et al. (Jallerat, 1984) studied the effects of bicarbonate and carbonate on localized corrosion in chloride solutions of AISI 304L and 316L stainless steel, alloy 800, and alloy 625. The concentrations of all anionic species varied from 0.1M to 1M. The pH of the bicarbonate solutions measured 7.5 - 8.2 while those of the carbonate solutions 10.5 - 11. The test temperature was 90°C. They found that bicarbonate and carbonate inhibit localized corrosion of all alloys. The effect of bicarbonate went beyond just the effect of alkalinity since addition of NaOH to the same pH did not inhibit localized corrosion as effectively. The relationships between bicarbonate and chloride in terms of inhibition of localized corrosion are given below for three alloys:

304L stainless steel:	$Log\ (Cl^-) = 2.05\ Log\ (HCO_3^-)$	
316L stainless steel:	$Log\ (Cl^-) = 0.23 + 2.02\ Log\ (HCO_3^-)$	(10)
Alloy 800:	$Log\ (Cl^-) = 0.08 + 1.19\ Log\ (HCO_3^-)$	

It must be noted from the above equation that the concentration of bicarbonate required for inhibition is far higher than the concentrations tested thus far in any of the repository programs. For example, for 0.1M Cl^- concentration, localized corrosion was inhibited on type 316L stainless steel with a concentration of 0.25M (15,000 ppm). The highest bicarbonate concentration tested thus far is 2000 ppm.

3.2.3.3 *Effect of Sulfate*

Sulfate as an inhibitor of localized corrosion in chloride environments has been investigated rather extensively. Leckie and Uhlig (Leckie, 1966) investigated the inhibitive action of SO_4^{2-} early one in an Fe-18Cr-8Ni stainless steel and found that an addition of 0.05M SO_4^{2-} to 0.1M Cl^- increased the E_p. However, since they did not conduct a reverse scan, the effect of SO_4^{2-} on E_{rp} was not known. Rosenfeld and Maksimchuk (Rosenfeld, 1967) performed essentially galvanostatic experiments on 18Cr-8Ni stainless steels and concluded that for a neutral 0.1N Cl^- solution, the SO_4^{2-}/Cl^- ratio must be at least 10 for inhibition. The ratio decreased for more acidic and alkaline solutions. Because they were detecting the start of potential oscillations for small anodic currents ($2\mu A/cm^2$), they were measuring localized corrosion initiation rather than repassivation.

Bogaerts and Van Haute (Bogaerts, 1985) examined the effect of several anions including sulfate, bicarbonate, and phosphate on localized corrosion of several stainless steels and Ni-base alloys. They found that addition of 0.1M SO_4^{2-} to a 0.1M Cl^- solution increased the pitting potential at all temperatures ranging from 50° to 175°C. This is illustrated for alloy 800 in Figure 24. However, since they did not measure repassivation potentials, the concentration of sulfate required for

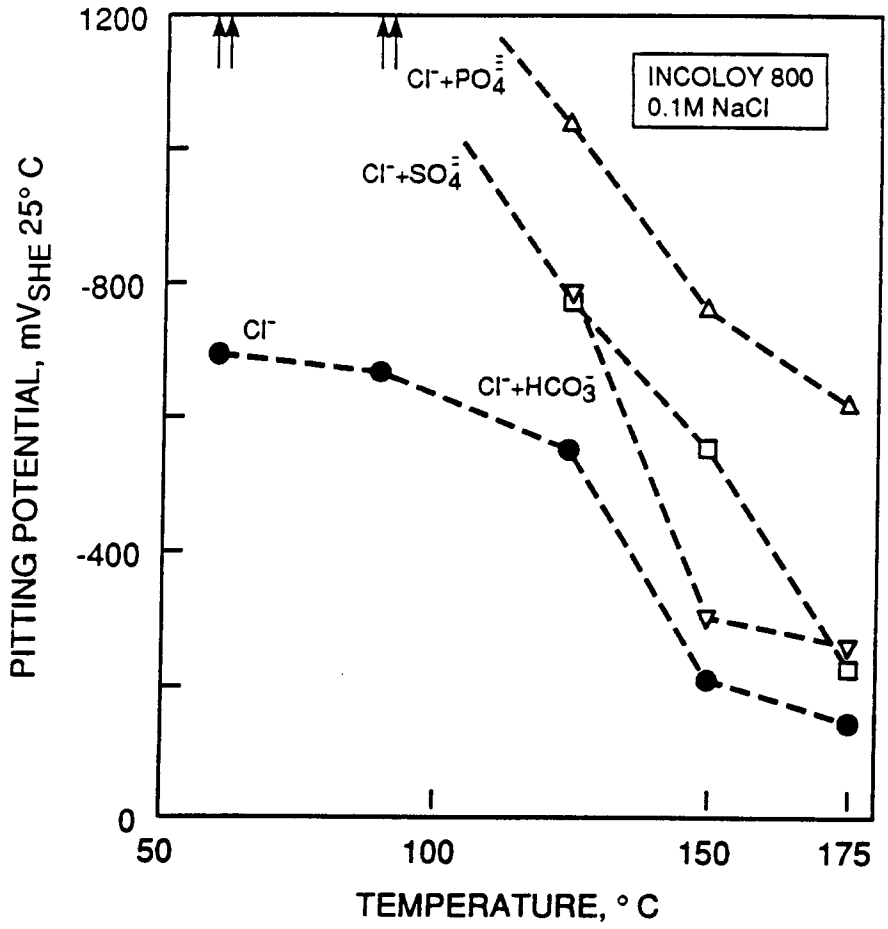

Figure 24. Influence of 0.1M PO_4^{3-}, SO_4^{2-}, or HCO_3^- additions to 0.1M chloride on pitting of alloy 800. (Bogaerts, 1985).

complete inhibition is not known. It can also be seen from Figure 24 that phosphate has a greater inhibitive capacity than sulfate.

Brookes and Graham (Brookes, 1989) showed that localized corrosion was inhibited for several ferritic stainless steels when suitable concentrations of sulfate were added. Based on the measurement of E_p, they established relationships between Cl^- and SO_4^{2-} for inhibition as shown below:

$$Log\ (Cl^-) = A\ Log\ (SO_4^{2-}) + B \qquad (11)$$

where A and B are constant dependant on the alloy composition and presumably temperature. For a Fe-18.5Cr-0.02%Ni stainless steel, inhibition is achieved in a 0.1M Cl^- solution only at a SO_4^{2-} concentration of 10M. However, for a Mo-containing ferritic stainless steel (18Cr-2Mo), the concentration of SO_4^{2-} required for inhibition is only 0.01M in a 0.1M Cl^- solution. Since, reverse scan was not conducted, the E_{rp} values were not considered for inhibition. As indicated in Table 6, sulfate has also been shown to inhibit crevice corrosion in aerated sea water. The mechanism by which sulfate inhibits localized corrosion is thought to be by competitive adsorption against chloride.

3.2.3.4 Effect of Nitrate and Nitrite

Nitrate and nitrite are well known inhibitors of localized corrosion in many alloy systems (Smialowska, 1986). Matsuda and Uhlig (Matsuda, 1964) examined several inhibitors of localized corrosion of Fe-18Cr-8Ni stainless steel and found that the inhibition efficiency decreased in the order: $OH^- > NO_3^- > SO_4^{2-} > ClO_4^- > CH_3COO^-$. Rosenfeld and Maksimchuk (Rosenfeld, 1967) examined the same type of stainless steel and arrived at a similar conclusion. In their investigation, the NO_3^-/Cl^- ratio for inhibition in neutral solution was 0.4 whereas the ratio of SO_4^{2-}/Cl^- for the same solution was 10. Many investigators have found an inhibitor potential, E_i in the presence of nitrate, which is more positive than the E_p. Beyond E_p current density increases due to pitting and beyond E_i, the current density is lowered drastically and no pitting is found. The E_i decreases with an increase in nitrate concentration and increases with an increase in temperature while E_p decreases with temperature (Smialowska, 1986) thus reducing the inhibition efficiency of nitrate at higher temperatures. The inhibition potential can be measured only by continuing scanning of potentials more anodic to E_p to very high current densities (greater than $10^5\ \mu A/cm^2$). While this is interesting from a mechanistic perspective, it is not relevant for many applications. Typically, in cyclic polarization curves, scanning is reversed once lower current densities are attained and, hence, E_i is not generally measured. However, nitrate and nitrite beyond certain concentrations depending on the alloy, increase E_p and also inhibit pitting completely on the reverse scan (Cragnolino, 1991a, 1991b). It must be noted that in many of these investigations, the concentration of nitrate/nitrite added was not sufficient to influence the corrosion potential by its redox reaction.

3.2.3.5 Effect of pH

The localized corrosion susceptibility in terms of E_p has been found to be relatively independent of pH over a wide range from 1.6 to 12.7 by some investigators and over a slightly narrower range of 3-8 by others (Smialowska, 1986). Under more alkaline conditions, E_p has been found to increase with pH and indeed OH^- is an efficient inhibitor of pitting as discussed before. Most of these studies have focused on relatively concentrated chloride solutions (0.1M and higher). Matamala (Matamala, 1987) investigated the localized corrosion of type 316 stainless steel in relatively low chloride

solutions (3 x 10^{-4}M) at pH ranging from 2.3 to 6.5 and found that E_p varied from 544 to 660 mV vs. SCE. The effect of pH on E_{rp} has not been examined extensively. In a recent report, decrease in pH was found to result in a much larger decrease in E_{rp} than E_p for alloy 825 in dilute chloride solutions (Cragnolino, 1991c).

3.2.3.6 Effect of Temperature

The effect of temperature on localized corrosion parameters depends on other factors such as the environmental composition and the alloy composition. The pitting and repassivation potentials generally follow an inverse sigmoidal relationship with temperature as illustrated in Figure 25 (Brigham, 1973) for E_p measured potentiostatically for a series of stainless steels. At the low temperatures, below 20°C for the 3.04% Mo alloy and below 50°C for the 7.3%Mo alloy, the E_p is near the oxygen evolution line and relatively independent of temperature. Beyond a certain temperature, E_p again becomes relatively independent of temperature, although in many cases this temperature is not attained. The inverse sigmoidal curve shifts to the right (higher temperatures) when the chloride concentration decreases as well as when the alloy content increases. Thus, for any applied potential, there is a temperature, called Critical Temperature, beyond which pitting/crevice corrosion will be observed in a given chloride solution. This is indicated for a Fe-20%Cr-25%Ni-4.5%Mo-1.5%Cu alloy in Figure 26 (Bernhardsson, 1980) which also shows that, for the low chloride concentrations, the critical temperature increases dramatically as the applied potential is lowered. At any potential, the critical temperature increases with an increase in pH, with the slope depending on the alloy. This is illustrated for alloy 825 in Figure 27 (Bernhardsson, 1983) which shows that in a pH = 8.5 solution of 3% NaCl (0.5M Cl), pitting does not occur below a temperature of about 60°C at an applied potential of 400 mV vs. SCE. It must be noted that in these tests crevice corrosion was rigorously avoided and repassivation potential was not considered. Other data by the same authors (Bernhardsson, 1983) indicate that critical crevice corrosion temperature for alloy 825 at an applied potential of 200 mV vs. SCE and in a 3% NaCl solution is 30 - 45°C.

This previous observation has been confirmed by the findings of Hodgkiess and Rigas (Hodgkiess, 1983) who found that in aerated sea water (approximately equivalent to 3.5% NaCl), alloy 825 showed a reduction in E_p from 1050 mV vs. SCE to 230 mV when the temperature was raised from 20 to 60°C. The E_{rp} decreased even more from 1030 mV to 0 mV vs. SCE. Cragnolino and Sridhar (Cragnolino, 1991b) found that the temperature dependance of E_p and E_{rp} varied as a function of chloride content. From the above discussions of the effect of temperature, it can be concluded that temperature dependance is related to a combination of alloy and environment conditions and critical temperature data must be used with great care taking into consideration the chloride (and other species) content, presence of crevices, and the likely corrosion potential (related to the E_h of the environment).

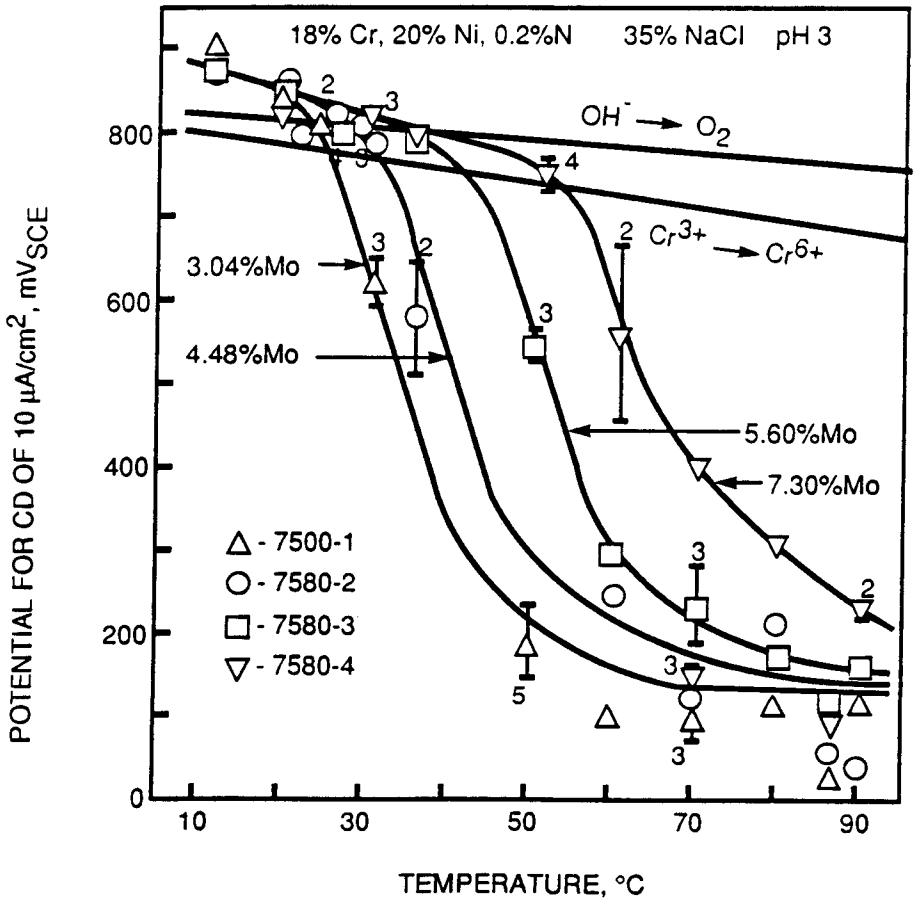

Figure 25. Effect of temperature on pitting potential in a potentiostatic test for a variety of austenitic alloys in 3.5% NaCl. (Brigham, 1973).

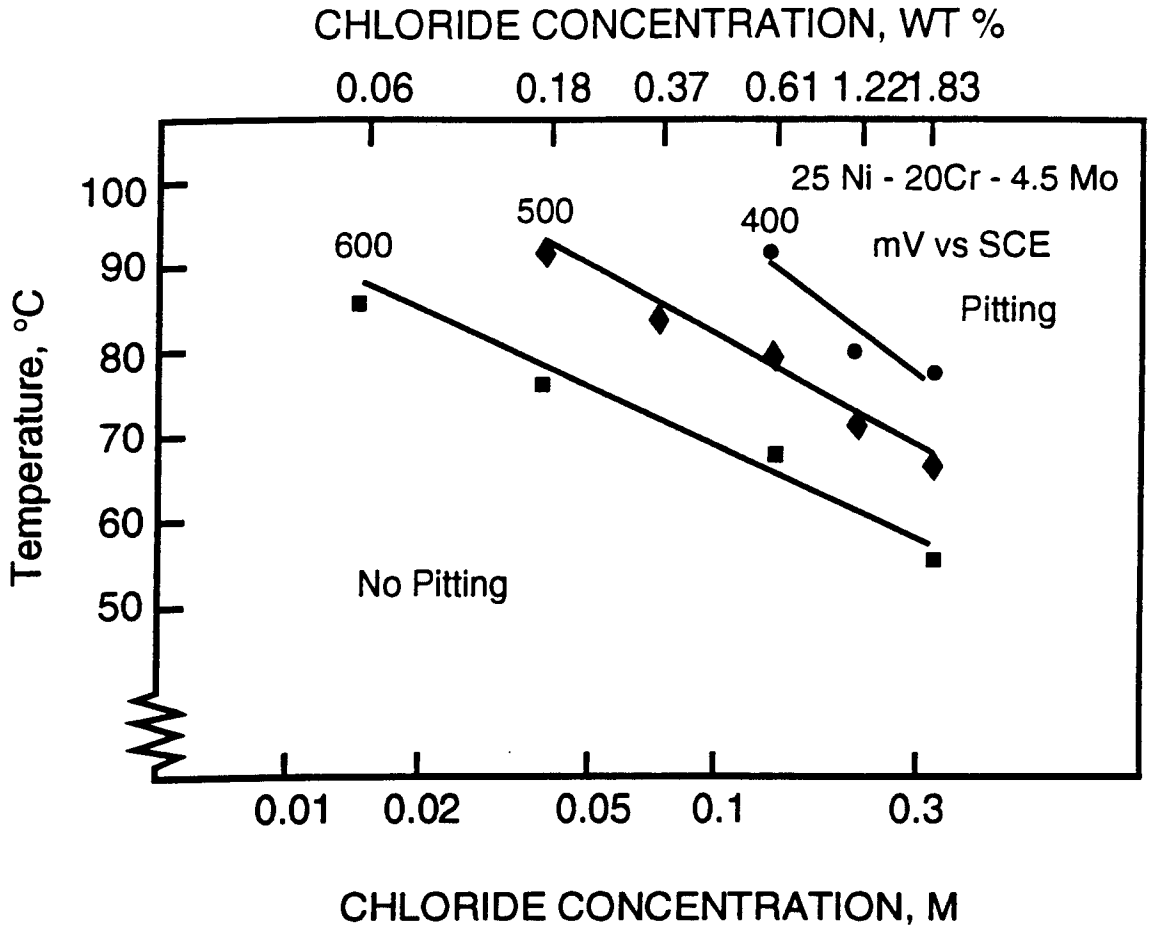

Figure 26. Effect of applied potential, chloride, and temperature on pitting of an austenitic stainless steel. (Bernhardsson, 1980).

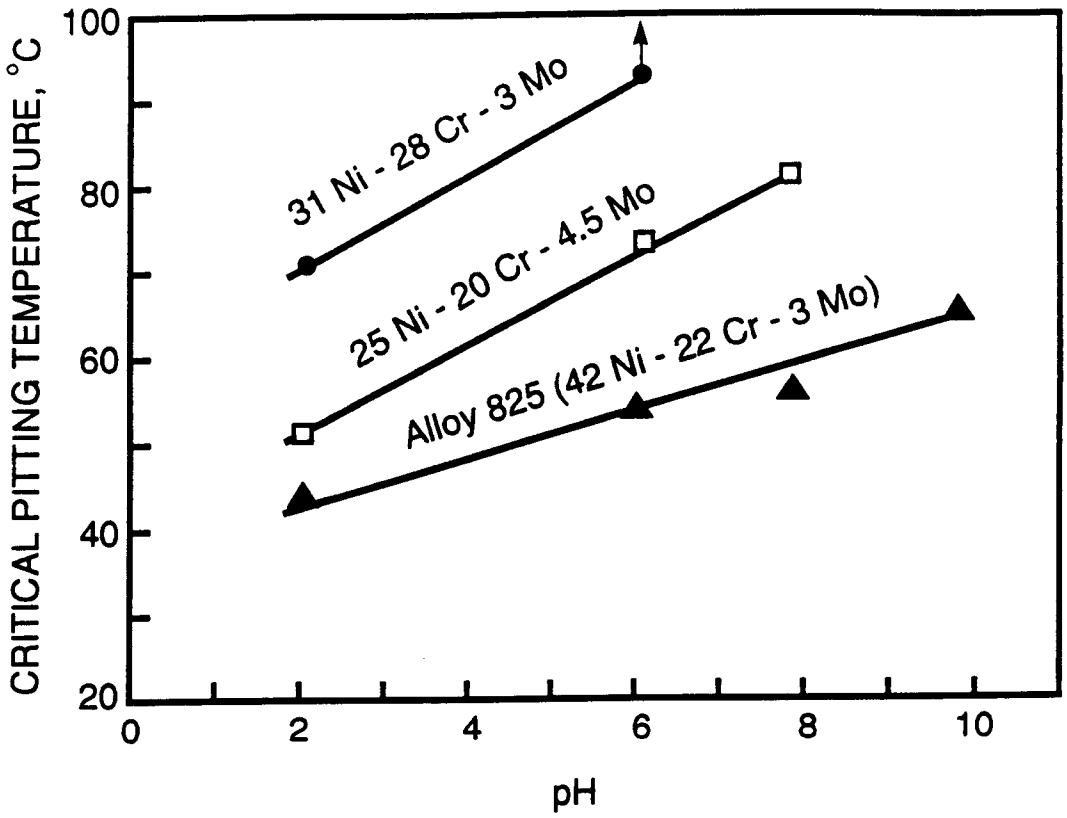

Figure 27. Effect of temperature and pH on pitting of three austenitic alloys in 3% NaCl solution at an applied potential of 400 mV_{SCE}. (Bernhardsson, 1983).

4. LOCALIZED CORROSION OF COPPER AND COPPER-BASED ALLOYS

4.1 HIGH-LEVEL WASTE RELATED LITERATURE

4.1.1 Electrochemical Experiments

4.1.1.1 DOE and LLNL Experimental Results

LLNL developed a limited test program for evaluating the corrosion behavior of copper and copper-based alloys (Table 7) as an alternative alloy system to the austenitic stainless steels and the high-nickel-base alloys for the environmental conditions of the proposed Yucca Mountain repository (McCright, 1985). Cyclic potentiodynamic polarization curves were used to determine the susceptibility of the candidate copper-based alloys CDA 102, CDA 613, and CDA 715 to localized corrosion in J-13 well water and in a solution in which the species present in J-13 water were concentrated by boiling under atmospheric pressure to reduce the volume to 1/100 of the original one. As it was noted (McCright, 1985), under such conditions sodium and calcium silicate precipitate from J-13 water and the pH of the supernatant, which was used in the tests, rises to values ranging from 10.1 to 10.3. It was claimed that soluble anions such as chloride, fluoride and carbonate remain in solution. In the case of carbonate, however, it is doubtful that the concentration increased 100-fold because some proportion has been lost through ex-solution of CO_2, which is in equilibrium with bicarbonate and carbonate in aqueous solutions. Undoubtedly, at pH above 10 carbonate predominates over bicarbonate. No analysis of the chemical composition of the final solution has been provided.

All the alloys were tested in the as-received annealed condition with the specimen surfaces mechanically polished with 600-grit SiC paper and finally with 5 and 1 μm Al_2O_3 slurry. The polarization curves were obtained at a potential scan rate of 1 mV/s. Although not indicated in the report, it is assumed that the solutions were not deaerated and, therefore, the concentration of oxygen was that corresponding to the equilibrium with air at the temperature of the test. A typical polarization curve is shown in Figure 28, in which the anodic behavior of CDA 102 in 100-times concentrated J-13 water at 25°C is displayed. A wide potential range in which the metal exhibited passive behavior was observed followed by an abrupt current increase at the pitting potential. Pitting was observed in the metal surface. The pits were found to be broad, but not very deep, and generally covered by bluish-green deposits of corrosion products. Although no remarks were made by the author, it is apparent that the surface repassivates during the reverse scan at a potential that is about 70 mV_{SCE}. For the purpose of comparison, the polarization curve for the same material in J-13 water is shown in Figure 29. It is clearly noticeable that in the more dilute solution the current density increases slowly in the passive range and no signs of an abrupt current increase related to pitting is observed during the forward scan.

Figure 30 summarizes the corrosion potentials measured for CDA 102, CDA 613 and CDA 715 in J-13 water and 100-times concentrated J-13 water at the three temperatures investigated: 23, 55, and 80°C. The bars indicate the range of values measured, and the symbols indicate the average value. It is clearly seen in all cases that corrosion potentials are more than 100 mV lower in the concentrated solution. It appears that for each environmental condition, in terms of solution composition and temperature, particularly in the concentrated J-13 water, the corrosion potential decreases in the order CDA 102 > CDA 613 > CDA 715. Also, the corrosion potential decreases with increasing temperature, particularly in the concentrated J-13 water. However, due to the lack of control of the environmental conditions in terms of dissolved oxygen concentration, pH, etc. these measurements are only useful for comparative purposes.

Table 7. NOMINAL CHEMICAL COMPOSITION IN WEIGHT PERCENT OF VARIOUS Cu-BASED ALLOYS OF INTEREST IN HIGH-LEVEL NUCLEAR WASTE DISPOSAL PROGRAMS

Alloy	UNS No.	C max	Cr	Cu	Fe	Mo	Ni	Ti	Others
Oxygen Free Cu	C10200	-	-	99.95 min.	-	-	-	-	-
Cu-Al	C61300	-	-	90	2.5	-	-	-	Al = 6.75 Sn = 0.35
Cu-30Ni	C71500	-	-	70	0.4-1 max	-	31	-	-
Cu-Al	C61400	-	-	90	2.5	-	-	-	Al = 7
Cu-10Ni	C70600	-	-	90	1-1.8 max	-	10	-	-

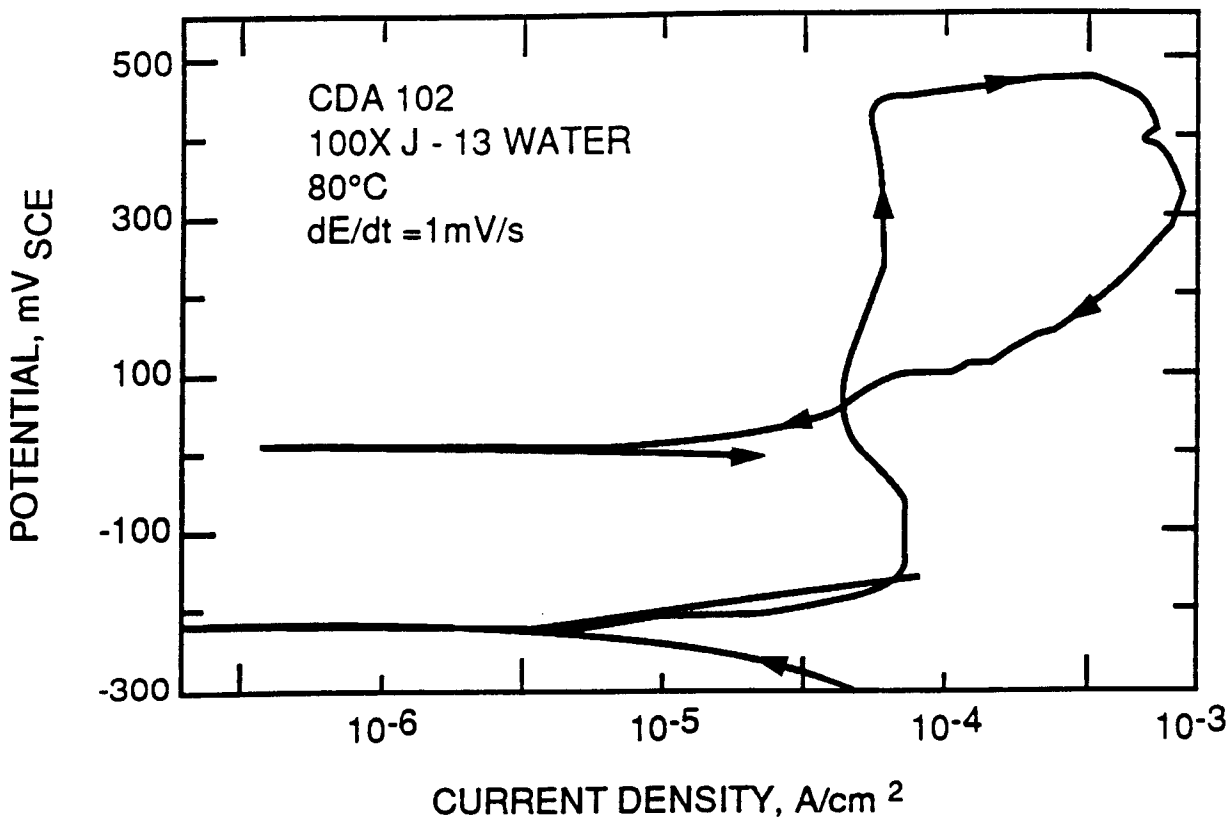

Figure 28. Cyclic polarization behavior of CDA-102 in 100X J-13 water at 80°C. (McCright, 1985).

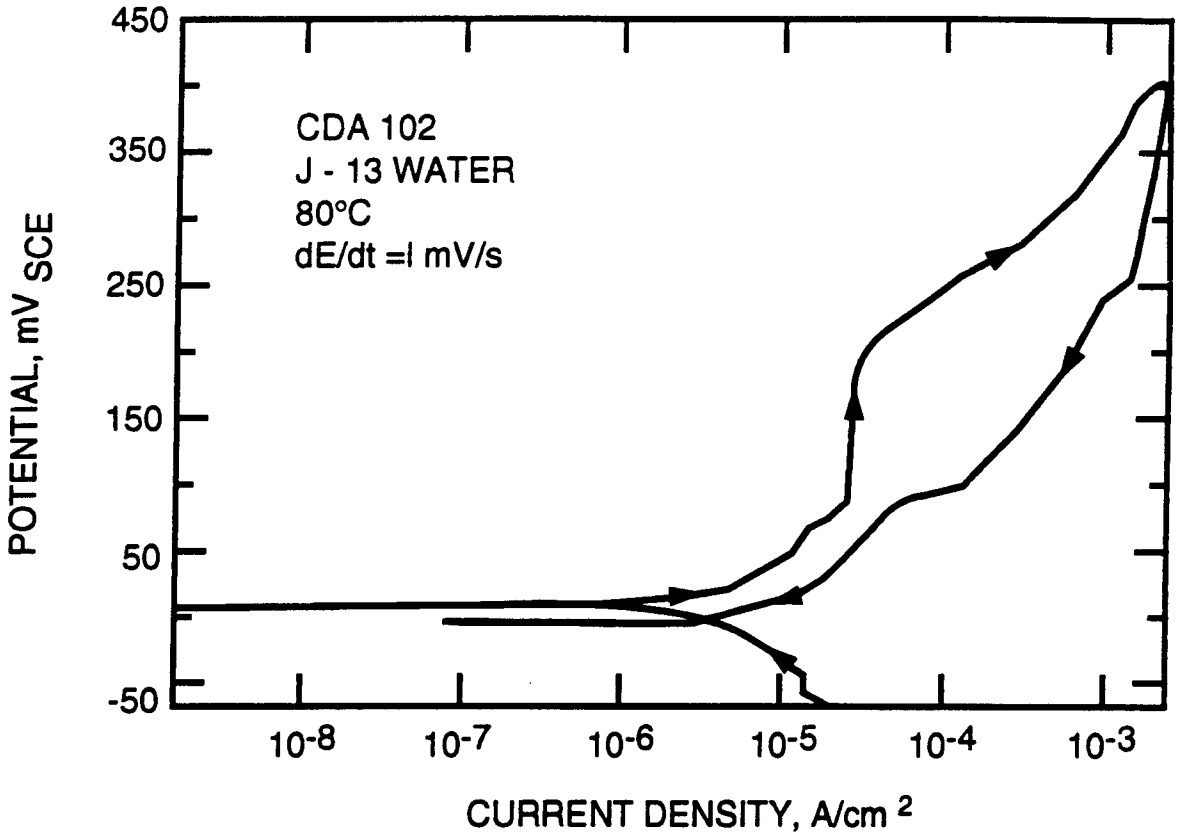

Figure 29. Cyclic polarization behavior of CDA-102 in J-13 water at 80°C. (McCright, 1985).

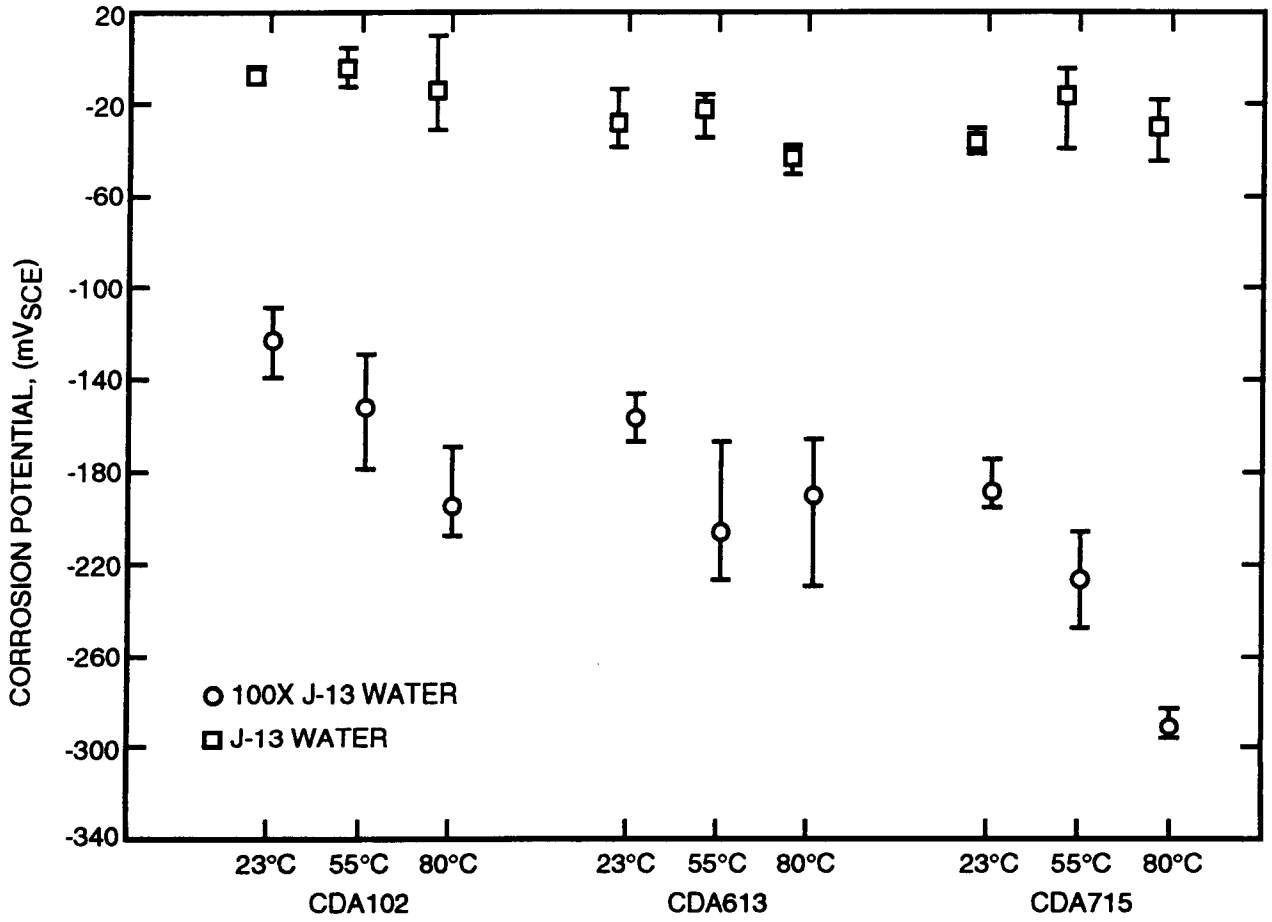

Figure 30. Corrosion potentials of copper alloys in J-13 and 100X J-13 waters vs. temperature. (McCright, 1985).

Pitting potentials are plotted in Figure 31, where the bars and symbols have the same meaning as above, for the three alloys in the various environmental conditions as presented in the original publication. Two aspects should be noted. First, the range of variability in the pitting potential is far more pronounced in the concentrated solution that in the original J-13 water. Secondly, the pitting potential in any given case is significantly higher in the more concentrated solution. However, as seen in Figure 29, there is no clear indication of a breakdown potential in the polarization curves obtained in the original J-13 water. No clear trend in terms of temperature can be discerned from the data reported, although it appears that for all alloys in the concentrated J-13 water, the highest pitting potentials are observed at the intermediate temperature. Also, the alloys exhibited higher pitting potential than pure copper (CDA 102) for most of the environmental conditions tested.

The differences between the pitting potential and the corrosion potential were reported for each alloy in J-13 water and concentrated J-13 water at the three temperatures tested (McCright, 1985). Although large values are displayed, in particular for the concentrated solution, the information cannot be considered relevant. As noted above, the corrosion potentials were measured under conditions which were not well defined and may increase significantly in the presence of higher concentrations of oxygen or other oxidants. On the other hand, it is unfortunate that the repassivation potentials were not reported because this parameter needs to be considered in order to reach a conclusion regarding the susceptibility to localized corrosion of a particular alloy.

One of the main limitations in this study is the possible variation in the composition of the concentrated solution from experiment to experiment that leads to significant variations not only in the pitting potential, but also in the corrosion potential values. As noted by the author, a possible interpretation for the higher pitting potentials observed in the concentrated solution is the effect of inhibiting species that may become more concentrated. In particular, it should be noted that the pH of J-13 water was found to be 7.6 while that of the concentrated solution was 10.3. This difference implies a significant increase in the concentration of OH^- ions which may act as inhibitors for the development of pitting corrosion.

As in the case of austenitic stainless steel, the effect of gamma-radiation on the corrosion potential of CDA 102 and CDA 715 was studied in J-13 water (Glass, 1985). Figure 32 shows the variation of the corrosion potential of CDA 102 with time when the electrochemical cell was exposed to a dose rate of 3.3 Mrad/h. The corrosion potential shifted almost instantaneously to a value which is approximately 100 mV more positive than that in the absence of irradiation. Then, the potential decayed, exhibiting a behavior that is different than that shown in Figure 13 for AISI 316L SS, where the potential remained high for a extended period after a larger increase. Upon termination of the irradiation period, a value similar to that measured prior to irradiation was obtained.

A similar potential vs. time transient was observed for CDA 102 when H_2O_2 was added to unirradiated J-13 water. As in the case of AISI 316L, it was concluded that H_2O_2 generated by gamma radiolysis of water is the species determinant of the potential rise. The authors interpreted the faster decay observed in the case of copper as a result of a catalytic effect of this metal on the decomposition of H_2O_2. Additionally, a more significant effect of irradiation was noted for copper than for the stainless steel. After 15 days of irradiation, relatively severe corrosion was observed in the area exposed to the gaseous phase, probably as a result of the formation of nitrogen oxides.

Cyclic potentiodynamic polarization curves for CDA 102 in 20X concentrated J-13 water at 90°C were conducted to evaluate the effect of gamma-radiation (McCright,

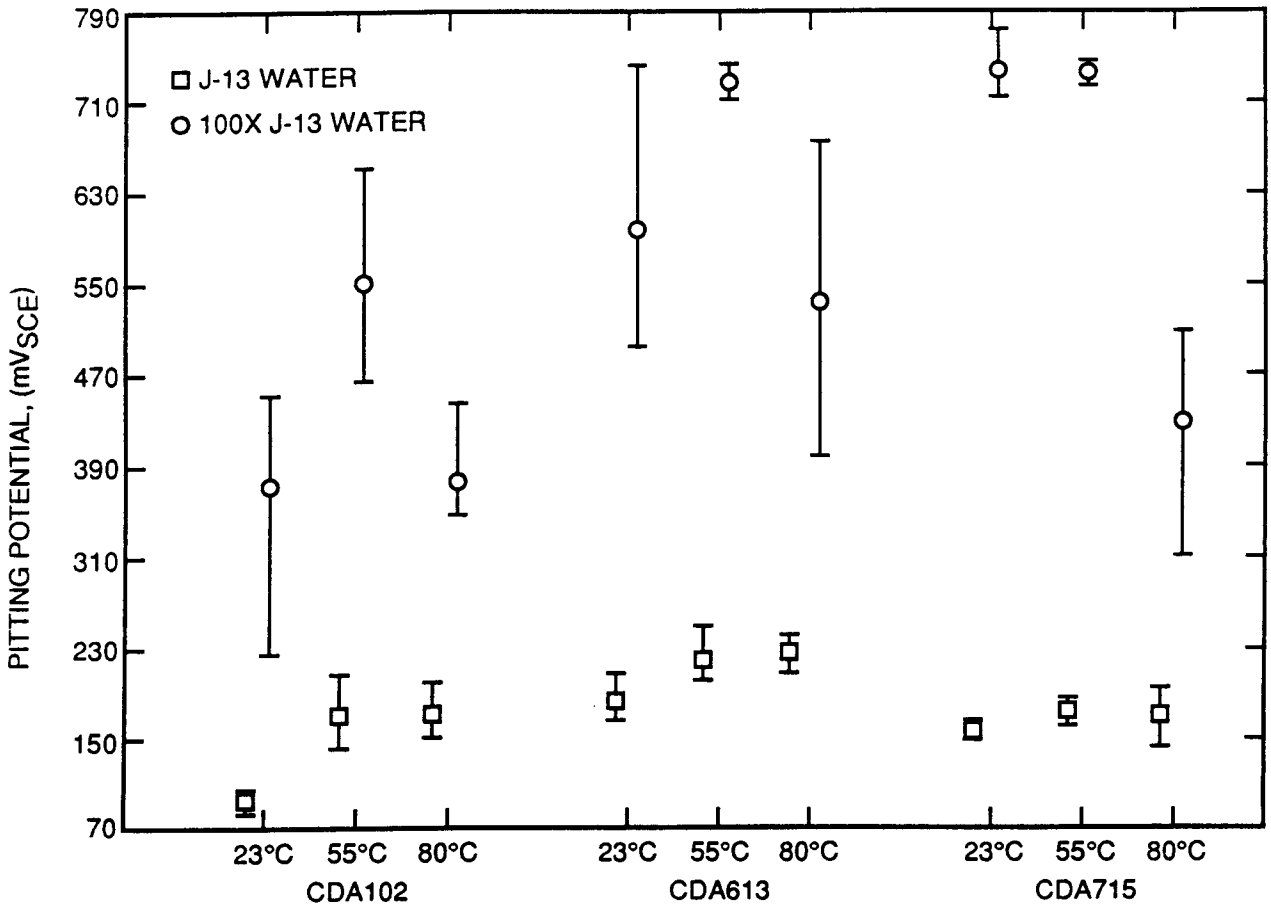

Figure 31. "Pitting potentials" of copper alloys in J-13 and 100X J-13 waters vs. temperature. (McCright, 1985).

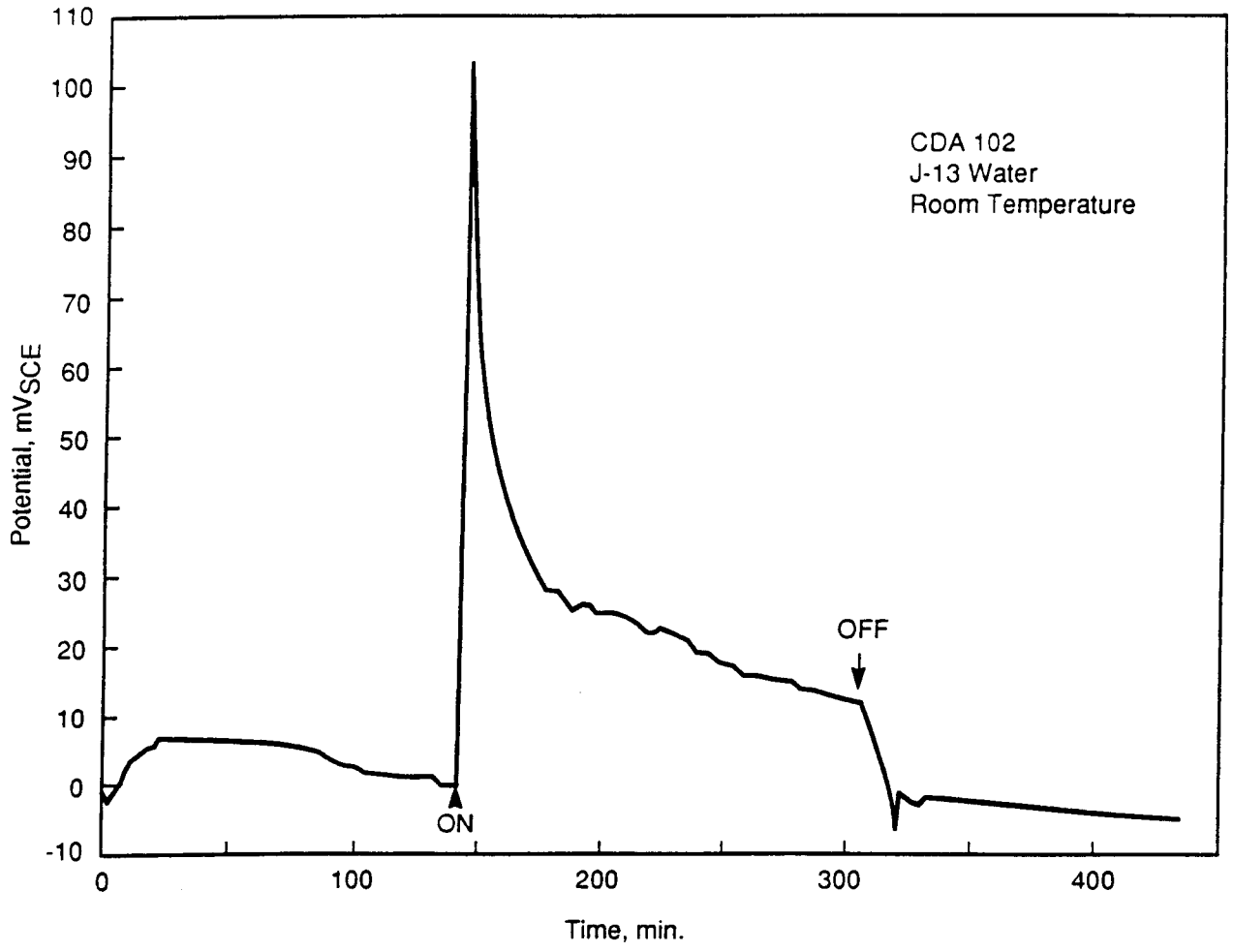

Figure 32. Corrosion potential behavior of CDA-102 in irradiated J-13 water. Gamma irradiation at 3.3 Mrad/h. (McCright, 1985).

1987). As shown in Figure 33, the presence of the gamma radiation field had a very minor effect on the polarization behavior. Apparently, no pitting corrosion occurred under either condition despite the large hysteresis loop.

It is apparent from the results reported above that more work is necessary to evaluate the propensity of the copper-based alloys to localized corrosion. The effect of irradiation on the corrosion of copper in the presence of humid air has been the subject of additional work conducted under DOE sponsorship. This work will be reviewed at a later date in the context of another task in the IWPE program.

4.1.1.2 Cortest Columbus Experimental Results

Two of the three copper-based alloys selected by LLNL have been studied by Cortest Columbus (Beavers, 1988b). They are Oxygen-free Copper (CDA 102) and 70-30 Cupronickel (CDA 715).

In a preliminary set of tests, the anodic behavior of CDA 102 was studied in actual and simulated J-13 well water by using cyclic potentiodynamic polarization curves. The purpose of these tests was to reproduce some of the results obtained at LLNL and validate the use of simulated J-13 water instead of the actual one. Very similar curves were obtained in tests conducted at 80°C at a potential scan rate of 1 mV/s in both environments under aerated conditions, following an initial exposure time of 1-2 hours before polarization. In additional tests, selected experimental conditions were changed, such as an increase in temperature to 90°C, an increase in the waiting period before polarization to 15 hours, and a decrease in the potential scan rate to 0.167 mV/s to attain anodic curves which were considered to be more representative of steady state conditions. A breakdown potential of 130 mV_{SCE}, which is approximately 120 mV lower than that determined at 60 mV/min, was measured at the low potential scan rate, but practically no difference was observed in the repassivation potential ($\sim$ -70mV_{SCE}).

Additional polarization curves were obtained in simulated J-13 water containing 1000 ppm Cl^-. For CDA 102, no region of passive behavior was observed and the current increased rapidly when the potential was scanned upwards from the corrosion potential ($\sim$ -80 mV_{SCE}). During the reverse scan, pronounced hysteresis was observed suggesting that localized corrosion occurred. However, no pitting or other form of localized corrosion was detected. The authors considered this an unusual observation, because they only observed a pronounced change in film coloration. Similar results were obtained for CDA 715. The breakdown potential was found to be around 180 mV_{SCE} in simulated J-13 water, whereas, in the presence of 1000 ppm Cl^- decreased to -30 mV_{SCE}. In both solutions significant hysteresis was noted but, as in the case of CDA 102, it was not related to localized corrosion.

The same statistical approach discussed above for AISI 304L SS and alloy 825 was used by Beavers and Thompson to evaluate the effect of environmental variables on the localized corrosion of CDA 102 and CDA 715 (Beavers, 1988b). In the case of the Copper-based alloys, the authors noted that pitting corrosion did not occur in many solutions although the cyclic polarization curves exhibited significant hysteresis. For that reason, they decided to replace the term "pitting potential" with "breakdown potential" in the description of their results.

By analyzing the test matrix it can be concluded that pitting corrosion of CDA 102, although detected in few solutions, was more commonly observed at 50°C than at 90°C and

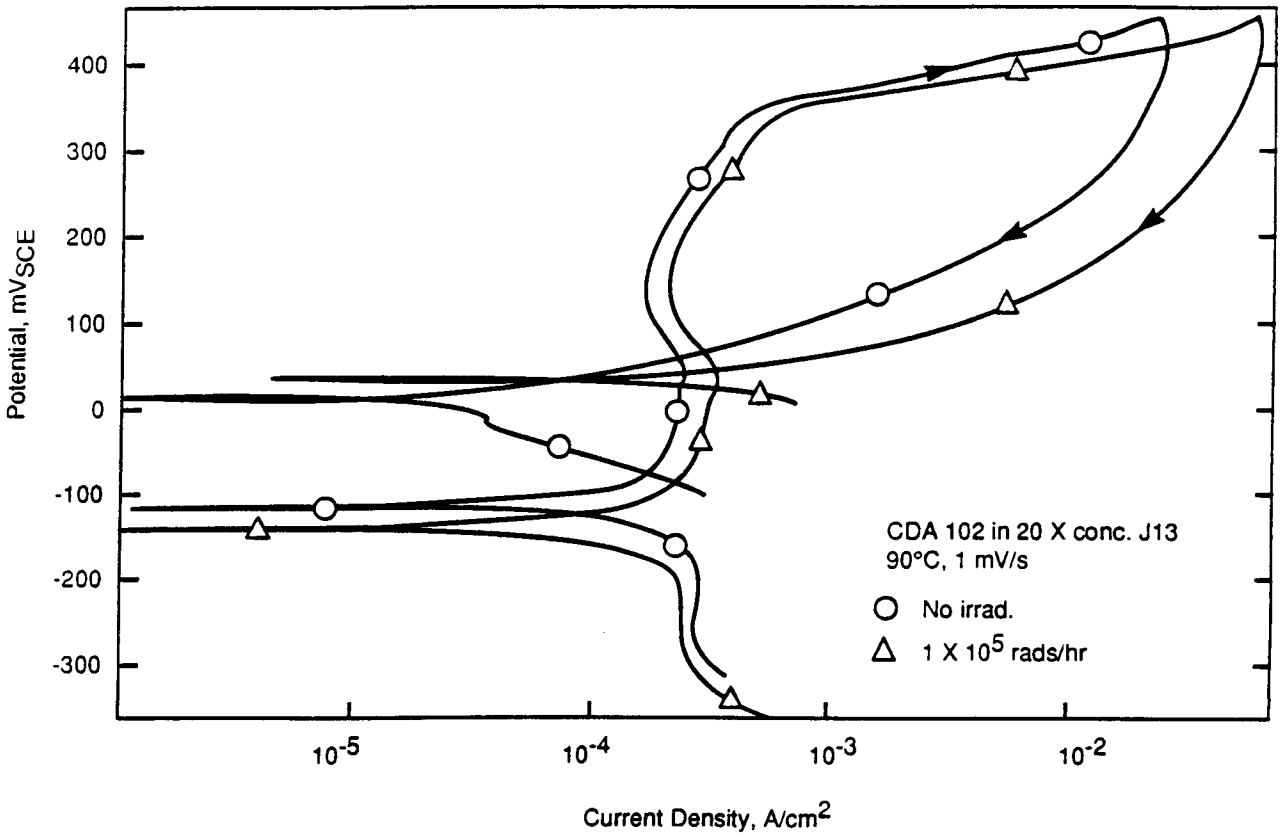

Figure 33. Effect of gamma irradiation on the cyclic polarization behavior of CDA-102 in 20X J-13 water at 90°C. (McCright, 1987).

also at pH 10 rather than at pH 5. It is also interesting to note that in these cases pitting occurred regardless of the Cl^- content, since it was observed in solutions containing 5 ppm as well as 1000 ppm. It is not possible to establish a trend in terms of the Cl^-/HCO_3^- concentration ratio. In several other solutions locally active attack was the dominant form of corrosion attack, as characterized by Beavers and Thompson.

The statistical analysis of the data was performed to assess the effect of the different environmental variables on the electrochemical parameters. As shown in Figure 34, Cl^- is the single anion that decreased the breakdown potential of CDA 102. On the other hand, the breakdown potential increased by the action of silicon, HCO_3^- and pH. Regarding the repassivation potential, it should be noted that its decrease is promoted by Cl^- and oxalic acid, whereas, its increase is due to silicon, F^- and NO_3^-. It is difficult to compare these results with observations reported in the literature. Pitting of copper has been observed in natural waters in the presence of relatively low concentrations of Cl^-, but at temperatures lower than 60°C, the presence of HCO_3^- and SO_4^{2-} in certain minimum concentration ratios with respect to Cl^- is required (Campbell, 1972). In addition, pitting corrosion occurs when the potential of the metal is above a critical value that in the particular case of copper corresponds to the equilibrium electrode potential for the couple Cu/Cu^{2+} (Pourbaix, 1972). It is assumed that in the acid solution existing inside pits, the stable species is Cu^{2+}, but outside the pits, precipitation of basic cupric carbonate occurs.

The effect of the environmental variables on the corrosion potential of CDA 102 is illustrated in Figure 35. As expected E_c increases with increases in the concentration of O_2 and H_2O_2, whereas, HCO_3^-, PO_4^{3-}, temperature, and pH have the opposite effect. It also appears that Si increases the corrosion potential, which is not the case for CDA 715. For this alloy Si, HCO_3^-, F^-, Cl^-, PO_4^{3-} and temperature decreases E_c, whereas, H_2O_2 is the single species that increases E_c. The effect of different species on the breakdown and repassivation potentials of CDA 715 is even more difficult to understand on the basis of the existing knowledge. No effect of Cl^- on the breakdown potential was found, although this anion decreases the repassivation potential. The breakdown potential is increased only by HCO_3^- and pH, whereas, many species have an effect on the repassivation potential. This is increased by the presence of Si, HCO_3^-, Mg^{2+} and oxalic acid, whereas, both Cl^- and NO_3^- have the opposite effect.

There were some tests in which pitting was detected, such as those quadruplicate tests in which the intermediate values of all the variables were studied. As illustrated in Figure 36, despite some variation in the value of the breakdown potential between different tests, the repassivation potential was practically the same. In this case the concentration of Cl^- was 250 ppm, whereas, that of HCO_3^-, which was found to be a strong inhibitor, was 500 ppm. Nevertheless, as noted above, pitting was observed.

In an attempt to understand the reasons for the occurrence of large hysteresis in the cyclic polarization curves without the concurrent development of localized corrosion, Beavers and Thompson (Beavers, 1989a) conducted several potentiostatic tests. The specimens were polarized by increasing the potential in 50 mV steps from the corrosion potential until a preselected potential was reached. At this constant potential, the current was monitored as a function of time for a certain period. The weight loss of the specimen was determined at the end of experiment. As an example, Figure 37 shows the method adopted by the authors for the presentation of their data in the case of CDA 715 exposed to J-13 water containing 1000 ppm Cl^- at 90°C. With the background of the cyclic polarization curve, the variation of current density during the period in which the specimen was potentiostated is represented by a horizontal arrow that extends from the initial to the final current density in the position

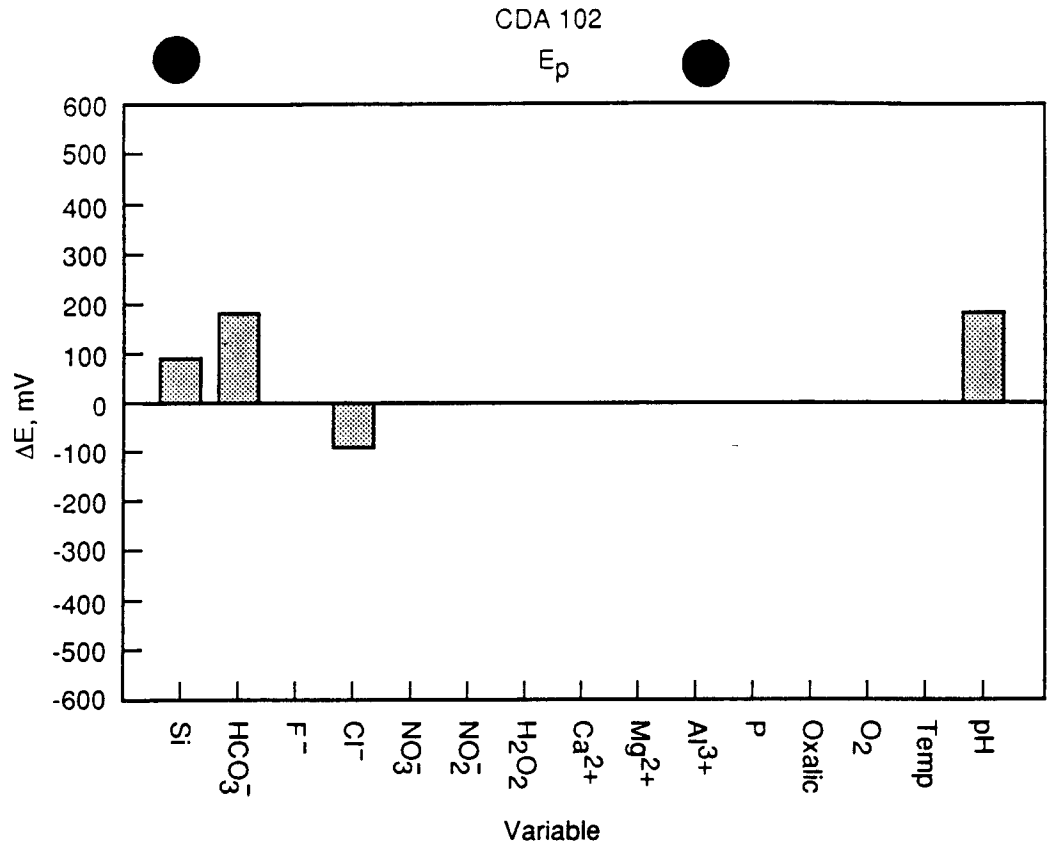

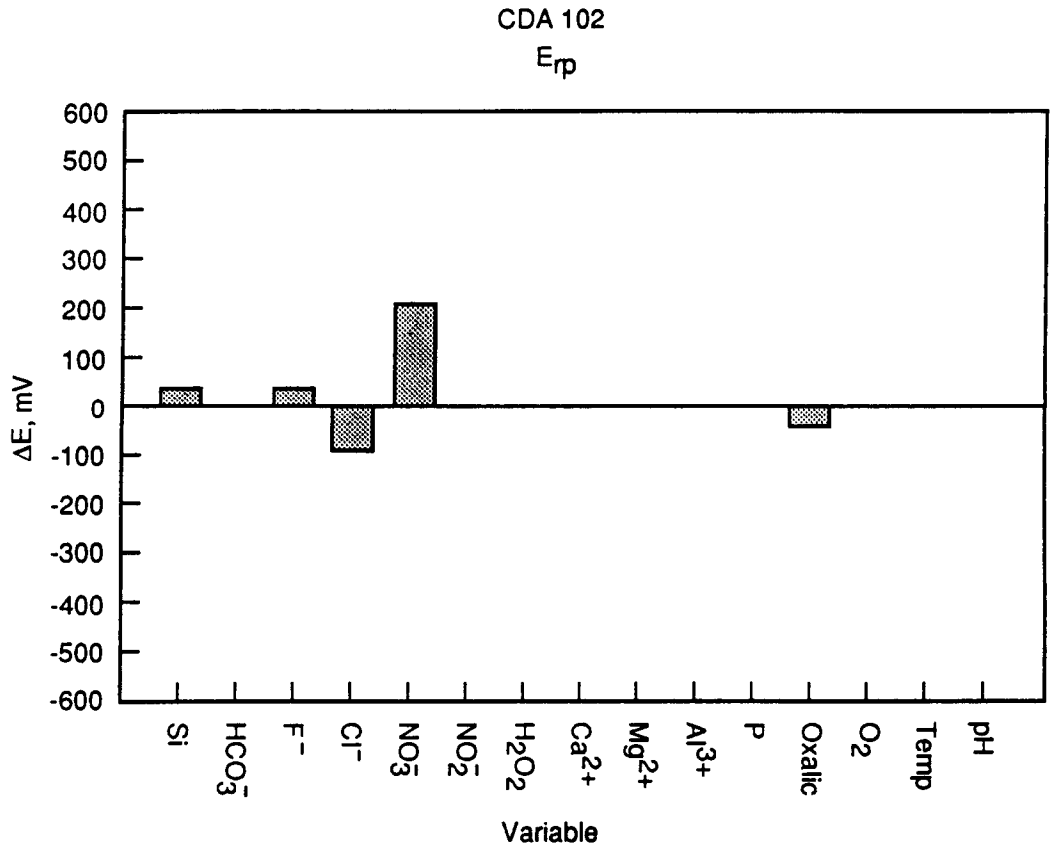

Figure 34. Amplitude of changes in E_p and E_{rp} due to changes in environmental factors (from min. to max.) as calculated by multiple regression analysis. CDA-102. (Beavers, 1990a).

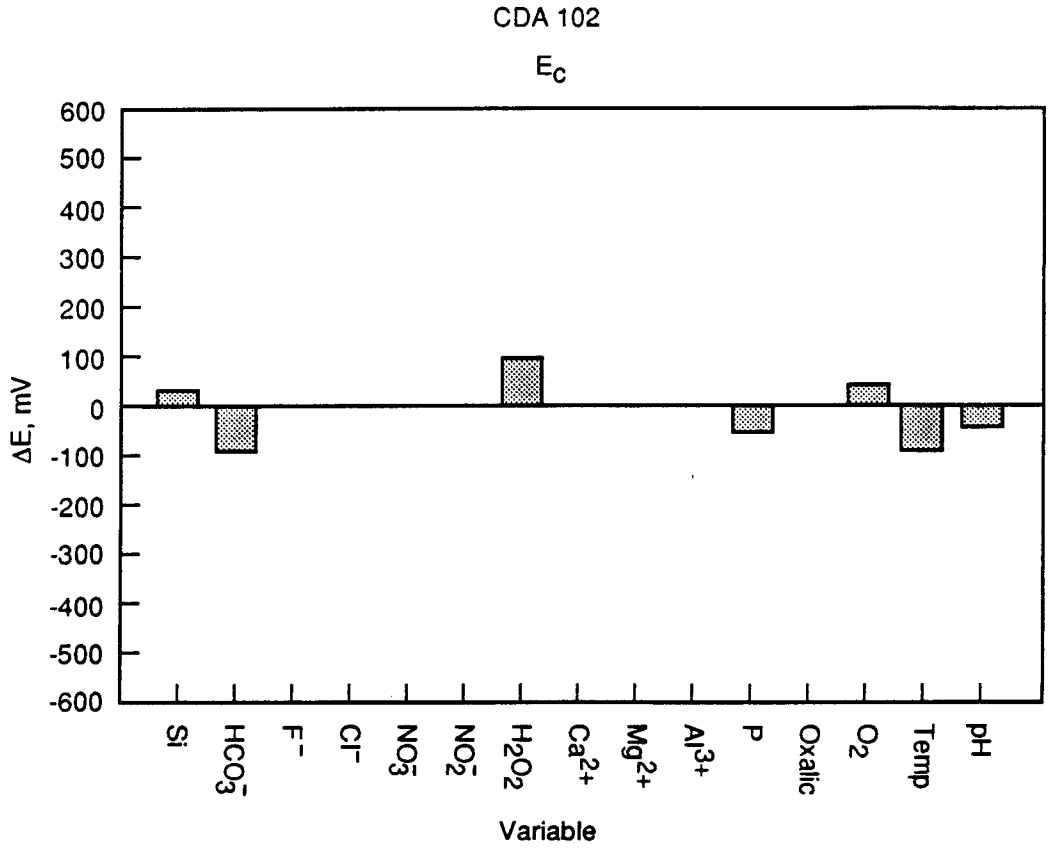

Figure 35. Amplitude of changes in E_c due to changes in environmental factors (from min. to max.) as calculated by multiple regression analysis. CDA-102. (Beavers, 1990a).

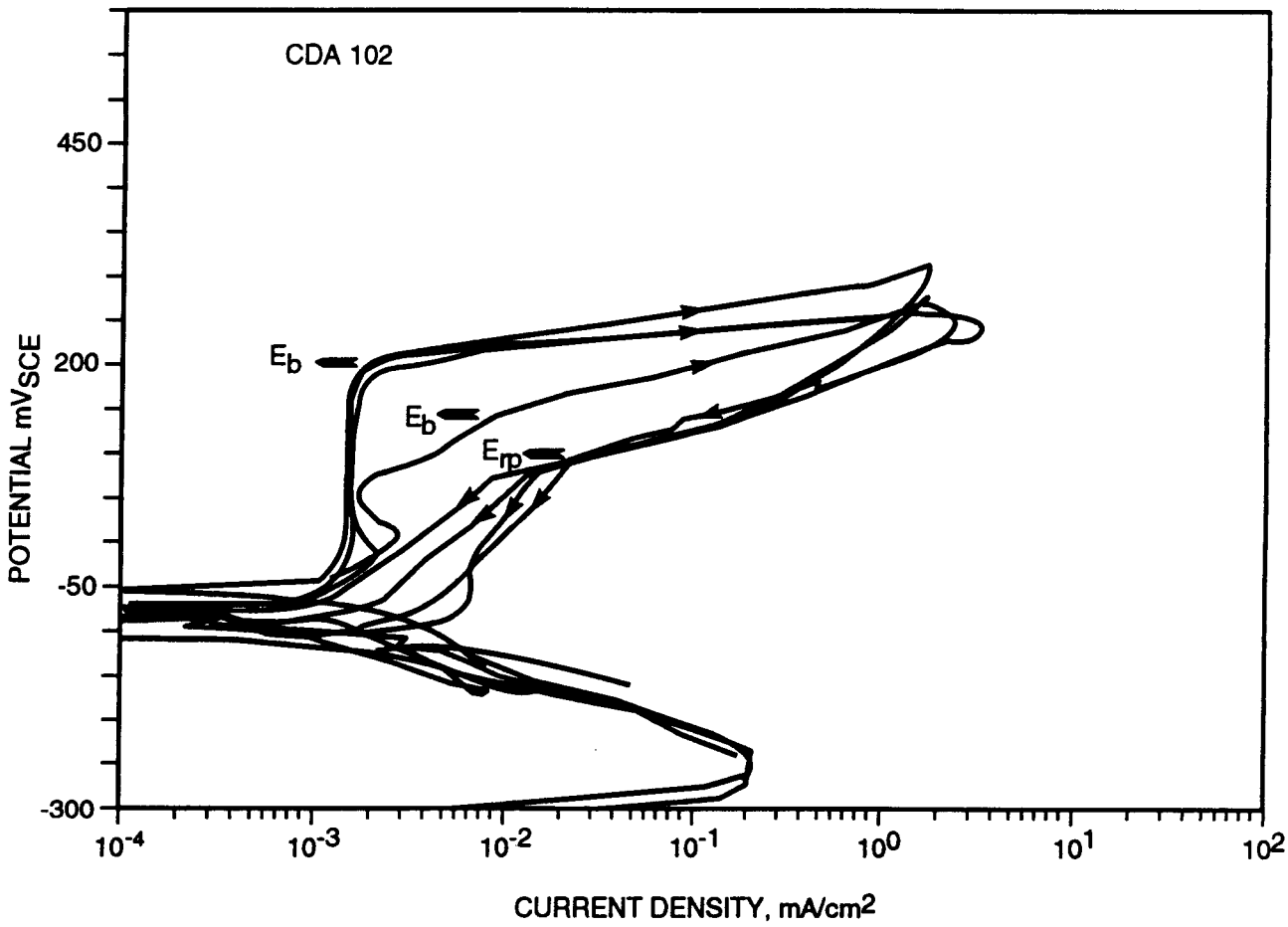

Figure 36. Cyclic polarization curves for multiple samples of CDA-102 in model test solution containing: 250 ppm Cl^-, 500 ppm HCO_3^-, 50 ppm F^-, 250 ppm NO_3^-, 50 ppm NO_2^-, 50 ppm H_2O_2, 50 ppm Oxalic, 15 ppm O_2 and at a pH of 7.5. Temperature: 70°C. (Beavers, 1988b).

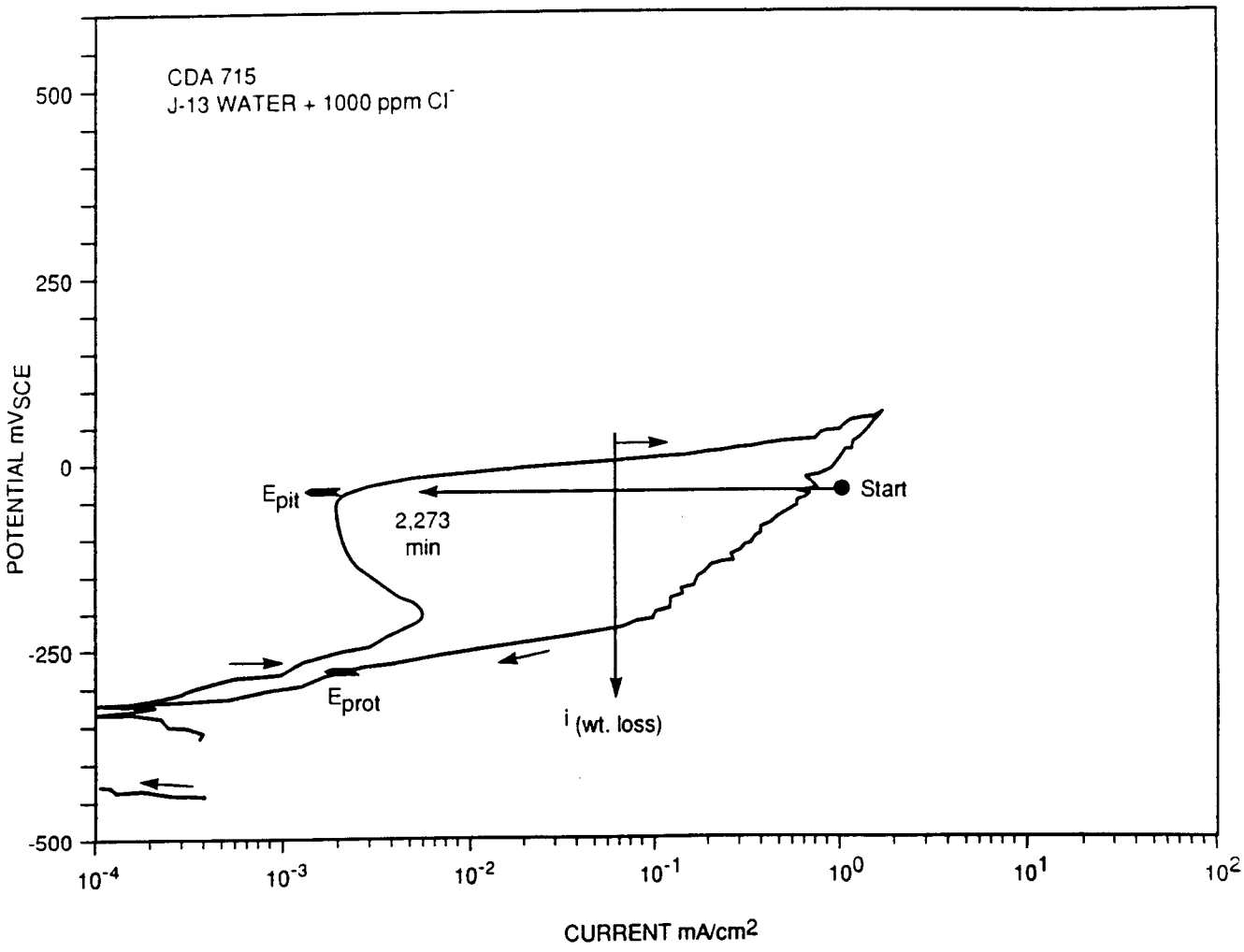

Figure 37. Effect of potentiostatic polarization at -40 mV SCE on the anodic current vs. time for CDA-715. The potentiostatic behavior is superimposed on cyclic polarization curve. No pitting, but severe active attack was observed. (Beavers, 1989a).

corresponding to the applied potential. The vertical arrow indicates the calculated current density corresponding to the measured weight loss.

A qualitative agreement between the weight loss measurements and the variation of current density was found in most of the cases studied, since the current density calculated from the weight loss lies within the current density range observed, as shown in Figure 37. Although hysteresis was found in the potentiodynamic curve, no pitting initiation was observed in the potentiostatic test and the current, as illustrated in Figure 37, decreased to passive values. The authors remarked that an active attack, though somewhat localized, occurred underneath a corrosion product layer.

Several other cases of anodic behavior than cannot be interpreted unequivocally from the analysis of the cyclic polarization curves were reported for both CDA 102 and CDA 715 in some of the solutions used in the statistical test matrix. Beavers and Thompson concluded that hysteresis in the cyclic polarization curves for the copper-based materials does not necessarily correspond to the growth of pits. In some cases the dominant form of corrosion was found to be a local active attack underneath an oxide or a corrosion product layer.

It is unfortunate that in this extensive work no analysis of the composition of the films and/or corrosion product layers by using surface analytical techniques is reported. These types of observations may become extremely useful to interpret the localized corrosion behavior in terms of film stability as related to the composition of the environment. It could be also particularly useful for analyzing the results of long-term tests. The authors commented that the potentiostatic current density vs. time curves exhibited various patterns indicating anodic behaviors that make long-term prediction from the cyclic polarization curves difficult. Unfortunately, these curves were not reported and therefore it is not possible to analyze them in terms of passivation, dissolution-precipitation processes, etc. In most of the cases, the authors indicated that no pitting was observed and instead a severe locally active attack developed.

A set of experiments to study pit propagation was conducted using an artificial pit geometry (Beavers, 1989b). The pit cavity was packed with a corrosion product paste to create occluded cell conditions and accelerate the initiation of pit propagation. The same configuration was used previously in a study of the localized corrosion of carbon steels in simulated groundwater for the basalt repository project (Beavers, 1987; Beavers, 1990). With this geometry the current flow between the artificial pit and the boldly exposed surface (BES) was monitored by means of a zero resistance ammeter.

The alloy studied was CDA 102 exposed to one of the solutions used in the statistical test matrix at 90°C. The solution was selected because it was found to promote pitting of CDA 102 at 50°C with a pitting potential of 60 mV_{SCE} and a repassivation potential of 20 mV_{SCE}. The solution contained 1000 ppm Cl^-, 1000 ppm NO_3^-, 10 ppm HCO_3^-, and 1 ppm F^- as predominant anionic species and had a pH equal to 10.

Several experiments were conducted in which the aspect ratio of the pit was changed from 1:5 to 1:2; a paste originally made with cuprous oxide was replaced by one formed with products of the anodic dissolution of copper in the same solution and, finally, cathodic polarization of the uncoupled pit was tried in different attempts to promote pit propagation (Beavers, 1989b; Beavers, 1990a). Only in the presence of 200 ppm H_2O_2 in the solution was a substantial galvanic current measured. However, as a result of the relatively rapid decomposition of H_2O_2, successive additions on a daily basis were necessary to maintain the activity of the pit. In this case the potential of the BES was

temporarily above the E_p for CDA 102 in the same solution and weight-loss measurements at the end of the experiment revealed corrosion rates in qualitative agreement with the magnitude of the galvanic current and the polarity of the pit/BES couple.

A typical anodic current transient for the experiment described above is shown in Figure 38. It can be noted that the current decreased to very low values, and even turned negative, after approximately 200 min following the addition of H_2O_2. By using a microcapillary the potential was measured down the depth of the artificial pit with the pit and the BES coupled, before and after the addition of H_2O_2. As shown in Figure 39, a potential gradient of about 100 mV from the mouth to the tip of the pit developed after the H_2O_2 addition, whereas, no such gradient existed prior to the addition. The potential gradient indicates that an anodic current was flowing from the pit in correspondence with the anodic transient presented in Figure 38.

Additional experiments were described (Beavers, 1990a) in which the role of H_2O_2 was simulated potentiostatically. It is, however, unfortunate that no additional experiments were done under naturally corroding conditions using different concentrations of oxygen or other oxidizing species of interest in solution. Nevertheless, it should be recognized that further work according to a planned test matrix for copper base alloys, including CDA 102 and CDA 715, in which J-13 water and solutions selected on the basis of the cyclic polarization tests would be used, was not conducted due to the termination of the program. Apparently, no work using the artificial pit geometry was planned for the Fe-Cr-Ni-Mo alloys.

4.1.2 Crevice Corrosion Studies

4.1.2.1 DOE and LLNL Experimental Results

No experimental studies on crevice corrosion of copper and copper-based alloys have been reported by DOE. As a result of a literature survey (Farmer, 1988b), crevice corrosion was not considered a severe limitation for this class of alloys and other areas of research were prioritized. However, it should be noted that in many applications localized corrosion of these alloys (in the form of pits) takes place under deposits and, therefore, can be considered as a particular case of crevice corrosion.

McCright et al. (McCright, 1987) have concluded in a previous report that water of a composition similar to J-13 water should not be particularly corrosive to copper. They have claimed that the relatively high ratio of bicarbonate to sulfate is expected to mitigate localized attack. In particular, they have pointed out that J-13 water does not contain significant concentrations of species, such as Fe^{3+} and manganese ion (sic), that are known to favor pitting attack in copper-base alloys. In addition, they noted that sulfide ion, which is a harmful species able to promote localized corrosion on copper and copper-base alloys, is not expected to be found under the mildly oxidizing conditions of the repository. Most of these statements were included previously in a review of the literature prepared for the Copper Development Association (Myers, 1986) and included as an Appendix in the publication of a workshop on Copper-Base Waste Package Container Materials (Van Konynenburg, 1990). In this specific review, most of the scarce experimental work quoted in support of those statements was obtained in tests conducted under a limited set of environmental conditions, typical of flowing water systems.

4.1.2.2 Cortest Columbus Experimental Results

Very limited work on crevice corrosion of copper-base materials has been conducted by Cortest Columbus. Long-term exposure tests, in which simulated J-13 water was allowed

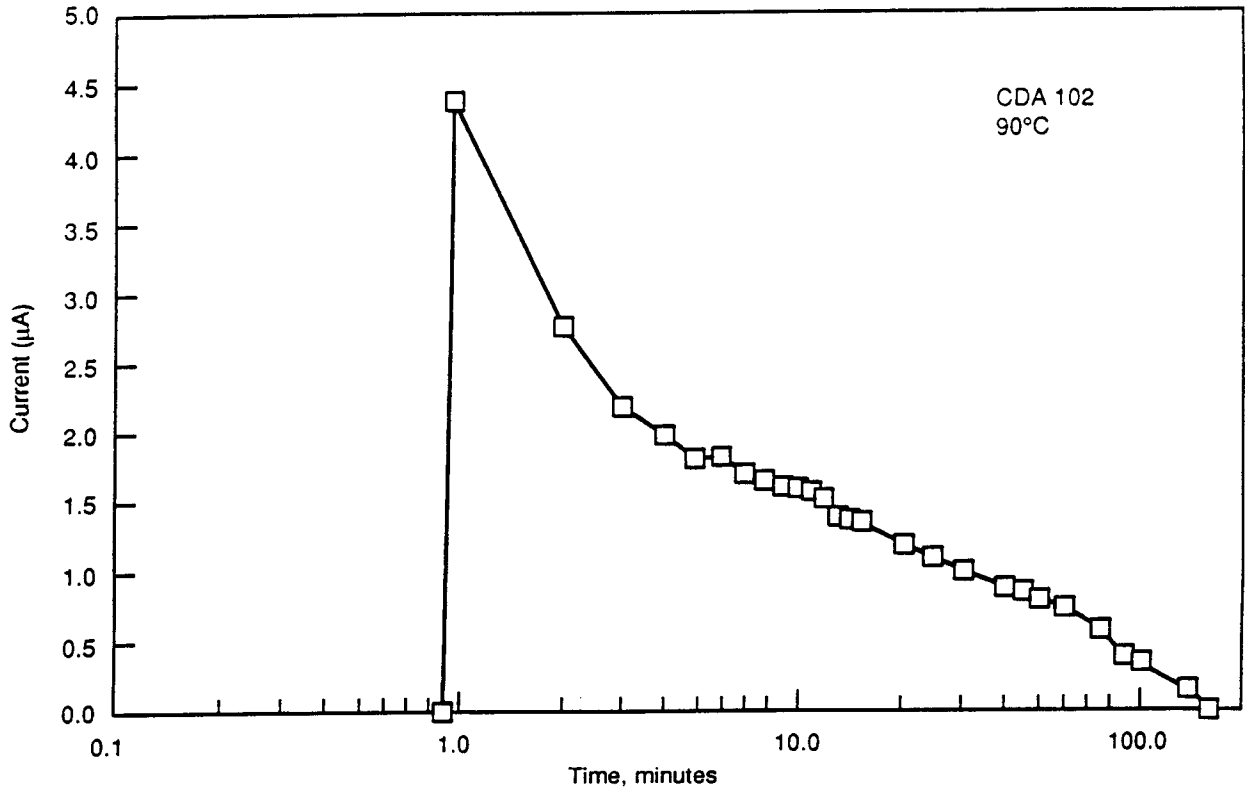

Figure 38. Typical anodic current transient for CDA 102 following addition of H_2O_2. Solution: 1000 ppm Cl^-, 10 ppm HCO_3^-, 1000 ppm NO_3^-, 200 ppm H_2O_2, 200 ppm oxalic, pH 10, temp. 90°C. (Beavers, 1989b).

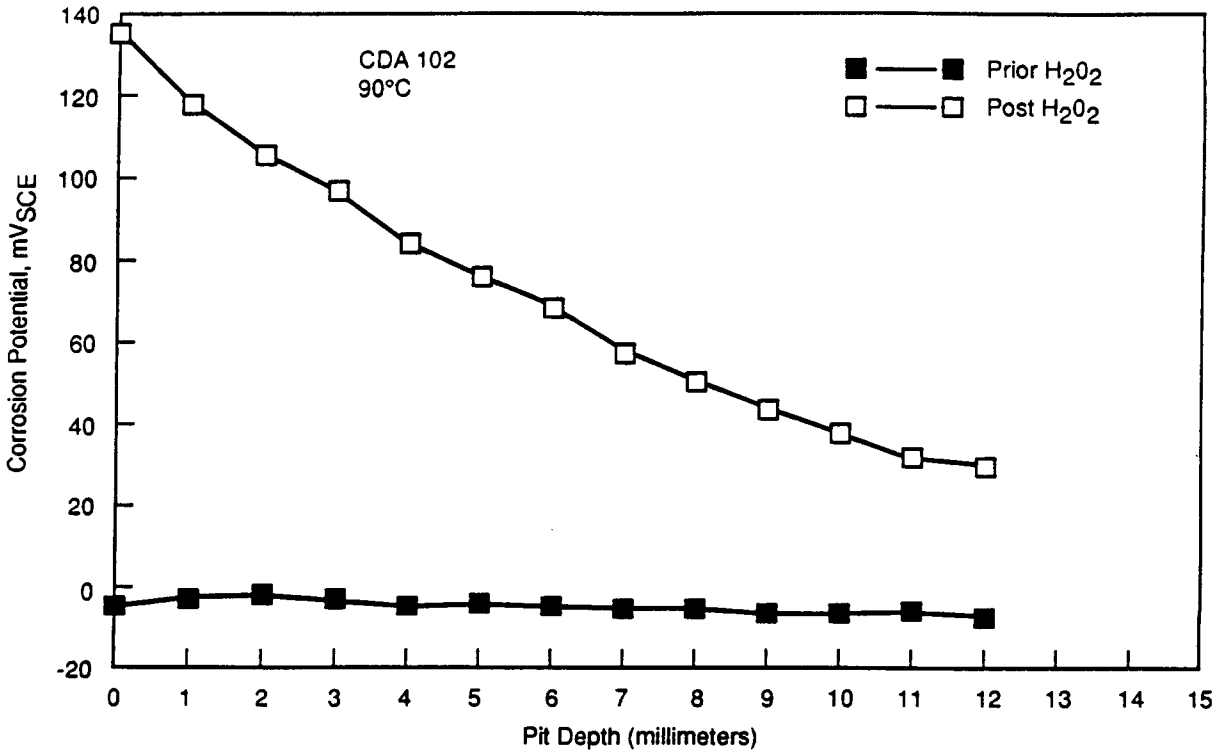

Figure 39. Potential vs. depth in an artificial pit specimen of CDA-102. Solution: 1000 ppm Cl^-, 10 ppm HCO_3^-, 1000 ppm NO_3^-, 200 ppm H_2O_2, 200 ppm oxalic, pH 10, temp. 90°C. (Beavers, 1989b).

to boil-down, were conducted for up to 8064 hours, as described for AISI 304L SS and alloy 825 in Section 3.1.2. Optical examination and weight-loss measurements were made on CDA 102 and CDA 715 coupons provided with serrated PTFE washers to create a crevice. In the case of CDA 715, a corrosion rate of 0.02 μm/y was reported. Very light scaling was noted accompanied by localized etching in the crevice area. For CDA 102, the corrosion rate was found to be 0.65 μm/y after 8064 hours exposure, but for 4033 hours exposure, the corrosion rate was 1.16 μm/y. This seems to indicate a decrease in the corrosion rate with time. Heavy etching of the specimens was reported, as well as slight pitting for only one of the three specimens removed after 4033 hours.

Corrosion potentials were also measured as a function of time. The potential for CDA 715 was consistently higher than that of CDA 102. For CDA 715, the potential varied between -80 and -175 mV_{SCE}, whereas, for CDA 102, the potential ranged from -150 to -300 mV_{SCE}.

No crevice corrosion has been observed in these tests. However, due to the limited scope of these tests, it cannot be concluded that the copper base alloys are not susceptible to crevice corrosion under the environmental conditions of the tuff repository. It is apparent that more systematic work is necessary in this area.

4.2 GENERAL LITERATURE

Unlike the case of Fe-Cr-Ni-Mo alloys, localized corrosion in Cu-base alloys can occur in a variety of forms under a variety of seemingly disparate environmental conditions. In the literature, localized corrosion of copper and copper alloys has been discussed under a variety of categories: 1. Type-1 localized corrosion that occurs at relatively low temperatures in hard waters (Campbell, 1974; Pourbaix, 1974), 2. Type-2 localized corrosion which occurs at higher temperatures mainly in soft waters (Mattsson, 1968; Shalaby, 1989), 3. "Horse Shoe" type localized corrosion under turbulent flow conditions (Bianchi, 1978), 4. Localized corrosion in the presence of sulfides such as in polluted waters (Syrett, 1980), 5. Crevice corrosion in chloride environments (Efird, 1977), and 6. A more recent type of pitting corrosion morphology termed "Ant-nest Corrosion" (Notoya, 1990). Other forms of localized corrosion include dealloying type corrosion for Cu-Al and Cu-Ni alloys and microbiologically influenced corrosion. However, only the localized corrosion occurring in soft waters at higher temperatures and crevice corrosion are of interest for the repository environment and these will be examined. Localized corrosion in hard waters at low temperatures will also be included because of the extensive research in this area and because some of the conclusions from these investigations can be extended to the soft waters. Ant-nest corrosion seems to be a new type of corrosion mainly observed due to exposures to organic chlorides (e.g., degreasers) and in some wet-dry environments. Because of the lack of sufficient information available on this form of corrosion, it will not be discussed in this report.

4.2.1 Pitting in Hard and Soft Waters - Effect of Environmental Variables

Pitting in hard waters and at low temperatures (close to ambient temperatures) has been observed to be shallow and wide and covered by a thick corrosion product of malachite ($CuCO_3 \cdot Cu(OH)_2$). Inside these pits, are found layers of CuCl and crystallites of Cu_2O (Campbell, 1974; Shalaby, 1989). The reactions occurring inside these pits have been examined by Pourbaix (Pourbaix, 1974) in terms of an equilibrium between copper, Cu_2O, and CuCl. This is shown in Figure 40. Pourbaix proposed the following reactions as governing the behavior of copper inside pits or occluded areas:

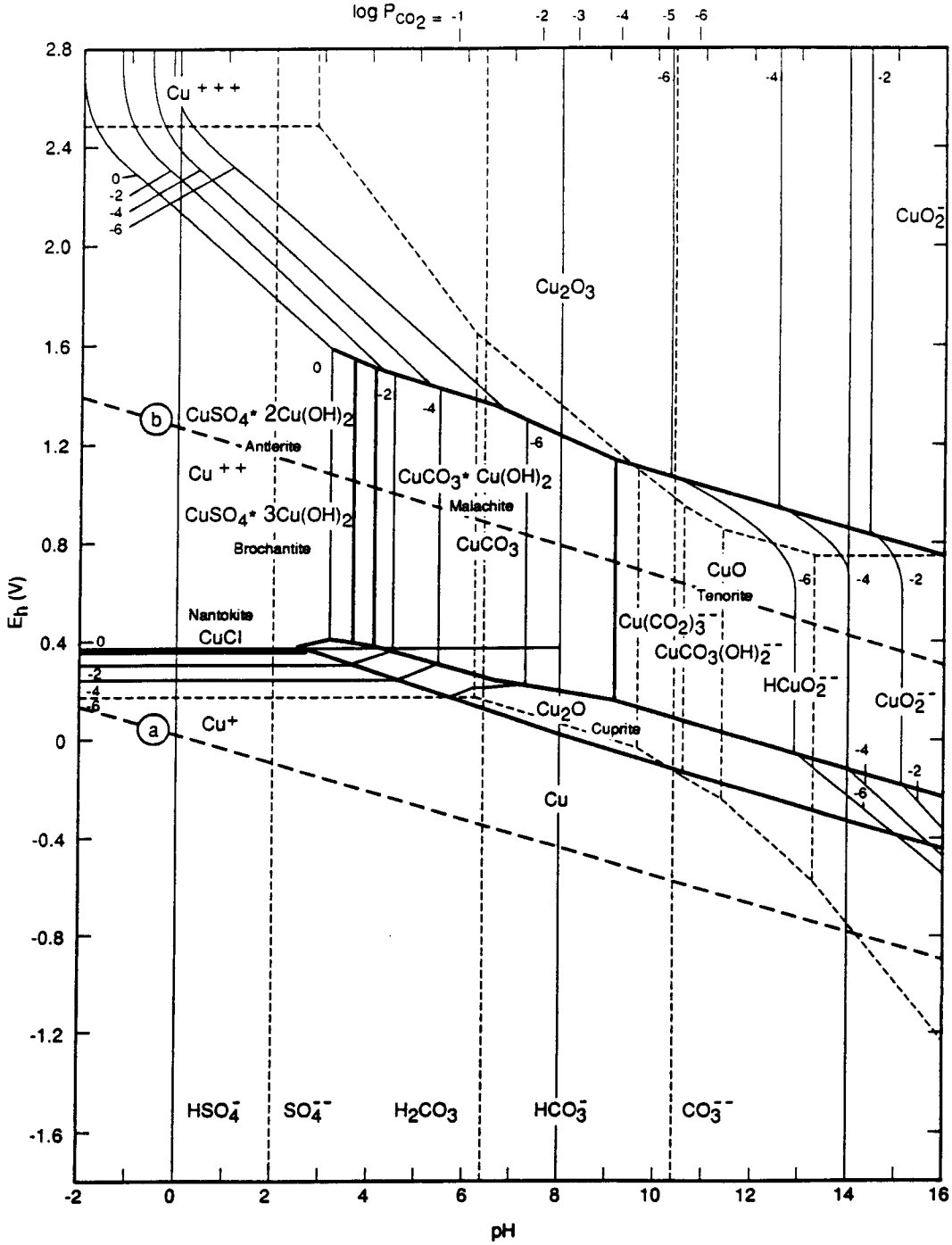

Figure 40. Potential-pH equilibrium diagram for copper in the system: $Cu\text{-}Cl^-\text{-}SO_4^{2-}\text{-}H_2O$ at 25°C (for solutions containing Cl^-: 22 ppm, CO_2:229 ppm and SO_4^{2-}:46 ppm). (Pourbaix, 1974).

$$Cu = Cu^{+} + e^{-} \; ; \; E = 0.520 + 0.059\,Log\,(Cu^{+}) \tag{12}$$

$$Cu = Cu^{2+} + 2e^{-} \; ; \; E = 0.337 + 0.0295\,log\,(Cu^{2+}) \tag{13}$$

$$Cu + 2Cl^{-} = CuCl_2^{-} + e^{-} \; ; \; E = 0.208 + 0.0591\,log\,(CuCl_2^{-}) - 0.118log\,(Cl^{-}) \tag{14}$$

$$Cu + Cl^{-} = CuCl + e^{-} \; ; \; E = 0.137 - 0.0591\,log\,(Cl^{-}) \tag{15}$$

$$2CuCl + H_2O = Cu_2O + 2Cl^{-} + 2H^{+} \; ; \; pH = 5.66 + log\,(Cl^{-}) \tag{16}$$

with electroneutrality dictated by:

$$2(Cu^{2+}) + (Cu^{+}) + (H^{+}) = (Cl^{-}) + (CuCl_2^{-}) + (OH^{-}) \tag{17}$$

Based on the above reactions, copper dissolves to form cuprous ions which react to form cuprous chloride. Since cuprous chloride is stable only in acidic conditions, it hydrolyses in neutral water to form acidic conditions inside the pit. At 25°C, Pourbaix predicted that the concentration of chloride inside a pit will be about 265 ppm and the pH will be about 3.5. Additionally, both experiments and theory concluded that the behavior of copper inside the pits was reversible and the potential inside the pit was 20 mV vs. SCE. Above this potential, copper dissolved to release Cu^{+} and below this potential copper plated out from Cu^{+}. Since there is a diffusion potential difference between the inside and outside of the pits, the potential outside was approximately 150 mV more positive than the inside the pit. By this reasoning, Pourbaix rationalized the observed phenomena of protection potential for copper in cold Brussels water of about 170 mV vs. SCE. One can also understand on the basis of this reasoning why deposition of a carbon film on the inner walls of copper tubing is detrimental to hard water pitting. Carbon acts as a cathodic site polarizing the copper to a higher potential than 170 mV vs. SCE. Formation of malachite ($CuCO_3 \cdot Cu(OH)_2$) is incidental in this model since it will occur (with reference to Figure 40) on the outside in the presence of CO_2 and at high anodic potentials set up by the presence of oxygen or carbon.

Thomas and Tiller (Thomas, 1972a, 1972b) studied the breakdown of protective films on copper systematically in various mixtures of $NaHCO_3$ and NaCl. The effect of bicarbonate on anodic behavior of copper at 25°C is shown in Figure 41 (Thomas, 1972a). It can be seen that bicarbonate additions increase the "passive" region of the electrochemical response of copper and increase the breakdown potential i.e., the potential at which a dramatic increase in current was observed. Examination of the samples exposed to conditions beyond the breakdown potential revealed deep, narrow pits. The surface film formed in the passive region was found to be mixture of Cu_2O and $Cu(OH)_2$ with increasing amounts of Cu_2O with increasing HCO_3^{-}. The breakdown potentials were decreased only slightly by the addition of up to 0.1M Cl^{-} to a 0.1M HCO_3^{-} solution. However, addition of chloride resulted in the formation of a mixture of CuCl and malachite film. The addition of 1M Cl^{-} resulted in general corrosion because of the unprotective nature of the CuCl film. It was also observed that the localized corrosion was a function of time in the chloride solution. If the samples were maintained in the open-circuit condition for 24 hours before polarization, no breakdown potential was observed and only a general corrosion was observed. Similar behavior was observed in chloride solutions without bicarbonate. On the basis of these observations, they argued that the potential for inducing pitting in

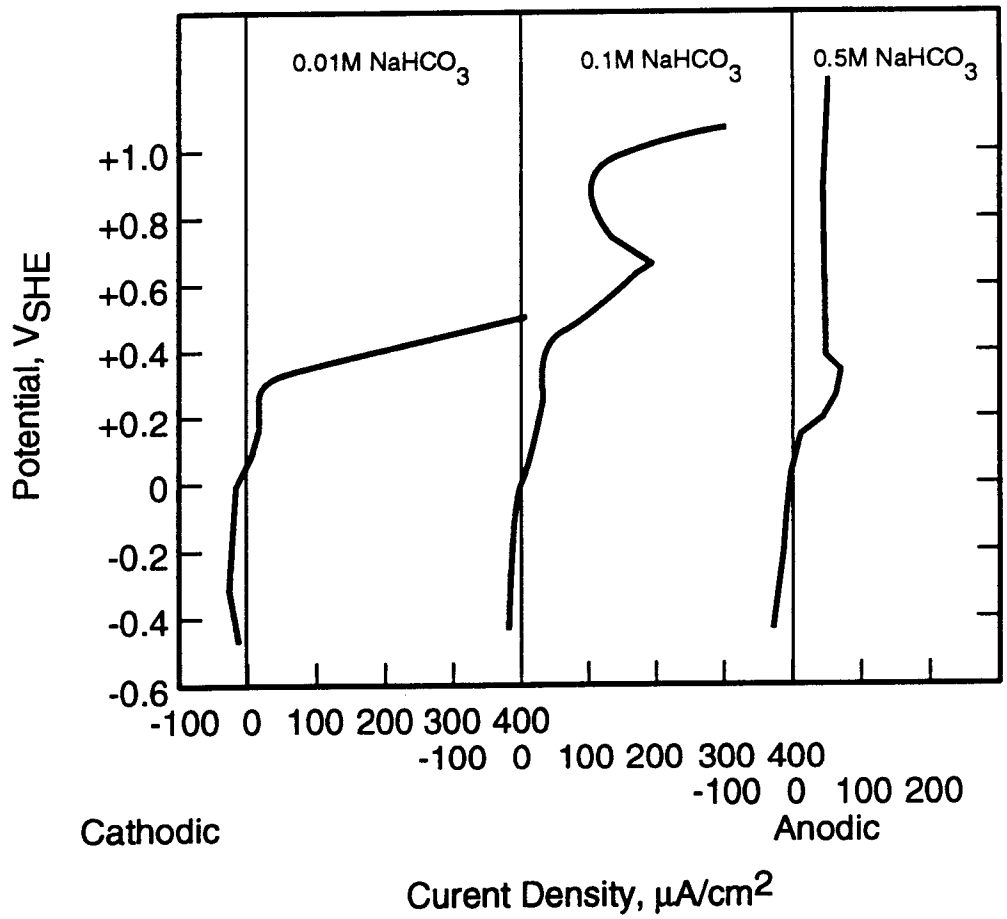

Figure 41. Potentiodynamic anodic polarization of copper in $NaHCO_3$ solutions at 25°C. (Thomas, 1972a).

copper corresponds to the potential for breakdown of the oxide film formed on copper in bicarbonate solutions rather than to the equilibrium potential of copper inside flaws as claimed by Pourbaix (Pourbaix, 1974). They claimed that the conditions proposed by Pourbaix prevail once a pit starts propagation. In this viewpoint, chloride is incidental for the breakdown event since the breakdown potentials were not affected by chloride.

The effect of temperature on breakdown behavior was studied by Thomas and Tiller (Thomas, 1972b). The effect of temperature on the anodic behavior of copper in bicarbonate solutions without chloride is shown in Figure 42a. It can be seen that increasing temperature increases the protective nature of the film and increases the breakdown potential. However, in the HCO_3^- + Cl^- mixtures and Cl^- solutions, temperature had an opposite effect as shown in Figure 42b. It was found that in NaCl solution that the corrosion was primarily general at 25°C, but with increasing temperatures resulted in greater localization of corrosion.

Mattsson and Fredriksson (Mattsson, 1968) examined the propagation of pitting of copper in hot (75°C), soft water using an artificial pit. In this case, a sample of copper enclosed by a glass capillary was electrically connected to another sample of copper freely exposed to the same solution and the current flowing between the samples was measured at a given applied potential difference (500 mV), this being an indicator of the rate of pit dissolution. Although it was not explicitly stated, it is assumed that the sample enclosed in the capillary was anodic to the open sample. A variety of solutions containing HCO_3^- in the range of 15 - 280 ppm, Cl^- in the range 0 - 4 meq./l (0 - 142 ppm), SO_4^{2-} 0.1 - 1 meq./l (4.8 - 48 ppm) and pH in the range of 6-9. They found that the current was increased when the concentration of sulfate was increased and the pH was decreased. Chloride had a less pronounced effect than sulfate. Pitting in these experiments is driven by the applied potential difference between the open and artificial pit samples and, hence, the conclusions reached can only be translated to that occurring under natural conditions in a qualitative manner. They also conducted a survey of soft water failures in copper tubing and found that pitting did not occur in hot water when the hardness was high, when the pH was above 7.4 or when the HCO_3^-/SO_4^{2-} (on a ppm basis) was higher than 1.

Shalaby et al. (Shalaby, 1989) examined the pitting of copper in warm (50°C) and cold (20°C) waters. The water had the following composition: HCO_3^-: 15 ppm, Cl^-: 52 ppm, SO_4^{2-}: 75 ppm, SiO_2: 4 ppm, Total Hardness ($CaCO_3$, mg/l): 93, pH: 8.1. Both potentiodynamic (no reverse polarization scan) and potentiostatic tests were used and detailed characterization of the surface film and pit morphology were performed using scanning electron microscopy (SEM). Both potentiodynamic and potentiostatic tests indicated that pitting occurred at a potential of 240 mV vs. SHE (-2 mV vs. SCE). However, in their long term potentiostatic tests, the anodic currents slowly decreased over a period of 20 hours. This phenomenon was not examined by the authors in detail. SEM examination indicated that during the initial stages of pitting, the surface was covered by an essentially oxide scale containing some chloride. Analysis of the pit insides showed only copper and chlorine indicating formation of cuprous chloride. At intermediate stages of pit growth, hemispherical pits lined with crystallites of cuprous chloride were observed. Only after relatively long exposure times (5 days) were sulfur peaks observed away from pits, indicating formation of sulfate. Based on these observations, they suggested that chloride is the most important factor in pitting in terms of breakdown and both sulfate and bicarbonate were incidental. The proposed mechanism for pitting in cold, soft water is shown in Figure 43.

Systematic examination of the effects of bicarbonate and sulfate on localized corrosion of Cu-Ni alloys have not been attempted. However, the effect of chloride on pitting on 90Cu-10Ni alloy in alkaline, borate buffer solutions is of interest (Milosev, 1991). Breakdown of the passive film, which consisted of an inner layer of Cu_2O and an outer layer of $CuO/Cu(OH)_2$, occurred in the borate buffer

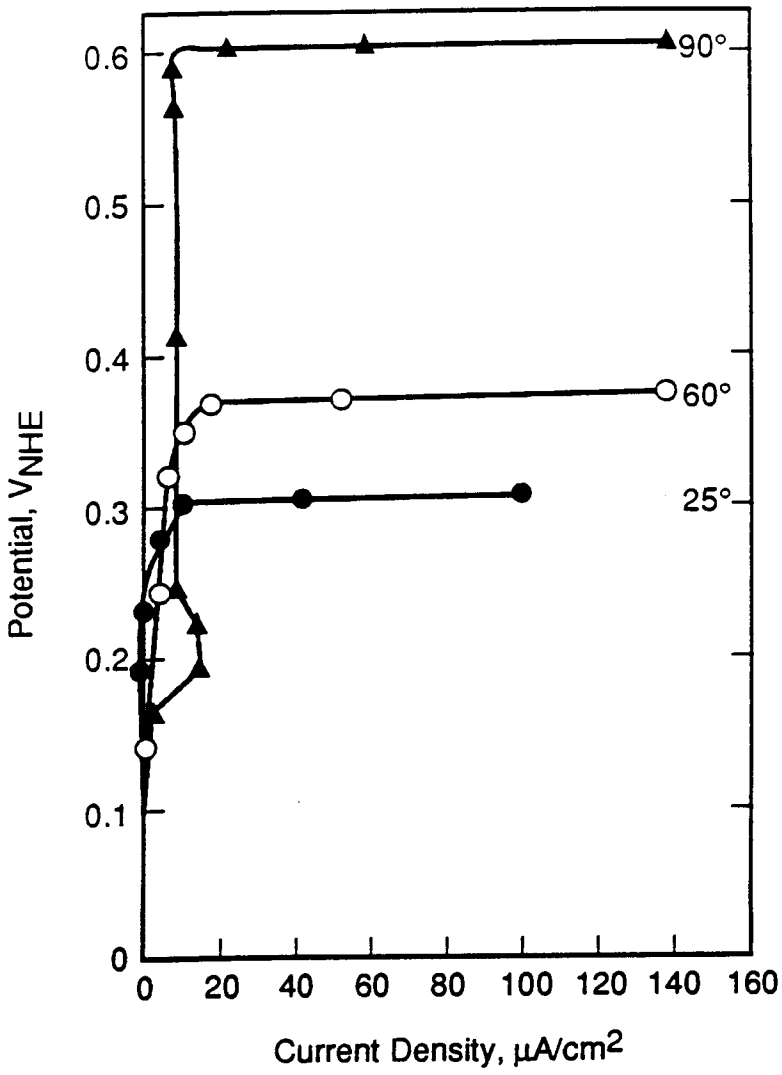

Figure 42a. Effect of temperature on potentiodynamic polarization curves of copper in 0.01M HCO_3^- solution. (Thomas, 1972b).

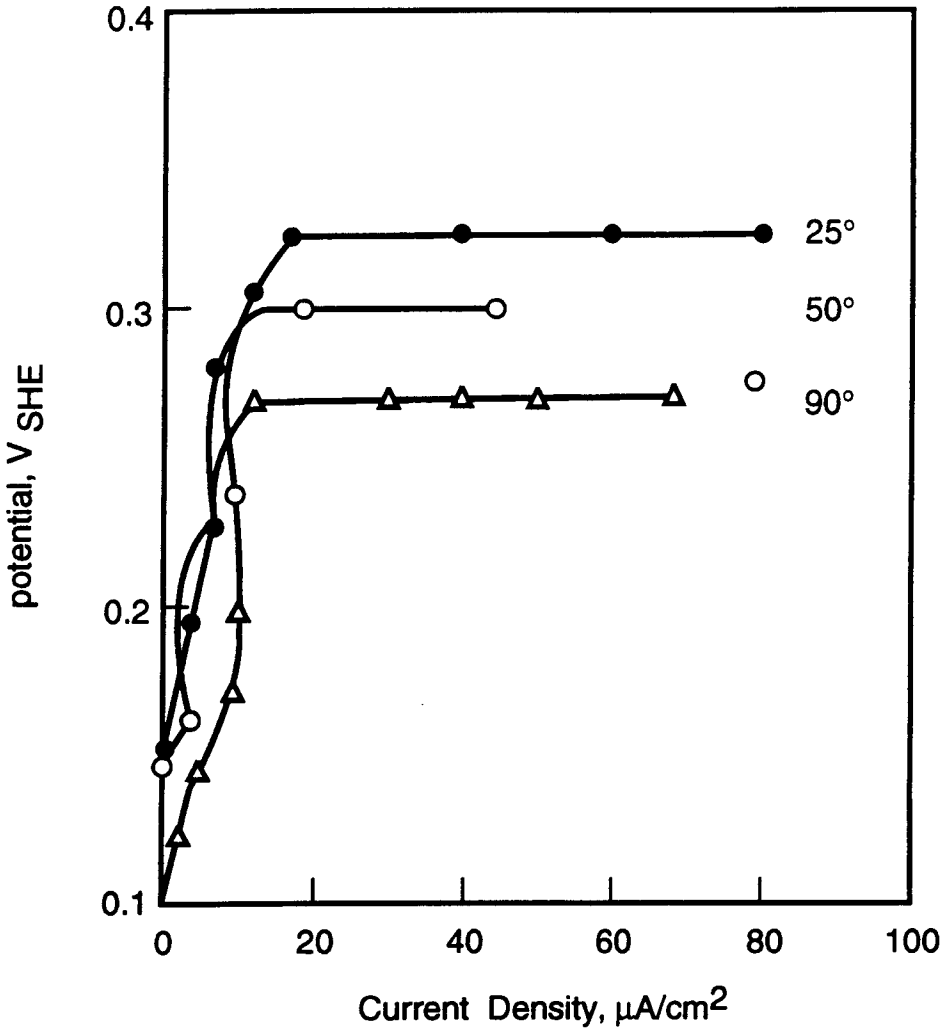

Figure 42b. Effect of temperature on potentiodynamic polarization curves of copper in 0.01M HCO_3^- + 0.01M Cl^- solution. (Thomas, 1972b).

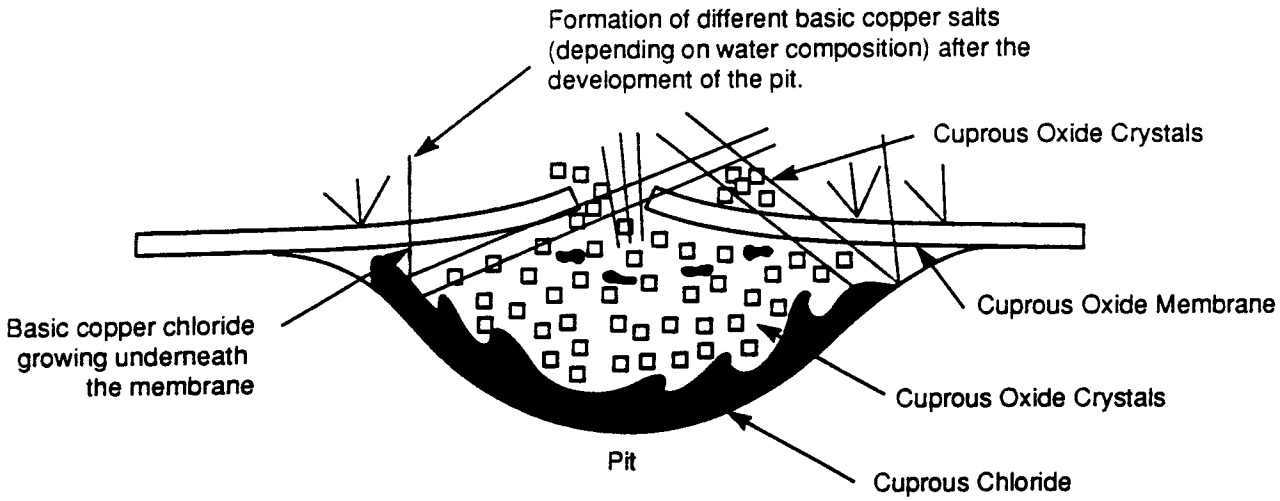

Figure 43. Schematic, unified representation of pitting in copper in a variety of waters. (Shalaby, 1989).

+ 0.05M chloride solution above 450 mV vs. SCE. It must be noted that this pitting potential is similar to that measured by Thomas and Tiller (Thomas, 1972a) on copper in a 0.1M bicarbonate with and without chloride. When the chloride concentration was increased to 0.5M, the breakdown potential decreased in a logarithmic fashion according to:

$$E_p = A - B \log (NaCl) \tag{18}$$

where B = 0.385 V. The value of A was not given, but may be calculated from the data to be about -0.05 V. They also found, based on potentiostatic measurements over a relatively short period of time, that the critical concentration of chloride in this solution for pitting was 0.019M.

Nishikata et al. (Nishikata, 1990) report localized corrosion of copper under wet/dry conditions in carbonate-chloride conditions. However, they did not elaborate the environmental conditions and the mode of corrosion. In alkaline carbonate + chloride solutions that simulate the condensate environment found under wet/dry conditions, Cl^-:0.5N and CO_2^-: 4N, breakdown of protective film and localized corrosion were observed at potentials exceeding 700 mV vs. Ag/AgCl electrode. Increasing the chloride concentration lowered the breakdown potential.

4.2.2 Crevice Corrosion

In the case of austenitic stainless steels and Ni-base alloys, it is well recognized that crevice corrosion is more important than pitting. This is not always found to be the case in copper-based alloys, mainly because of the effects of differential aeration. For example, the location of attack for most copper alloys has been stated to be just outside the crevice site (Polan, 1988). However, many investigators have evaluated corrosion of copper and Cu-Ni alloys inside creviced areas (Efird, 1977). Hence, it is important to examine the differences in the environmental or materials conditions that may lead to these divergent observations of crevice corrosion.

Most of the crevice corrosion studies in copper and copper-base alloys have been in sea-water environments. Hence, this environment is examined in detail. One of the earliest systematic observations of crevice corrosion in sea water was made by Bailey (Bailey, 1951) who examined a variety of Cu-Ni-Fe alloys containing Ni ranging from 5 to 30% (wt.) and Fe ranging from 0-32% (wt.). While the emphasis of the paper was on impingement attack due to flowing sea water, some tests on crevice corrosion in stagnant sea water were conducted using a loose deposit of sand as the crevice forming device. Tests were conducted at 40°C to accelerate corrosion. They found that crevice corrosion occurred in alloys containing more than about 12% Ni and 1% Fe. In alloys containing 30% Ni (similar to CDA 715), crevice corrosion was especially severe if the Fe content increased beyond 1%. They recommended an optimum Fe content of 0.2%. Bailey also reported detrimental effects due to growth of Fe-rich particles upon thermal treatment of the Cu-10% Ni alloy at 600°C. The effect of thermal treatment was worse for lower Ni alloys indicating the lack of solubility of Fe in copper.

Efird and Verink (Efird, 1977) examined the conditions leading to the crevice corrosion of a 90%Cu-10%Ni alloy in a 0.1M Cl^- solution at a bulk pH of 10.3. They used an occluded cell experiment as shown in Figure 2, where the crevice area is simulated by a sample in a small volume of solution that is in restricted communication through a glass frit with the bulk solution in which another sample of the same material is immersed. The two alloy samples are electrically coupled. The changes in pH and chloride content of the restricted solution ("crevice solution") was measured as a function of

the potential applied to the external sample. It was noted that at an applied potential of 0.14 V vs, SHE, a discontinuous change in "crevice solution" pH and chloride concentration was observed. When the applied potential was above this value, the pH inside the "crevice solution" decreased below the bulk value to about 5.5 and the corresponding Cl^- concentration was higher by a small amount (0.005M). Active dissolution of the sample in the crevice solution was noted. When the potential was below 0.14 V vs. SHE, the pH of the "crevice solution" was 10.4 - 11.1. No corrosion of the sample in the crevice solution was noted. Thus, the potential of 0.14V was termed protection potential. These changes in pH as a function of applied potential are shown in Figure 44, superimposed on an experimental potential-pH diagram. Also indicated are general corrosion and passivation areas. In the case of points 1 - 4, the crevice solution pH values are indicated by points 1' - 4'. According to Efird and Verink, crevice corrosion proceeds by the following mechanism: Above the protection potential corresponding to 1, a passive film forms which restricts general corrosion. However, a small dissolution of copper results in the formation of CuCl which hydrolyzes near the surface to lower the pH, thus, destabilizing the film. Once film breakdown occurs, the decrease in pH is hastened by faster metal dissolution and the pH inside the breakdown area moves to point 1' which is in the active dissolution area of the potential-pH diagram. When the external potential is below the protection potential as in point 6, reduction of pH due to hydrolysis shifts the pH to another area in the potential-pH diagram that also induces passivation. While there are many attractive features of this mechanism for crevice corrosion, there are many uncertainties associated with the potential-pH diagram for the alloy which is not thermodynamically derived. Additionally, the effect of temperature or other environmental factors needs to be recognized. Further experimental work defining the crevice corrosion protection potential as well as the potential-pH behavior of Cu-Ni alloys needs to be evaluated.

King et al. (King, 1981) examined copper in simulated saline ground water environments pertaining to high level waste disposal in the Canadian program. In one solution, containing 68 ppm HCO_3, 6460 ppm Cl^-, 1040 ppm SO_4, 33 ppm NO_3, and a pH of 7, crevice corrosion was noted in a deaerated solution at 150°C and the corrosion rate increased with aeration. However, in these experiments, the crevice was accidental and, hence, no attempt was made to measure the crevice corrosion rate in a controlled manner. In a much higher chloride environment, containing 34,260 ppm Cl^-, 10 ppm HCO_3, 790 ppm SO_4, 50 ppm NO_3, and at a pH of 7, King and Lidke (King, 1986) found no evidence of localized corrosion in copper at 150°C even in the presence of sulfides. It must be noted that under these high chloride, low bicarbonate conditions, the passive film is not stable and corrosion is likely to take place under active dissolution conditions.

The above discussions indicate that crevice corrosion in Cu and Cu-based alloys can occur under conditions which lead to the formation of a protective film on the boldly exposed surfaces. As mentioned in previous sections, these conditions include presence of bicarbonate, higher than neutral pH, and relatively low chloride. The uncertainties include the effects of sulfate and temperature. While early literature indicated that increasing Ni content may be detrimental to crevice corrosion, this aspect has not been explored further. The detrimental effect of iron beyond about 1% has been well documented, but the effects of long-time thermal treatments on alloys with more than 1% Fe that may lead to iron segregation and localized corrosion needs further investigation. Aluminum bronzes have not been investigated in any great detail for localized corrosion and may be especially susceptible to crevice corrosion because of the protective film formation as well as hydrolysis of Al and Cu inside creviced areas.

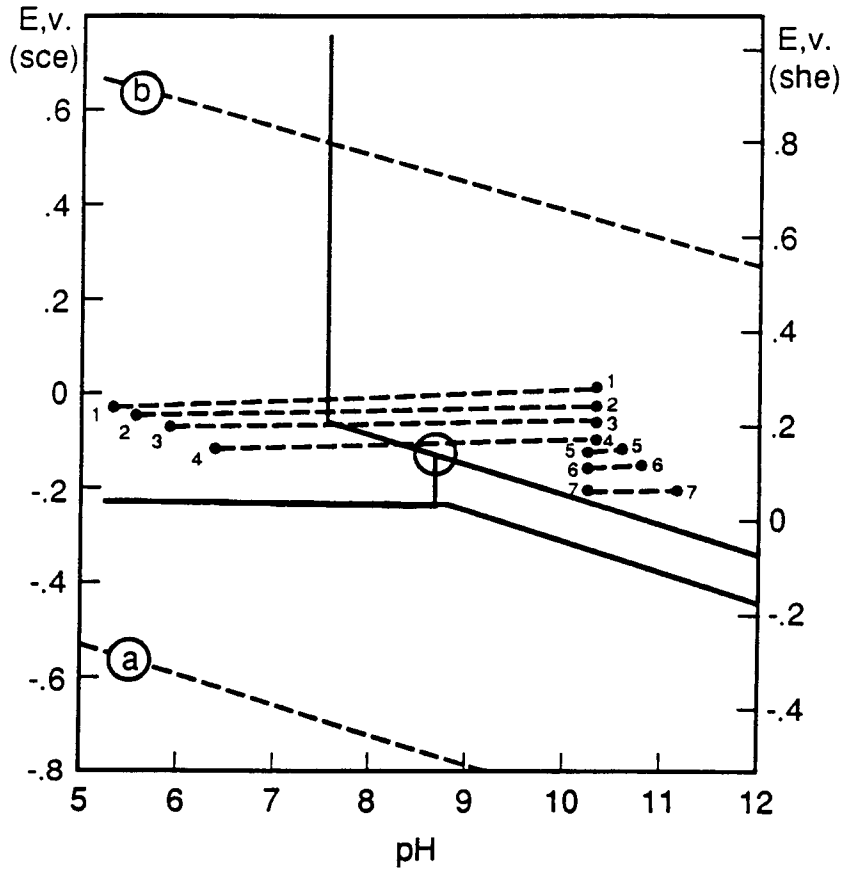

Figure 44. Influence of external applied potential on crevice pH and conditions for protection in 90Cu-10Ni alloy. The experimental data is superimposed on a experimentally derived potential-pH diagram for the alloy. (Efird, 1977).

5. SUMMARY AND RECOMMENDATIONS

The advantages and limitations of the different test techniques available to characterize localized corrosion are discussed in this review to guide the selection of the most appropriate experimental methods for assessing the performance of container materials over very extended periods of time. Both electrochemical and nonelectrochemical techniques are described and examined to evaluate the validity of different parameters used to characterize the resistance to pitting or crevice corrosion. The need for accelerated tests that yield suitable parameters for long-term extrapolation of material performance is discussed. It is concluded, for example, that the repassivation potential for crevice corrosion could be used as a bounding parameter, provided it can be demonstrated that it is a time-independent parameter, as suggested by the results of some of the experimental work reviewed in Section 2.3. On the other hand, a parameter such as pitting potential is not a suitable bounding parameter because pit growth or crevice corrosion may occur at potentials lower than that critical potential. Nevertheless, the pitting potential concept is useful in terms of relative ranking of materials and for the determination of environmental conditions leading to pitting corrosion.

Potentiostatic or potentiodynamic polarization techniques for the determination of critical potentials, such as pitting and repassivation potentials, are valuable methods for comparing the resistance to localized corrosion of different candidate materials in a given environment or evaluating the role of various environmental factors on the response of a particular alloy. The need for visual evidence of localized corrosion is emphasized to avoid misleading interpretations based in the consideration of the polarization curves alone. Experimental aspects of these techniques are discussed covering a wide range of factors from those that affect reproducibility (i.e., electrical noise associated to low conductivity solutions) to the influence of variables intrinsic to the technique, such as potential scan rate, threshold current, etc. In the case of crevice corrosion, particular attention is paid to the description of different devices or cells, taking into consideration the importance of the geometrical factors (crevice/bold area ratio, crevice gap, crevice depth, etc). A distinction is made between tests oriented to the determination of design parameters and those used for mechanistic studies.

Besides the discussion of more conventional electrochemical techniques based in d.c. measurements, certain advantages offered by the use of a.c. impedance methods are discussed on the basis of recent experimental work presented in the literature. It is emphasized, however, that the application of a.c impedance techniques to localized corrosion requires the development of appropriate mechanistic models or realistic electric circuit analogs to represent the electrochemical processes occurring at the metal/solution interface.

All the experimental work conducted by LLNL and Cortest Columbus Technologies on localized corrosion of the candidate Fe-Cr-Ni alloys is discussed in detail. In most of the electrochemical experiments conducted in both laboratories, cyclic potentiodynamic polarization curves were measured. It can be concluded that no pitting occurs on any of the candidate alloys (AISI 304L SS, AISI 316L SS, and alloy 825) exposed to J-13 water, which has been adopted as the reference groundwater for the proposed repository studies, at temperatures ranging from 50 to 95°C. However, it is clearly emphasized that a range of environmental conditions should be evaluated. While in the LLNL work only the effect of higher Cl^- concentration on AISI 304L SS was studied, Cortest Columbus used an extended test matrix to evaluate the action of fifteen environmental variables, including temperature and pH, on the pitting corrosion of AISI 304L SS and alloy 825. The interdependence of some of the variables selected by Cortest is discussed to reveal how some of the results may be affected, but at least, from a qualitative point of view, certain conclusions seem to be in agreement with previous results in the literature and our

more recent findings. The main conclusions of this work can be summarized as follows: a) For AISI 304L SS, chloride promotes a significant decrease of E_p and E_{rp}, whereas, nitrate, acting as an inhibitor, increases both potentials. No other variable was found to affect E_{rp}. E_p increases with pH and HCO_3^- and decreases with temperature, and b) For alloy 825, no anion was found to decrease E_p, but F^- increases it. E_{rp} decreases with pH and Cl^- and increases with NO_3^- and oxalic acid. Both Mg^{2+} and H_2O_2 decrease E_p and E_{rp}. Also, in this work, the superior resistance to localized corrosion of alloy 825 over AISI 304L SS is clearly demonstrated, as expected, from the greater Cr and Mo content.

Very limited work on crevice corrosion of the candidate Fe-Cr-Ni alloys was conducted by LLNL, mainly in J-13 water at 100°C. It was concluded (Glass, 1984) that any one of the candidate alloys could meet the 300-1000 year containment objective. However, as discussed in Section 3.3.2.1, the possibility of passivity breakdown cannot be disregarded in some test results. Although Cortest Columbus conducted additional tests for AISI 304L SS and alloy 825, it was reported that no crevice corrosion occurs over a extended testing period (8065 hours) upon exposure to J-13 water in a weekly wet-dry cycle. Under different testing conditions in a solution containing 1000 ppm Cl^-, pitting was observed in the creviced area. It should be noted, however, that the studies described above have been conducted under a very limited set of conditions. Crevice corrosion initiation is critically related, besides environmental conditions, to the geometry and dimensions of the crevice. There is a need to evaluate more rigorously the effects of geometrical and environmental factors on crevice corrosion.

In the review of the open literature on localized corrosion of Fe-Cr-Ni alloys, particular attention is paid to the effect of alloy composition and microstructure. The role of the main alloying elements is discussed in some detail, in particular, the combined effect of Cr and Mo (and also Nb and W) in conferring resistance to localized corrosion to this class of alloys. Many of the microstructural features that affect localized corrosion, such as precipitates and inclusions, are also discussed, although it is recognized that, at the present time, the main effort is in the selection of an appropriate alloy. However, the effect of closure methods is briefly discussed in this context.

The main emphasis in the review of the open literature is in the effect of environmental variables since this a very important aspect in the correlation between accelerated tests and long-term prediction, as well as phenomenological description and modeling. The role of the main anions present in groundwaters is carefully assessed, and it can be concluded that chloride is the main promoter of both pitting and crevice corrosion, whereas, bicarbonate, sulfate, nitrate and nitrite are inhibitors. However, the complex interrelation between anions that arises from the required concentration ratio for inhibition is clearly illustrated in this review. The effect of pH appears related to the role of OH^- as inhibitor, but it has not been examined extensively in relation to E_{rp}. In the temperature range of interest it appears that for most of the alloys a temperature increase promotes a decrease of E_p and E_{rp}, although the effect on the latter parameter has been far less investigated. Most of the effect of these environmental variables is common to pitting and crevice corrosion, but the quantitative aspects of their influence should be carefully investigated for potential bounding parameters, such as E_{rcrev}.

As discussed in Section 4.1.1, LLNL investigated the anodic behavior of the candidate copper alloys in J-13 water and in 100X-J-13 water at temperatures ranging from room temperature to 80°C. No clear trend emerged from the results reported because, among other factors, the composition of the concentrated solution is not known. Precisely, one of the main conclusions of the review of the open literature is that the concentration ratio of the anions in natural waters, in particular HCO_3^-, SO_4^{2-} and Cl^-, is extremely critical for the development of pitting corrosion on copper.

Cortest Columbus used a statistical approach for evaluation of the effect of environmental variables on the localized corrosion of the copper alloys. Among other findings, it was concluded that for CDA 102 Cl^- decreases E_p and E_{rp}. Other observations, as noted in Section 4.1.1.2, are difficult to interpret in terms of the available literature. However, one of the main claims in this work is that the hysteresis loop observed in the cyclic potentiodynamic polarization curves is not necessarily related to pit growth. The review of the open literature clearly illustrated the complex environmental conditions that lead to the localized corrosion of copper in natural waters. Discussed in detail is the role of HCO_3^- in improving the passive film and, as a consequence, the promotion of deep pitting instead of shallow attack in the presence of Cl^-. As the chloride content is increased, localized corrosion tendency is replaced by more general corrosion. In addition, it is emphasized that even though copper-based alloys are less prone to crevice corrosion than Fe-Cr-Ni alloys, by no means can the possibility of this phenomenon be neglected under the environmental conditions prevailing in groundwaters.

One of the main recommendations that arises from this review is that more effort should be dedicated to the study of crevice corrosion for both classes of candidate container materials. In particular, the concept of repassivation potential for crevice corrosion should be fully explored to determine its usefulness as a bounding parameter for performance assessment. In this context, the role of the main anionic species present in groundwater should be carefully assessed, as well as the relative importance of pH and temperature effects.

Obviously, in a review of this nature many points are not adequately covered. Recognizing this limitation, it should be noted that in a later review, programmed as a major milestone in Task 1 of the IWPE program, in addition to an update of the information currently provided, the following aspects will be discussed in detail: a) updated examination of crevice corrosion of Fe-Cr-Ni alloys; b)localized corrosion of DOE alternate materials, including new concepts for waste package components; c) effect of chromium depletion on the localized corrosion of Ni-based alloys, such as alloy 825; d) effect of gamma radiation on the semiconductive properties of passive films and its impact on localized corrosion.

TERMINOLOGY

E_c, E_{corr}	-	Corrosion or open-circuit potential
E_p, E_{tp}	-	Pit initiation potential
E_{rp}	-	Repassivation potential for pits
E_{prot}	-	Protection potential
T_p or CPT	-	Critical pitting temperature
E_{crev}	-	Crevice corrosion initiation potential
E_{rcrev}	-	Repassivation potential for crevice
pH_d	-	Depassivation pH
E_h	-	Redox or mixed potential of an environment
T_c or CCT	-	Critical crevice corrosion temperature
t_i	-	Initiation time
R_{tot}	-	Total resistance without the solution resistance (pit and open areas of surface)
Z_{tot}	-	Total impedance (pit and open areas)
C	-	Capacitance
R_t	-	Charge transfer resistance
SCE	-	Saturated calomel electrode
SHE	-	Standard hydrogen electrode
M	-	Molar (Moles/liter)
i	-	Current density (current per unit area)
i_p	-	Passive current density
mpy	-	mils per year (calculated uniform corrosion rate)
R_s	-	Solution Resistivity
R_{ox}	-	Resistance to charge transfer through the passive film
R_{pit}	-	Resistance to charge transfer in the pit
C_{ox}	-	Capacitance associated with passive film surface
C_{pit}	-	Capacitance associated with pit surface
i_{corr}	-	Corrosion current density at open-circuit potential
B_a, B_c	-	Anodic and cathodic Tafel slopes
R_p	-	Polarization resistance
B	-	Stern-Geary Constant

REFERENCES

Abraham, T., H. Jain and P. Soo. 1986. Stress Corrosion Cracking Tests on High-Level Waste Container Materials in Simulated Tuff Repository Environments. NUREG/CR 4619. Brookhaven National Laboratory.

Accary, A., 1985, Corrosion Behavior of Container Materials for Geological Disposal of High-level Radioactive Waste, EUR 9386 EN, Commission of European Communities, Luxembourg.

Bailey, G. L., 1951, Copper-Nickel-Iron Alloys Resistant to Sea-water Corrosion, J. of Institute of Metals, V. 79, No. 5, pp. 243-292.

Bandy, R. and D. Van Rooyen, 1983, Pitting Resistant Alloys in Highly Concentrated Chloride Media, Corrosion, V. 39, pp. 227-236.

Beavers, J. A., and N. G. Thompson. 1988a. Container Corrosion in High Level Nuclear Waste Repositories. NRC Contract No. NRC-04-87-009. Year 1, First Semi-Annual Report. Columbus, Ohio: Cortest Columbus, Inc.

Beavers, J. A., and N. G. Thompson. 1988b. Container Corrosion in High Level Nuclear Waste Repositories. NRC Contract No. NRC-04-87-009. Year 1, Second Semi-Annual Report. Columbus, Ohio: Cortest Columbus, Inc.

Beavers, J. A., and N. G. Thompson. 1989a. Container Corrosion in High Level Nuclear Waste Repositories. NRC Contract No. NRC-04-87-009. Year 2, First Semi-Annual Report. Columbus, Ohio: Cortest Columbus, Inc.

Beavers, J. A., and N. G. Thompson. 1989b. Container Corrosion in High Level Nuclear Waste Repositories. NRC Contract No. NRC-04-87-009. Year 2, Second Semi-Annual Report. Columbus, Ohio: Cortest Columbus, Inc.

Beavers, J. A., and C. L. Durr. 1990a. Container Corrosion in High Level Nuclear Waste Repositories. NRC Contract No. NRC-04-87-009. Year 3, First Semi-Annual Report. Columbus, Ohio: Cortest Columbus, Inc.

Beavers, J. A., and C. L. Durr. 1990b. Container Corrosion in High Level Nuclear Waste Repositories. NRC Contract No. NRC-04-87-009. Year 3, Second Semi-Annual Report. Columbus, Ohio: Cortest Columbus Technologies.

Beavers, J. A., and N. G. Thompson. 1990c. Environmental Effects on Corrosion in the Tuff Repository. NUREG/CR-5435. Nuclear Regulatory Commission, Washington, D.C.

Beavers, J. A., N. G. Thompson, and W. V. Harper, 1990d. Potentiodynamic Polarization Studies of Candidate Container Materials in Simulated Tuff Repository Environments, Mat. Res. Soc. Symp. Proc., Vol. 176, p. 533, Materials Research Society.

Bernhardsson, S., R. Mellstrom, and B. Brox, 1980, Limiting Chloride Contents and Temperatures with Regard to Pitting of Stainless Steels, CORROSION/80, Paper No. 85, NACE, Houston, Texas.

Bernhardsson, S., R. Mellstrom, 1983, Performance of a Highly Alloyed Stainless Steel in Marine Environments, CORROSION/83, Paper No. 72, NACE, Houston, Texas.

Bertocci, U., M. Koike, S. Leigh, F. Qiu, and G. Yank, 1986, A Statistical Analysis of Fluctuations of the Passive Current, J. Electrochem. Soc., V. 133, pp. 1782-1786.

Bianchi, G., G. Fiori, P. Longhi, and F. Mazza, 1978, "Horse Shoe" Corrosion of Copper Alloys in Flowing Sea Water: Mechanism, and Possibility of Cathodic Protection of Condenser Tubes in Power Stations, Corrosion, V. 34, pp. 396-406.

Bogaerts, W. et al., 1981, Influence of Cl^-, HCO_3^-, and SO_4^{2-} on the Corrosion of Fe-Ni-Cr Alloys in Hot Water Systems, Proc. 8th International Congress on Metallic Corrosion, V. II, p. 1887, DECHEMA, Frankfurt, Germany.

Bogaerts, W. F. and A. A. Van Haute, 1985, Chloride Pitting and Water Chemistry Control in Cooling or Boiler Circuits, Corros. Sci., V. 25, pp. 1149-1161.

Brigham, R. J., 1972, Pitting of Molybdenum Bearing Austenitic Stainless Steel, Corrosion, V. 28, p. 177-179.

Brigham, R. J. and E. W. Tozer, 1973, Temperature as a Pitting Criterion, Corrosion, V. 29, p. 33.

Brigham, R. J., 1974, Temperature as a Crevice Corrosion Criterion, Corrosion, V. 30, pp. 396.

Brookes, H. C. and F. J. Graham, 1989, Influence of the Electrolyte and Alloy Composition on the Pitting Behavior of Stainless Steel Alloys, Corrosion, V. 45, pp. 287-293.

Campbell, H. S., 1974, A Review: Pitting Corrosion of Copper and Its Alloys, Localized Corrosion, pp. 625-638, NACE, Houston, Texas.

Cottis, R. A., P. J. Laycock, D. Holt, S. A. Moir, and P. Scarf, 1987, The Statistics of Pitting Corrosion of Austenitic Stainless Steels in Chloride Solutions, Advances in Localized Corrosion, pp. 117-121, NACE, Houston, Texas.

Cragnolino, G. A. and N. Sridhar, 1991a, Localized Corrosion of a Candidate Container Material for High-level Nuclear Waste Disposal, CORROSION/91, Paper No. 35, NACE, Houston, Texas.

Cragnolino, G. A. and N. Sridhar, 1991b, Integrated Waste Package Experiments, Report on Research Activities for Calender Year 1990, CNWRA 90-01A, Prepared for the Nuclear Regulatory Commission, Contract No. NRC-02-88-005, Center for Nuclear Waste Regulatory Analyses, San Antonio, Texas, February 1991.

Cragnolino, G. A. and N. Sridhar, 1991c, Integrated Waste Package Experiments, Report on Research Activities for Second Quarter of January - March, 1991, CNWRA 91-01Q, Prepared for the Nuclear Regulatory Commission, Contract No. NRC-02-88-005, Center for Nuclear Waste Regulatory Analyses, San Antonio, Texas, April, 1991.

Crolet, J. L., L. Seraphin, and R. Tricot. 1977. Mechanisme d'action du soufre sur la resistance a la corrosion caverneuse des aciers inoxydables. Mem. Sci. Rev. Met., V. 74 (5), pp. 281.

Diegle, R. B. 1981. Electrochemical; Cell for Monitoring Crevice Corrosion in Chemical Plants. CORROSION/81, NACE. Houston, Texas.

Drugli, J. M. and E. Bardal, 1978, A Short Duration Test Method for Prediction of Crevice Corrosion Rates on Stainless Steels, Corrosion, V. 34, No. 12, p. 419.

Efird, K. D. and E. D. Verink, 1977, The Crevice Protection Potential for 90-10 Copper Nickel, Corrosion, V. 33, pp. 328-331.

Ehrhardt, W. C., 1990, IR Drop in Electrochemical Corrosion Studies, American Society for Testing and Materials, ASTM STP 1056, pp. 5-26, ASTM, Philadelphia, Pennsylvania.

Elfenthal, L., J. W. Schutz, and O. Meyer, 1989, The Simulation of Radiation in Oxide Films by Ion Implantation, Corrosion Sci., V. 29, pp. 343-361.

Farmer, J. C., R. A. Van Konynenburg, R. D. McCright, and D. B. Bullen, 1988a, Survey of Degradation Modes of Candidate Materials for High-level Radioactive Waste Disposal Containers, Vol. 3, Localized Corrosion and Stress Corrosion Cracking of Austenitic Alloys, UCID-21362, Vol. 3, Lawrence Livermore National Laboratory, Livermore, California.

Farmer, J. C., R. A. Van Konynenburg, R. D. McCright, and G. E. Gdowski, 1988b, Survey of Degradation Modes of Candidate Materials for High-level Radioactive Waste Disposal Containers, Vol. 5, Localized Corrosion of Copper-based Alloys, UCID-21362, Vol. 5, Lawrence Livermore National Laboratory, Livermore, California.

Farmer, J. C. and R. D. McCright, 1989, Localized Corrosion and Stress Corrosion Cracking of Candidate Materials for High-level Radioactive Waste Disposal Containers in U.S.: A Critical Literature Review, Mat. Res. Soc. Symp. Proc., Vol. 127, p. 359, Materials Research Society.

Garner, A., 1982, Corrosion of High Alloy Austenitic Stainless Steel Weldments in Oxidizing Environments, Materials Performance, V. 21 (No. 8), pp. 9-14.

Glass, R. S., G. E. Overturf, R. E. Garrison, and R. D. McCright, 1984. Electrochemical Determination on the Corrosion Behavior of Candidate Alloys Proposed for Containment of High Level Nuclear Waste in Tuff, UCID-20174, Lawrence Livermore National Laboratory, Livermore, California.

Glass, R. S., G. E. Overturf, R. A. Van Konynenburg, and R. D. McCright, 1986. Gamma Radiation Effects on Corrosion - 1. Electrochemical Mechanisms for the Aqueous Corrosion Processes of Austenitic Stainless Steel Relevant to Nuclear Waste Disposal in Tuff, Corrosion Science, Vol. 26, pp. 557-590.

Glass, R. S., R. A. Van Konynenburg, and G. E. Overturf, 1985. Corrosion Processes of Austenitic Stainless Steels and Copper-Based Materials in Gamma-Irradiated Aqueous Environments, UCRL-92941, Lawrence Livermore National Laboratory, Livermore, California.

Glassley, W. E. 1986. Reference Waste Package Environment Report, UCRL-53726. Lawrence Livermore National Laboratory, Livermore, California.

Glassley, W. E. 1990. Geochemical Interactions. Presentation to the Nuclear Waste Technical Review Board, January 18-19, 1990, Pleasanton, California. Livermore, California: Lawrence Livermore National Laboratory (LLNL).

Hack, H. P., P. J. Moran, and J. R. Scully, 1990, Influence of Electrolyte Resistance on Electrochemical Measurements and Procedures to Minimize or Compensate for Resistance Errors, ASTM STP 1056, pp. 5-26, American Society for Testing and Materials, Philadelphia, Pennsylvania.

Hibner, E. L., 1986, Evaluation of Test Procedures for Critical Crevice Temperature Determination for Ni-base Alloys in a Ferric Chloride Environment, CORROSION/86, Paper No. 181, NACE, Houston, Texas.

Hodgkiess, T. and S. Rigas, 1983, A Comparison of the Corrosion Resistance of Some Higher-alloy Stainless Steels in Sea-water at 20-100°C, Desalination, V. 44, pp. 283-294.

Ijsseling, F. P., 1980. Electrochemical Methods in Crevice Corrosion Testing, Br. Corrosion J., V. 15 p. 51.

Jallerat, N., F. L. Pari, F. Bourelier, and K. Vu Quang, 1984, Specific Inhibition Effect of Carbonate and Bicarbonate Ions on Pitting Corrosion of Stainless Steels and Ni-base Alloys, Proc. 9th International Congress on Metallic Corrosion, V. 4, pp. 404-406, National Research Council, Ottawa, Canada.

Kain, R. M., 1990, Crevice Corrosion Resistance of Stainless Steels in Waters Containing Chloride and Sulfate Ions, Corrosion in Natural Waters, ASTM STP 1086, pp. 37-53, American Society for Testing and Materials, Philadelphia, Pennsylvania.

King, P. and C. D. Lidke, 1986, The Corrosion Behavior of Copper Under Simulated Nuclear Fuel Waste Disposal Conditions, Proc. Second International Conference on Radioactive Waste Management, pp. 593-596, Canadian Nuclear Society, Toronto, Canada.

King, P. J., S. J. Thorpe, K. Lam, and D. P. Dautovich, 1981, The Corrosion Behavior of Copper Under Simulated Nuclear Fuel Repository Conditions, Proc. 8th International Congress on Metallic Corrosion, V. II, pp. 1650-1654, DECHEMA, Frankfurt, Germany.

Koch, G. H., J. M. Spangler, and N. G. Thompson, 1988. Corrosion Studies in Complex Environments. ASTM STP 970, American Society for Testing and Materials, Philadelphia, Pennsylvania.

Laycock, P. J., R. A. Cottis, and P. A. Scarf, 1990, Extrapolation of Extreme Pit Depths in Space and Time, J. Electrochem. Soc., V. 137, pp. 64-69.

Leckie, H. P. and H. H. Uhlig, 1966, Environmental Factors Affecting the Critical Potential for Pitting in 18-8 Stainless Steel, J. Electrochem. Soc., V. 113, pp. 1262-1267.

Lizlovs, E. A. and A. P. Bond. 1968. J. Electrochem. Soc. Vol. 115, pp. 1130.

Macdonald, J. R., 1987, Impedance Spectroscopy, J. Wiley & Sons, New York, New York.

Manning, P. E., 1985, An Improved Intergranular Corrosion Test for Hastelloy Alloy C-276, p. 437, ASTM STP 866, American Society for Testing and Materials, Philadelphia, Pennsylvania.

Manning, P. E., 1981. Comparison of Several Accelerated Laboratory Tests for the Determination of Localized Corrosion Resistance of High Performance Alloys, CORROSION/82, Paper 176, 1982, NACE, Houston, Texas.

Mansfeld, F. 1988. Don't be Afraid of Electrochemical Techniques - But Use them with Care! Corrosion. V. 44, pp. 856-868.

Marshall, P. I., 1986, Effect of Composition on Pitting Corrosion Resistance of High Alloy Austenitic Stainless Steel Weld Metals, Report No. 316/1986, The Welding Institute, Abington Hall, Abington, Cambridge CB1 6AL, U. K.

Matamala, R. G., 1987, Correlation model of the AISI 316 stainless steel pitting potential with cellulose bleach process variables, Corrosion, V. 43, pp. 97-100.

Matsuda, S., and H. H. Uhlig, 1964, Effect of pH, Sulfates and Chlorides on Behavior of Sodium Chromate and Nitrite as Passivators of Steel, J. Electrochem. Soc., V. 111, p. 156.

Mattsson, E. and A. M. Fredriksson, 1968, Pitting Corrosion in Copper Tubes - Cause of Corrosion and Counter Measures, Br. Corros. J., V. 3, p. 246-257.

McCright, R. D., 1985, FY 1985 Status Report on Feasibility Assessment of Copper-Base Waste Package Container Materials in a Tuff Repository. UCID-20509, Lawrence Livermore National Laboratory, Livermore, California.

McCright, R. D., H. Weiss, M. C. Juhas, and R. W. Logan, 1984. Selection of Candidate Canister Materials for High-Level Nuclear Waste Containment in a Tuff Repository, CORROSION/84, Paper No. 198, NACE, Houston, Texas.

McCright, R. D., W. G. Halsey, and R. A. Van Konynenburg, 1987. Progress Report on the Results of Testing Advanced Conceptual Design Metal Barrier Materials Under Relevant Environmenmtal Conditions for a Tuff Repository, UCID-21044, Lawrence Livermore National Laboratory, Livermore, California.

Murphy, W. M. 1989. Constraints on the Chemistry of Groundwater in the Unsaturated Zone of Yucca Mountain, Nevada and in the Proposed Repository at that Site (Draft). Nuclear Regulatory Commission Contract No. NRC-02-89-005. CNWRA. October 1989.

Nagaswami, N. S. and M. A. Streicher, 1983, Accelerated Laboratory Tests for Crevice Corrosion of Stainless Alloys, CORROSION/83, Paper No. 71, NACE, Houston, Texas.

Newman, R. C. and E. M. Franz. 1984. Growth and Repassivation of Single Corrosion Pits in Stainless Steel. V. 40, pp. 325.

Nishikata, A., M. Itagaki, T. Tsuru, S. Haruyama, and E. Fujii, 1990, Anodic Dissolution Mechanisms of Copper in Alkaline Carbonate-chloride Solutions, Corrosion Engineering, V. 39, pp. 15-24.

Notoya, T., 1990, Ant-Nest Corrosion in Copper Tubing, Corrosion Engineering, V. 39, pp. 353-362.

Okayama, S. et al., 1987, The Effects of Alloying Elements on Stainless Steel Depassivation pH, Corrosion Engineering, V. 36, pp. 631-638.

Oldfield, J. W., 1987, Test techniques for Pitting and Crevice Corrosion Resistance of Stainless Steels and Ni-base Alloys in Chloride-containing Environments, International Materials Review, V. 32, No. 3, p. 153.

Polan N. W., 1988, Corrosion of Copper and Copper Alloys, Metals Handbook, 9th Edition, Vol. 13, Corrosion, ASM International, Metals Park, Ohio.

Postlethwaite, J., R. J. Scoular, and M. H. Dobbin, 1988, Localized Corrosion of Mo-bearing Nickel Alloys in Chloride Solutions, Corrosion, V. 44, pp. 199-203.

Redmerski, L. S., J. J. Eckenrod, and C. W. Kovach, 1983, Crevice Corrosion of Stainless Steel Welds in Chloride Environments, Materials Performance, V. 22 (No.6), pp. 31-39.

Rosenfeld, I. L. and I. S. Danilov, 1967, Electrochemical Aspects of Pitting Corrosion, Corr. Sci., V. 7, pp. 129-142.

Robitz, E. S., M. D. McAninch, and E. W. Edmonds, 1990, Closure Development for High-level Nuclear Waste Containers for the Tuff Repository, Phase 1 Final Report, UCRL-15964, Lawrence Livermore National Laboratory, Prepared by Babcock & Wilcox.

Scully, J. R., R. P. Frankenthal, K. J. Hansen, D. J. Siconolfi, and J. D. Sinclair, 1990, Localized Corrosion of Sputtered Aluminum and Al-0.5%Cu Alloy Thin Films in Aqueous HF Solution, J. of Electrochem. Soc., V. 137, pp. 1365-1373.

Sedriks A. J., 1979. Corrosion of Stainless Steels, J. Wiley & Sons, New York, New York.

Sedriks A. J., 1982. Corrosion Resistance of Austenitic Fe-Cr-Ni-Mo Alloys in Marine Environments, International Metal Reviews, Vol. 27, p. 321.

Sedriks, A. J., 1990, Effects of Alloy Composition and Microstructure on the Localized Corrosion of Stainless Steels, p. 253, Advances in Localized Corrosion, Ed. H. Isaacs et al., NACE-9, Houston, Texas, 1990.

Shalaby, H. M., F. M. Al-Kharafi, V. K. Gouda, 1989, A Morphological Study of Pitting Corrosion of Copper in Soft Tap Water, Corrosion, V. 45, pp. 536-547.

Shibata, T. and T. Takayama, 1977, Stochastic Theory of Pitting Corrosion, Corrosion, V. 33, pp. 243-251.

Shih, H. and F. Mansfeld, 1989, A Fitting Procedure for Impedance Spectra Obtained for Cases of Localized Corrosion, Corrosion, V. 45, pp. 610-614.

Silence, W. L. and P. E. Manning, 1983, Laboratory and Field Corrosion Test Results Related to Flue Gas Desulfurization Systems, CORROSION/83, Paper No. 185, NACE, Houston, Texas.

Sridhar, N., G. A. Cragnolino, and W. Machowski, 1990, Environmental Effects on Localized Corrosion of a High-level Nuclear Waste Container Material, Mat. Res. Soc. Symp., V. 212, pp. 269-277, Materials Research Society.

Sridhar, N. and J. Kolts, 1987, Effects of Nitrogen on the Selective Dissolution of a Duplex Stainless Steel, Corrosion, V. 43, pp. 646-651.

Sridhar, N., 1990, Effect of Alloying Elements on Localized Corrosion Resistance of Nickel-Base Alloys, Advances in Localized Corrosion, p. 263, NACE, Houston, Texas.

Syrett, B. C. and S. S. Wing, 1980, Effect of Flow on Corrosion of Copper-Nickel Alloys in Aerated Sea Water and in Polluted Sea Water, Corrosion, V. 36, pp. 73-85.

Szklarska-Smialowska, Z., 1986. Pitting Corrosion of Metals, National Association of Corrosion Engineers, Houston, Texas.

Thomas, J. G. N. and A. K. Tiller, 1972a, Formation and Breakdown of Surface Films on Copper in Sodium Hydrogen Carbonate and Sodium Chloride Solutions - Effects of Anion Concentrations, Br. Corrosion J., V. 7, pp. 256-262.

Thomas, J. G. N. and A. K. Tiller, 1972b, Formation and Breakdown of Surface Films on Copper in Sodium Hydrogen Carbonate and Sodium Chloride Solutions - Effects of Temperature and pH, Br. Corrosion J., V. 7, pp. 263-267.

Thompson, N. G. and J. A. Beavers, 1990. Effect of Ground-Water Composition on the Electrochemical Behavior of Carbon Steel: A Statistical Experimental Study." ASTM STP 1086, American Society for Testing and Materials, Philadelphia, Pennsylvania.

Tsujikawa, S. et al., 1987, The Effect of Alloying Elements on the Repassivation Potential for Crevice Corrosion of Stainless Steel in 3% NaCl Solution, Corrosion Engineering, V. 36, pp. 157-168.

Tsujikawa, S., and Y. Hisamatsu, 1982, Repassivation Potential As Crevice Corrosion Characteristic for Austenitic and Ferritic Stainless Steels, Proceedings of 3rd Soviet-Japanese Seminar on Corrosion and Protection of Metals, NAUKA Publishers, Moscow, USSR.

Tsujikawa, S. and Y. Kojima, 1990, Repassivation Method to Predict Long-Term Integrity of Low Alloy Titanium for Nuclear Waste Package, Mat. Res. Soc. Symp., V. 212, pp. 261-268, Materials Research Society.

Wilde, B. E., 1974, On Pitting and Protection Potentials: Their Use and Possible Misuses for Predicting Localized Corrosion Resistance of Stainless Alloys in Halide Media, Localized Corrosion, pp. 342-352, NACE, Houston, Texas.

Williams, D. E., C. Westcott, and M. Fleischmann, 1985, A Statistical Approach to the Study of Localized Corrosion. Passivity of Metals and Semiconductors, pp. 217-228, Elsevier Science Publishers, Amsterdam B.V., The Netherlands.